Technical University of Crete

Undergraduate Thesis

Development of microelectronic system for maximizing the energy generated by flexible photovoltaic cells

Author:
Christos Konstantopoulos

Committee of inquiry:
Supervisor: Assistant Prof. Koutroulis Eftyhios,
Prof. Kalaitzakhs Konstantinos,
Dr. Tsikalakis Antwnios Phd Researcher of Technological Educational Institute of Crete

Chania, 2012

Abstract

Thin-film flexible Photovoltaic (PV) modules have set a new era at the PV market. Their flexible structure and their lightness have revealed new possible applications. The purpose of this thesis is the thorough experimental examination of the characteristics of these flexible PV modules under non-uniform solar irradiation conditions and the evaluation of Maximum Power Point Tracking (MPPT) algorithms, which are able to handle with these conditions. Within the framework of this thesis, a newly developed MPPT algorithm (Hybrid Chaotic PSO) is proposed, which was experimentally tested under non-uniform solar irradiation conditions. The experimental results have shown that the proposed algorithm provides a faster and more accurate convergence to the global maximum power point compared to the past-proposed MPPT algorithms.

Acknowledgement

Thanks to all of you with your invaluable help to carry off 760 different measurements of power-voltage characteristic. Special thanks to the committee of the inquire of my Thesis: my supervisor Assistant Prof. Koutroulis Eftychios, Professor Kalaitzakhs Konstantinos and Dr. Tsikalakhs Antwnios ,Researcher of Technical Education Institute of Crete.

Contents

1 Flexible Thin-Film Photovoltaic Modules **5**
1.1 Characteristics 5
1.1.1 Manufacturing Technology 5
1.1.2 Modeling of flexible PV modules 7
1.2 Applications of flexible PV modules 13
1.2.1 Building-Integrated PV Applications 13
1.2.2 Clothing Integrated Photovoltaics 16
1.2.3 Remote Power Applications 16
1.3 Future development 18

2 Flexible PV Module Power Management **19**
2.1 PV System Concepts 19
2.1.1 Centralized Architecture 19
2.1.2 Semi-Centralized Architecture 19
2.1.3 Module Integrated Converter Architecture 20
2.2 Power Converters 22
2.3 Maximum Power Point Tracking 23
2.3.1 MPPT Algorithms concerns 23
2.3.2 Conventional MPPT methods 24
2.3.3 MPPT methods for non-uniform radiation 26

3 System Implementation **36**
3.1 Hardware 36
3.1.1 Flexible PV module 36
3.1.2 Module integrated converter 37
3.2 Software 42
3.2.1 Switching frequency generation 42
3.2.2 USART connection 42
3.2.3 Sensor Interface 43
3.3 System Evaluation 45
3.3.1 Power-Voltage & Current-Voltage characteristics under non uniform irradiation 45
3.3.2 MPPT Algorithms Evaluation 54

4 Conclusions **86**

A Photos **91**

Introduction

Thin-film flexible Phovotoltaic (PV) module provides an alternative way of solar energy harvesting. Their native flexibility as well as their lightweight construction disclose new applications that crystalline pv modules and solid thin-film pv modules cannot cater for. Several emerging technologies overwhelm the photovoltaic market. Building integrated photovoltaic modules based on flexible thin-film technology, apparel integrated modules and portable flexible solar power generation units(portable solar charger e.t.c.) are some of the applications that flexible PV modules suit for. Fig.1 depicts a possible application of flexible PV modules.

As technology goes forward, electronic devices become more energy efficient. However due to self-reliance powering issues, energy harvesting units should be more efficient and in case of solar applications should be applicable in every type of solar cell and conform to every environmental change. Flexible solar modules, due to their inherent flexibility are exposed to unpredictable and non uniform environmental changes that alter module's electrical characteristics (power voltage and current voltage characteristic changes). In that case there is a need of developing a power management unit that tracks the environmental changes and be capable to extract the maximum available power.

Several studies concern the partial shade effect that affects the electrical characteristics of PV module in case that the it is covered by both unshaded and shaded areas. However, partial shading is not the only effect of non uniform incidence irradiation. Due to flexibility, thin-film modules are affected by the non-uniform bending as solar beams incident in different angles at the module's surface. As a result PV electrical characteristic varies in terms that have not been modeled so far and cannot be theoretically estimated. Non-uniform irradiation of a flexible solar module consists a field that no study has dealt with so far.

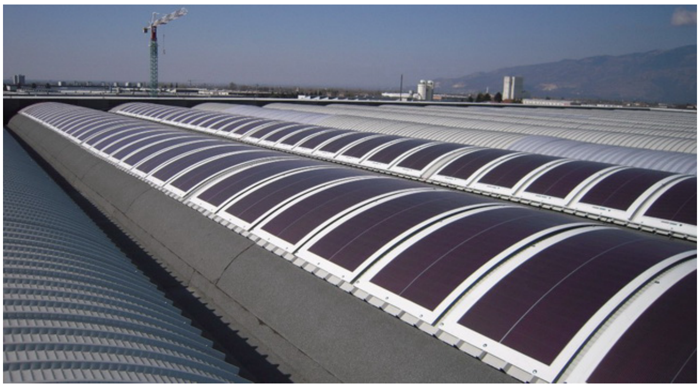

Figure 1: Application of Flexible PV modules.

Within the frame of this thesis a thorough investigation of the electrical characteristics of the flexible pv module was carried off. In order to investigate the power-voltage and current characteristics under several non-uniform irradiation conditions an arc shape static model was constructed that provide a testing platform of the PV module under non-uniform conditions. For the maximization of the non convex power-voltage characteristics that were extracted by the module integrated converter, MPPT algorithms specialized for the non convex characteristic were deployed. Furthermore within the frame of the thesis a newly MPPT algorithm was developed that makes use of the convergence mechanism of Particle Swarm Optimization and the deterministic nature of the chaotic sequences.

The first chapter of the thesis makes an introduction to the thin film technology. Various manufacturing technologies as well as the modeling of the thin film solar cells are presented. Furthermore an introduction to the bend shape model takes place and several applications that take the benefit of the flexible pv module are shown. Chapter 2 describes the flexible power management solutions as regard the concepts of the PV systems and the MPPT methods including the newly developed CPSO algorithm that maximizes the power-voltage characteristic under non uniform irradiation. Chapter 3 presents the results of the tested algorithms and the evaluation the tested algorithms.

Chapter 1

Flexible Thin-Film Photovoltaic Modules

1.1 Characteristics

1.1.1 Manufacturing Technology

The fabrication of a thin-film solar cell involves depositing a layer of semiconductor material (such as amorphous silicon, copper indium gallium diselenide or cadmium telluride) on a low-cost substrate, such as glass, metal or plastic. Current deposition techniques can broadly be classified into physical vapor deposition (PVD), chemical vapor deposition (CVD), electro-chemical deposition (ECD), plasma enhanced chemical vapor deposition (PECVD) or some kind of combination of the above.

Thin-film modules are produced in either single-junction or multi junction configuration. Every junction has a distinct energy gap of radiation that allows its conversion into electricity being manufactured in either P-I-N or N-I-P structures. In case of multi junction pv module, cells with different band gaps are stacked together for wider spectrum absorption of the incident light thus allowing better utilization of light and higher conversion rates. The major categories of thin-film technologies that most manufacturers have focused on are: a-Si, CdTe, CIGS, plastic solar cells and flexible DSSC [1].

a-Si Amorphous Silicon pv technology involves organic material silicon in non-crystalline form. As a-Si cells use approximately 1% of the silicon that is needed for typical c-Si cells ,a-Si cells are thinner and cheaper than crystalline counterparts. Due to their efficiency that is about %5 a-Si pv modules are usual triple -junction cells with three different cells capturing radiation with different band gap [1]. The top cell's band gap is about 1.8eV for blue photons using an a-Si alloy for the i-layer. The middle cell's i-layer is an amorphous silicon-germanium alloy for capturing the optical gap of 1.6eV (green photons). The bottom cell uses an i-layer of SiGe alloy with an optical gap of 1.4eV. Flexible back reflector as well as flexible stainless steel substrate are both used for light trapping.

Amorphous silicon technology (a-Si) is widely used in flexible PV modules today. Due to low manufacturing cost as well as the capturing ability of greater percentage of the incident light energy compared to crystalline silicon modules, gain an increasing portion of market. Amorphous silicon PV modules show better performance in warm, sunny conditions due to their lower power loss temperature coefficient [2]. In addition, a-Si modules perform better during overcast and environmental conditions with diffuse light, which is richer in blue illumination.

CIGS Cu(In,Ga)Se (CIGS) is an excellent absorber material that allows 99% of the available light to be absorbed. High absorption coefficient is succeeded due to the Gallium additive into CuInSe base [1] widening its light-absorption band. CIGS based solar cells have yielded the highest conversion efficiency of thin-film solar cells reaching efficiency over 20% [3].

Roll to roll production line is a usual method in case of CIGS solar cells. Mass manufacturing process involves deposition of CIGS materials onto a thin flexible and unbreakable substrate. Continuous roll to roll coating of thin-film makes use of electrodeposition of CIGS material under vacuum environmental conditions [4].

Plastic solar cells Plastic solar cells are molecular bulk heterojunction cells that are formed by ink jet printing technology [1]. Conjugated polymers that show semiconducting properties and produce photocurrent in heterojunction configuration, posses a processing advantage as they are soluble in common organic solvents and can be deposited by printing on flexible substrates[5]. In summary, polymer solar cell's production properties possess the advantages of lightweight final product, cost effective roll-to-roll printing technique, production ability of semi-transparent colored PV module and significant reduction of production energy consumption [5] during production.

DSSC Dye-sensitized solar cells are based on a photoelectrochemical process that mimics photosynthesis. They consist of semiconducting titanium dioxide crystals covered with photosensitizer dye. In case of photon incidence, the photosensitize dye absorbs the photon and charge injection occurs from the dye into the semiconductor.

1.1.2 Modeling of flexible PV modules

PV cell is illustrated in 1.1.The equivalent circuit of a the I-V characteristic of the PV cell is given by 1.1:

$$I = I_L - I_0(e^{\frac{q(V+IRs)}{nkT}} - 1) \tag{1.1}$$

$$I_L = I_L(T_1) + K_0(T - T_1) \tag{1.2}$$

$$I_L(T_1) = I_{sc}(T_{1,nom})\frac{G}{G_{nom}} \tag{1.3}$$

$$K_0 = \frac{I_{sc}(T_2) - I_{SC}(T_1)}{(T_2 - T_1)} \tag{1.4}$$

$$I_0 = I_0(T_1) * (\frac{T}{T_1})^{\frac{3}{n}} e^{\frac{qV_q(T_1)}{nk(1/T)-1/T_1}} \tag{1.5}$$

$$I_0(T_1) = \frac{I_{SC}(T_1)}{(e^{\frac{qV_{OC}(T_1)}{nkT_1}} - 1)} \tag{1.6}$$

I_D normal diode current, I_L photocurrent described by 1.2 depends on temperature and irradiation level. I_0 is the reverse saturation current which varies with temperature,I_{sc} short circuit current, V_{oc} is the open circuit voltage, n is the quality factor of diode,q is the electron's charge, k is Boltzman constant, T is the cell temperature (K) and G the solar irradiance(W/ m i_2). Finally, T_1 and T_2 refer to the reference cell temperatures when the values of I_{sc} and V_{oc} are taken.

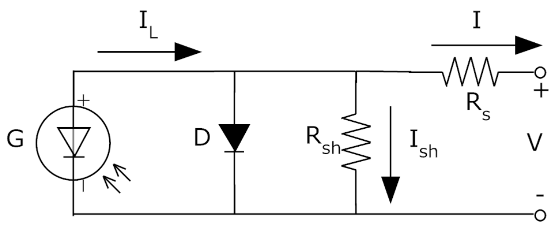

Figure 1.1: Equivalent of PV cell

PV modules consist of several photovoltaic cells connected in a parallel, series or a combined wiring. Due to several external factors the PV module may be partial shaded. Performance of PV module is adversely affected in case that one or more cells are not illuminated as equally as others. In case that the cells are connected in series, they are forced to carry the same current and may get reversed biased , acting as loads by dragging down the current of the entire string and consequently draining power from fully illuminated cells[6]. In parallel wiring, under the partial shading effect the voltage is forced to remain the same across the PV module affecting the total output current as the shaded PV cell consumes power, behaving as a resistor.

In order to avoid a possible damage of PV cells due to overheating when the difference in the illumination with the non-shaded solar cells is intense, bypass and blocking diodes are connected in parallel to with the PV cells. Consequently,for every PV cell that is shaded (assuming that every PV cell is provided with bypass diode) the open circuit voltage drops for 0.6V. Blocking diodes wired in series with the PV cells are used when strings of cells are wired in parallel. The diode gets reversed biased in case of shaded cells that belong to the string and prevents them from reverse-biasing.

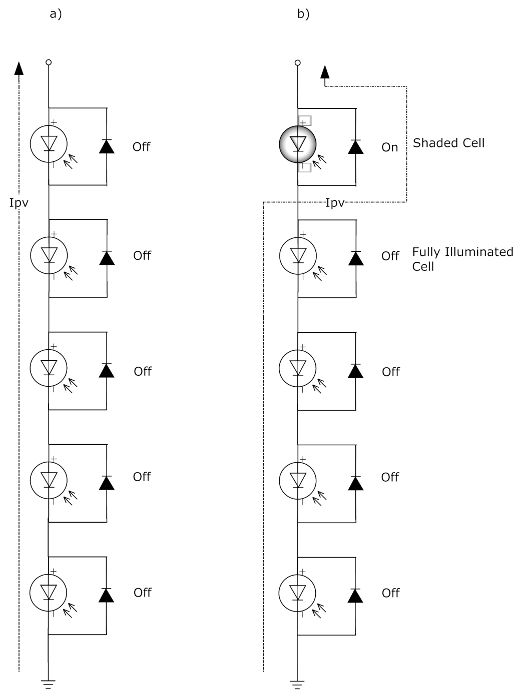

Figure 1.2: Solar cells in series wiring under: a)uniform irradiation, b) partial shading.

Figs. 1.2a depicts a PV module that consists of several of PV cells wired in series under uniform radiation across the PV module.A case of partial shading with a PV cell under shading is illustrated in Fig. 1.2b. Due to the fact that every solar cell is wired in parallel with a bypass diode, the current bypass the solar cell that is shaded.

Figs. 1.3 shows strings of PV cells that are wired in parallel comprising a PV module. In this case, the module is under partial shade as two cell in first string are shaded, consequently drop of voltage occurs across the first PV string. Due to the presence of blocking diodes the current is blocked in the first string. Power-voltage characteristic of a partial shaded PV module emerges from the composition of individual PV cell characteristics [7]. When PV cells are connected in series, for a certain current ,Ipv, the voltage across all PV cells is added to determine the resultant PV voltage. In parallel connection,in order to obtain the overall resultant characteristic a common voltage is considered ,while the overall current is calculated by the summation of the individual currents [7], [6]. Due to the interpolation of unequal power-voltage characteristics, local maximum points appear in the emerged characteristic. The power-voltage characteristic turns into a non-convex space where conventional Maximum Power Point Tracking (MPPT) methods fail to operate efficiently[8]. Figs. 1.4 depicts a PV module system [9] under partial shading conditions. The system's power-voltage characteristic is derived from the interpolation of the individual strings' power-voltage characteristic (Figs. 1.5).

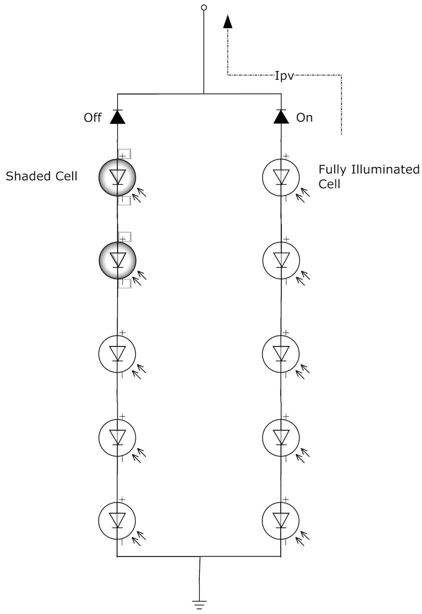

Figure 1.3: Solar cells in parallel wiring under partial shade.

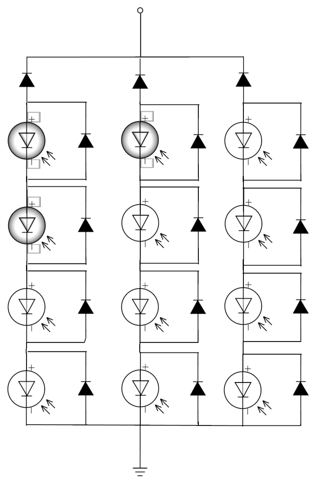

Figure 1.4: A PV module under partial shading.

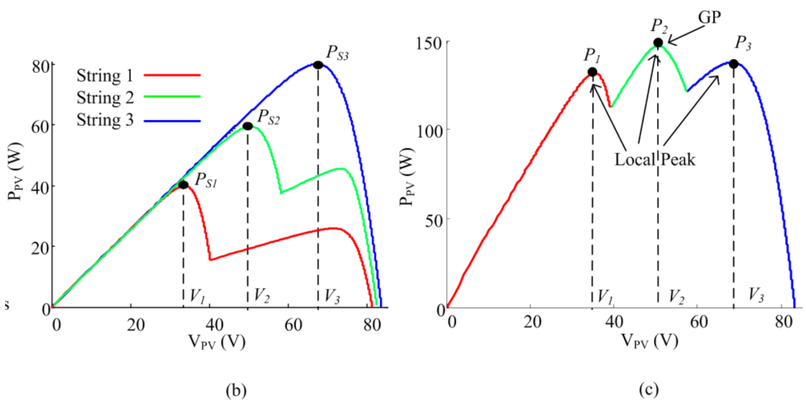

Figure 1.5: Figs. a) The power-voltage characteristic individual strings & b) the composed power-voltage characteristic of the partial shaded PV module.

Due to their inherent flexibility of thin-film PV modules the incident radiation can be in different angle at the individual cells across the same PV module. Figs. 1.6 shows a bended flexible PV module. The incidence angle $\hat{\alpha}$ between the edge and the center of PV module varies according to the degree of bending. The length of arc coincides with the length of PV module.

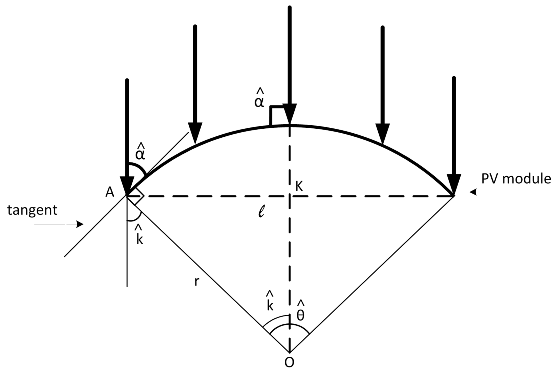

Figure 1.6: Flexible PV module as a portion of circle

The arc shape as shown in Figs. 1.6 as a portion of a circle with radius ,r, a center angle $\hat{\theta}$,chord λ and the length of the arc.

$$\frac{\text{portion of circle}}{\text{whole circle}} = \frac{\hat{\theta}}{360} = \frac{arcLength}{2\pi r} \tag{1.7}$$

resulting in:

$$r = \text{arc length} * \frac{360}{2\pi\hat{\theta}} \tag{1.8}$$

Also, according 1.7 it holds that:

$$\tan(\hat{k}) = \frac{AK}{OK} \tag{1.9}$$

$$AK = l/2 \tag{1.10}$$

$$\hat{k} = \frac{\hat{\theta}}{2} \tag{1.11}$$

$$\hat{\alpha} = 90 - \hat{k} = 90 - \hat{\theta}/2 \tag{1.12}$$

$$AO^2 = KO^2 + AK^2 \tag{1.13}$$

From 1.13 and 1.9 it results that:

$$AO^2 = (\frac{AK}{tan(\hat{k})})^2 + AK^2 \tag{1.14}$$

Combining 1.11, 1.14 and 1.10 :

$$r^2 = (\frac{l/2}{tan(\frac{\hat{\theta}}{2})})^2 + l/2^2 \tag{1.15}$$

$$l * \sqrt{\frac{1}{tan(\theta/2)^2} + 1} = 2 * r \tag{1.16}$$

substituting 1.16 in 1.7:

$$l * \sqrt{\frac{1}{tan(\theta/2)^2} + 1} = 2 * \text{arc length} * \frac{360}{2\pi\hat{\theta}} \tag{1.17}$$

$$l = \frac{2}{\sqrt{\frac{1}{tan(\theta/2)^2} + 1}} * \text{arc length} * \frac{360}{2\pi\hat{\theta}} \tag{1.18}$$

Given that the incidence radiation on the top of the arc forms an angle of 90° with the tangent line at this point, the incidence angle $\hat{\alpha}$ varies from 90° (center) to 90°-$\hat{\theta}/2$ (edge) degrees as expression 1.12 indicates. Equation 1.18 expresses the length of chord in accordance with the center angle $\hat{\theta}$, given the length of the PV module. Given a desired variance of the solar incidence angle across the PV module of a certain length using equation 1.19 length is calculated, which belongs to the arch that is formed: Angle $\hat{\alpha}$ indicates the solar incidence angle at the edge of PV module where Fig. 1.7 indicates the length of chord in meters for different center angles given an arc length of 2.8m.

$$l = \frac{2}{\sqrt{\frac{1}{tan(90-\hat{a})^2} + 1}} * \text{arc length} * \frac{360}{2\pi(180 - 2\hat{a})} \tag{1.19}$$

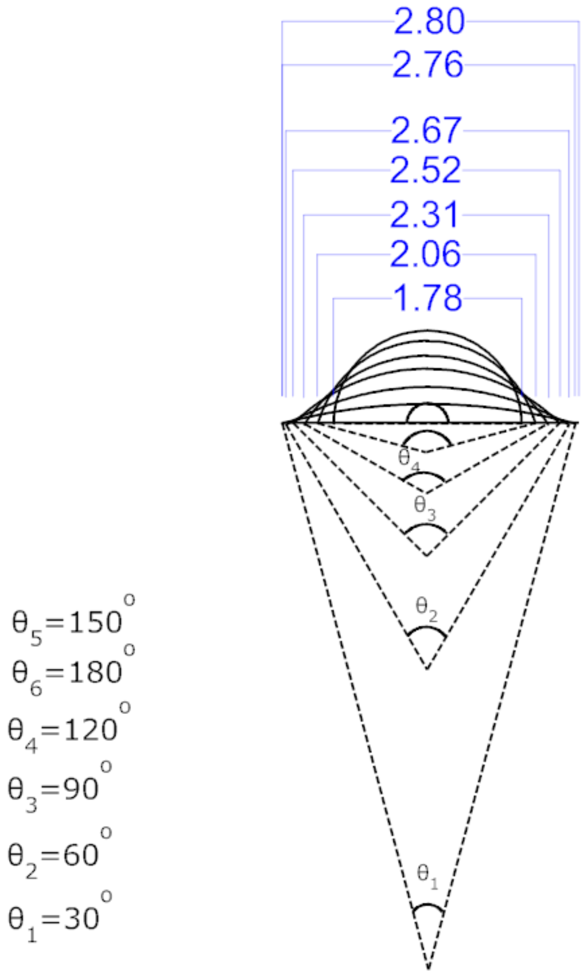

Figure 1.7: The chord length (metres) for different center angles in case that the arc length id equal to 2.8m.

1.2 Applications of flexible PV modules

Today, the flexible photovoltaic modules own a considerable portion of market. Due to their inherent characteristic of flexible and light structure, disclosed new market and applications possibilities that the alternative crystalline PV modules cannot fulfill their requirements. Several applications require standalone energy harvesting systems, which are able to adapt their function and environment. Newly developed CIGS technology has increased the efficiency of thin-film PV modules for over 19% as compared to crystalline silicon-based cell maximum efficiencies of 20% [3]. This increase in the performance, as well as the imminent reduction of manufacturing cost due to the mass production set a new era for thin-film PV modules.

1.2.1 Building-Integrated PV Applications

Photovotaic modules are used as modern building materials replacing conventional building structures. The Building-Integrated PV (BIPV modules retain the same construction ability providing an energy generation module as well as a daylighting and constructing element. Individual solar cells are interconnected, encapsulated, laminated on glass or flexible substrates and framed to form a BIPV module. This kind of photovoltaic modules is ideal for roofs, skylights or facades.Depending on the construction individual solar cells BIPV facades may allow partial light to come through the module providing in the same time interior natural light as well as power production.

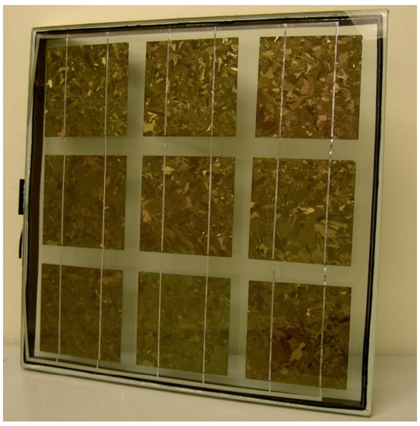

Figure 1.8: Monocrystalline PV modules encapsulated in glass.

thin-film BIPV module The monocrystalline and polycrystalline types of PV cell are mainly integrated in BIPV applications, however, due to the inability of transparency thin-film modules obtain an incrementing portion of BIPV market (Figs. 1.9). Newly developed manufacturing methods of thin-film modules achieve higher transparency than predecessor thin-film types, as well as higher energy conversion coefficient. Furthermore, modern architectonic tides adopt curly and arch-type forms that flexible thin-film PV module best fit. The PV rooftop installations based on flexible module become much more attractive than the crystalline counterparts, as they can be integrated on the roofing surface without the need of roof penetration, minimizing the mounting hardware and the overall weight load. Moreover, due to their minimal profile, they achieve zero wind load.

Figure 1.9: BIPV module based on thin-film technology.

A recent roof top BIPV module developed by SRS Energy(srsenergy.com) replaces the common clay tile with a curved polymer base integrated with a flexible PV module (Figs. 1.10). This combination allows a lightweight PV rooftop installation (Figs. 1.11) integrated into the building with aesthetic and functional advantage.

Figure 1.10: BIPV module Sole Power-Tile manufactured by SRS Energy.

Figure 1.11: Sole Power-Tile integratedon on a building roof.

Another implementation about BIPV based on flexible PV modules refers to portable shade structures or urban architectures. Konarka manufacturing company of Power Plastic flexible PV module, shows off several BIPV applications based on Power Plastic PV modules. For example Wi-Fi enabled transit shelter(Figs. 1.12)is based on Konarka's product.Figs. 1.13 depicts Flexible modules installed at curved roof.

Figure 1.12: Wi-Fi enabled transit shelter in San Francisco based on Power Plastic PV module

Figure 1.13: PV flexible modules installed on curved roof

1.2.2 Clothing Integrated Photovoltaics

Unlike the rapid development of wireless and mobile technology,the energy that should be available for mobile devices powering purposes is strictly limited .Recent studies have dealt with the development of sustainable mobile power sources that can power portable devices. Photovoltaic fibers that can be woven and produce smart textiles [10] as well as flexible PV modules integrated in garments [11], have been recently developed and tested. However, due to the challenges that arise in case of photovoltaic fibers like the moving interconnects, shadowing etc. a woven solar module in unlikely to be seen in the foreseeable future [12]. Figs. 1.14 depicts PV module mounted on flexible substrate integrated in wearing gear.

Figure 1.14: PV modules integrated in wearing gear

1.2.3 Remote Power Applications

Remote power applications consist a complete power management system of solar energy which is able to supply portable and remote electronic applications. Remote sensors, portable personal devices and space applications require extended power autonomy, however a power management system that is dependent only on energy stored at batteries has a restricted operational lifetime. In that case, systems that rely on sustainable energy sources have a beyond comparison advantage. The advantage of the lightweight and flexible structure of thin-film PV module complements the portable and remote nature of these applications. The development of a complete lightweight and flexible energy management system that produces, manages and stores solar energy, sets a new era of the future remote power applications.

Flexible PV modules integrated with energy storage, as well as a power management system are ideal for remote power applications where the portability and the overall system weight play significant role. These systems are able to supply and store enough power in order to operate devices that are portable or unable to be connected to the power grid. Solar charger SunPack which is developed by solar company FlexCell (www.flexcell.com), is able to power portable devices such as mobile phones and store the surplus energy in a Li-ion battery. SunPack's flexible PV module is based on amorphous silicon technology.

Figure 1.15: Flexcell Sunpack ion+ System

Modular Cylindrical Photovoltaic Array consists a modular photovoltaic platform that is based on a cylindrical design, which provides a wide angle of incidence light [13]. The main body of the platform is consisted from a flexible thin-film photovoltaic cell wrapped around of a cylindrical body forming a cylindrical PV array. The proposed portable platform offers the necessary housing for battery storage and related system electronics as well as the ability of interconnection among multiple modules. Figs. 1.16 depicts the modular cylindrical photovoltaic array, indicating the individual components.Also, the main advantage of the array is the improved energy density collection as well as the scalability and modularity compared to common PV modules that are currently used.

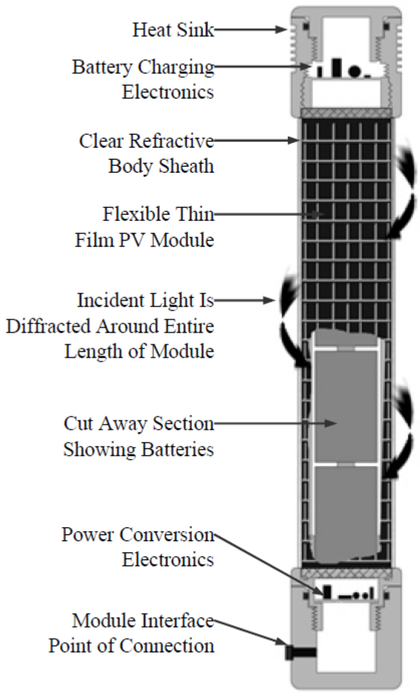

Figure 1.16: Modular cylindrical PV Array

Newly researches have developed power generation units for space applications that combine flexible PV module integrated with solid state thin-film battery and flexible power management units. A recently developed power generation system in [14] utilizes CIGS photovoltaic material as well as thin-film solid state battery storage, which consists of newly developed solid-state electrolyte. The system includes an electronic management unit manufactured on flexible substrate in order to interface the PV module.

1.3 Future development

The present cost-efficiency ratio of thin-film PV modules set a hindrance at the market penetration today. Crystalline PV has the cost advantage right now with more sufficient panels below the barrier of one dollar per watt. However, thin-film modules have better efficiency in low light conditions as well as in hot environment. These advantages turn into an equal power generation production to crystalline modules over the entire day. Due to the mass production of flexible PV modules , the manufacturing cost is imminently reduced and in combination with the increasing efficiency this leads to better future expectations. The flexible and lightweight construction of thin-film PV modules discloses new application possibilities where crystalline module cannot be applied.

Chapter 2

Flexible PV Module Power Management

Flexible PV modules have been widely used in several applications nowadays [14, 15, 16, 17, 18, 19, 11]. However, due to the inherent flexible structure the incidence radiation on the surface constantly varies non uniformly. Consequently the PV module's power voltage characteristic may exhibit local MPP and in this case the conventional power management methods that are used in straight surface PV modules fail. Conventional configurations of power management systems cannot meet the requirements of rapid varying environment and non uniform surface conditions. An ideal power management unit interfaces the flexible PV module and the central power conditioning unit extracting the maximum power that is available providing therefore maximum efficiency and rapid response under any surface conditions.

2.1 PV System Concepts

2.1.1 Centralized Architecture

In a centralized system (Figs. 2.1), PV modules are usually series connected as a string and plenty of strings are connected in parallel through string diodes to achieve the expected power level. However when non uniform irradiation incidence across the PV system the centralized architecture cannot interface the pv system . As a result the efficiency and the reliability drops significantly.

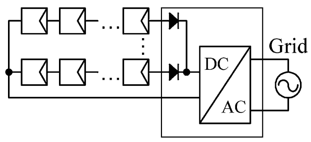

Figure 2.1: Centralized PV architecture.

2.1.2 Semi-Centralized Architecture

In semi centralized PV system configuration (Figs. 2.2), the PV modules' strings are connected to a dc-dc converter and a common DC/AC inverter is used to interface the system with the power grid. The mismatch problem of parallel - connected string is avoided, and the system's reliability is improved [20].Due to high dc voltage, the elimination of string diodes and the ability of adopting MPPT procedure to each individual string the system efficiency can be significantly increased.

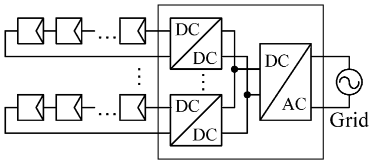

Figure 2.2: Multistring PV configuration.

2.1.3 Module Integrated Converter Architecture

Module Integrated Converter (MIC) technology is one approach that assists in driving down the balance of system (Bos) to secure an improved total system cost [21] ,and eliminating the MPPT mismatches between panel and the inverter [22]. This type of converter can be used integrated in building block such as tiles, facades etc. [23], therefore, comprising the power generating nodes of a wider power network. The electrical junction box that is used in usual photovoltaic installations is replaced by a power converter and a control unit that performs the MPPT procedure, as well as system monitoring [24]. The MICs individual are connected with dc-link and the communication with the central management unit is performed by power line communication methods or a wireless link.

The power converter boosts the lower output voltage of PV module to a high DC-link voltage of about 200 or 400 V. Conventional central high efficient -single stage inverter is needed, which acts as an interface between the smart solar generation network and the electric grid. The main functions of the controller in the MIC module includes tracking the MPP by monitoring the PV module as well as, sending MIC's operational data to the central unit.

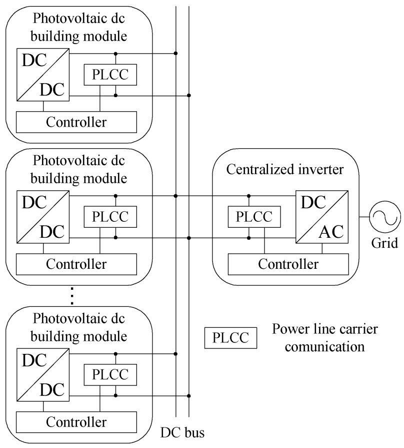

Figure 2.3: MIC-based System.

The advantages of MIC PV system compared to other topologies are the following:

- Individual MPPT process for every PV module. Every PV module operates in its individual MPP. Consequently the system is immune to non-uniform changes at the individual PV modules of the system. The MIC nodes are each other independent and can be installed at different positions and orientations to meet the building's requirements.

- Inherent and node individual data monitor. The status of every node is easy to be acquired and transmitted to the central monitor system via either the Power Line Communication (PLCC) protocol or wireless transmission. This provides individual node information for the entire PV network, therefore reassuring better maintenance and protection especially to PV systems consisting of a large number of nodes.
- Excellent expandability. Due to MIC's modular plug 'n' play design a system based on this technology can be easily enlarged by adopting more nodes.In that way energy storage arrays , such as lead-acid batteries or other distributed generation systems, wind generators can be easily integrated to the existing system.

Cost has been a barrier for further application expansion of the module integrated configuration [22]. Aside from the specifications of the components, it is also strongly influenced by the fact that the lower the power rating is, the higher is the cost per produced kWh. However the manufacturing cost can be reduced by mass production.

In order to maximize the PV generated energy, the perfect matching between the power management interface and the PV module is crucial. Especially when non-uniform irradiation across the PV module takes place, the converter should harvest the maximum power from the PV module using MPPT process that overcomes the barrier of the non convex space of the power-voltage characteristic. The non uniform incidence radiation on the surface of a flexible PV module can be exploited utmost by module integrated designs, as they can complement these special qualifications as mentioned above.

2.2 Power Converters

The Power Converter consists the main component of power management unit of the PV System power management unit. Simple conventional power converter topologies such as the boost converter, the buck converter or the flyback converter [25] have shown weaknesses, as the rated power level augments. Switching as well as transformer losses (in case of isolated topologies) should be taken into account when a high step up voltage is needed. The main concerns that are involved in the choice of power converter's choice [26]:

- High voltage DC gain
- Low input voltage ripple
- Compact topology and high converter efficiency
- High reliability

Several studies have proposed multistage isolated and non-isolated topologies that can handle with high step-up voltage and show increased efficiency without requiring high duty cycle values, [21, 22, 26]. Therefore losses at inductors and capacitors are diminished, diodes with short turn on-turn off time are not needed and switching transients as well as core susceptibility for fast changing flux intensity do not play significant role [22].

2.3 Maximum Power Point Tracking

Impedance matching is the main principle applied to attain maximum power transfer. In terms of the static resistance of photovoltaic module it is mandatory to match the load impedance in a manner that can be adapted according to environmental conditions as well as the non uniform radiation effects. Power converters with variable duty cycle operation and constant output voltage are used to change the voltage across the PV module. As a result the operating point alters and the current occurs according to the static resistance of PV module. Due to the fact that any I-V model hasn't been developed so far, which can characterize the static resistance of flexible thin photovoltaic cells under non-uniform radiance, it is necessary to develop efficient heuristic methods for the determination of static resistance. That are methods should be able to achieve impedance matching between the load and PV module by estimating the voltage across the module and tracking the maximum power point (MPP).

2.3.1 MPPT Algorithms concerns

The main concerns in designing an MPPT algorithm are :

System Independence and Parameters' Definiteness MPPT methods in order to estimate the environmental conditions and the operational point of photovoltaic module, monitors several system variables such as current, voltage, solar irradiation. Furthermore, look-up tables and mathematical models of power-voltage characteristic [27] make an quite fast algorithm. However, algorithms that dependent on these methods cannot be generic [28]. For instance MPPT methods employing state-space modeling, neural networks or fuzzy algorithms [29], [30] have system specific nature.

Time to converge to Global Maximum Power Point The number of duty cycle accesses that the algorithm needs to execute in order to converge into a MPP under a defined error margin provides an indication of the needed time that the algorithm needs to converge, without figuring the hardware and software complexity. Taking into account the notable settling time that the power converter needs for stabilization on every duty cycle change, the overall duty cycle steps of the algorithm should be considered.

Sense of tracking direction A major qualification of MPPT algorithm's efficiency is the most power point tracking ability and environment sense under rapid changing conditions. In terms of flexible thin solar module that subjects to constantly varying non uniform solar irradiation, the MPP tracking ability plays significant role. Without oscillation the algorithm should converge to the next most power point with minimum steps. That ensures the long term efficiency of algorithm under rapid changing environmental conditions.

Complexity of controller hardware Many MPPT methods utilize complex control hardware in order to maximize the power provided from the PV module. Hardware complexity increases the implementation cost of MPPT converter.

Software complexity In terms of searching and tracking the MPP, algorithms use routines of polynomial complexity as well as sorting routines that add additional overall complexity. The memory resources as well as the computational power of embedded microprocessors is limited,so the implementation of these algorithms increase the system's cost.

Many MPPT algorithms have been proposed so far [31]. However developing an algorithm that interface a flexible solar module and accomplishes the modular and generic design specifications of module integrated converter is a challenging task. The algorithm has to conform with the modular system design by monitoring a few system variables without employing complex mathematical models, as well as show off a rapid response and excellent MPPT ability under changing metereological conditions(i.e solar irradiation and ambient temperature). The ability of maximizing the power extracted from flexible photovoltaic modules takes for granted the ability of handling non convex power-voltage characteristics.

2.3.2 Conventional MPPT methods

Conventional MPPT methods are used complementary to other methods in order to approach the problem of non-uniform radiation on a PV array. They are basic MPPT methods that maximize the power extracted from PV modules under uniform irradiation [32]. In the case of a PV array connected to a power converter, perturbing the duty ratio of the power converter perturbs the PV array current and consequently perturbs the PV array voltage. Most of them like P&O and Incremental Conductance are based on the first order derivative of power in order to condition the current operation point and decide the next step of the algorithm.

P&O Considering that PV solar characteristic is convex under uniform irradiation, the P&O calculates and monitors the first order derivative of power extracted from the PV module. If there is an increase in power, the subsequent perturbation should be kept in the same direction to reach the MPP, otherwise in case of decrease the direction is reversed. Once the maximum power is extracted, the algorithm oscillates around the peak power point. The oscillation is minimized by reducing the duty cycle step. However, more duty cycle steps are needed for convergence in this case.

Incremental Conductance The Incremental Conductance method is based on the fact that the slope at the top of the power-voltage characteristic is equal to zero. Therefore by polling the variance of conductance, the algorithm tracks the maximum power point. Equation (2.1) proves the ability of tracking the MPP by perturbing the conductance of PV module

$$dP/dV = d(IV)/dV = I + V * dI/dV \tag{2.1}$$

Summarizing, the conditions of estimating the right perturbing direction are derived from 2.1 as follows:

$$\begin{cases} dP/dV = -I/V & \text{at MPP} \\ dP/dV > -I/V & \text{left of MPP} \\ dI/dV < -1/V & \text{right of MPP} \end{cases} \tag{2.2}$$

Fractional Open-Circuit Voltage Fractional Open-Circuit Voltage comprises a MPPT procedure that offers an approximation of the MPP. It has been shown that the MPP is proportional to the open circuit voltage [31],[32]:

$$V_{MPP} \approx k_1 * V_{OC} \tag{2.3}$$

where k is a constant of proportionality. However factor k is dependent on the characteristics of the PV module and as (2.4) is an approximation the PV module technically never operates at most power point. The algorithm periodically measure the open circuit voltage of PV module and calculates an estimation of MPP as the (2.4) indicates.

Constant Current Fractional short circuit current results from the fact that $\mathrm{I_{mpp}}$ is proportional linear related to the short circuit current Isc of the PV module.

$$I_{MPP} \approx k_2 * I_{OC} \tag{2.4}$$

Similarly to the Fractional Open-Circuit Method factor $\mathrm{k_2}$ is determined according to the PV module that is used. As the operating point consists an approximation of the actual MPP, the PV array is never perfectly matched to the converter [31].

Fuzzy Logic Control Fuzzy logic control consists of three stages: fuzzification, rule base look-up table, and defuzzication [31, 29],the following system variables are used for fuzzification:

$$\delta P = P(k) - P(k-1) \tag{2.5}$$

$$\delta I = I(k) - I(k-1) \tag{2.6}$$

$$\delta P_m = P_m(k) - P(k) \tag{2.7}$$

The output equation is the following:

$$\delta D = D(k) - D(k-1) \tag{2.8}$$

The variable inputs are divided into several fuzzy sets and the system's output is determined by Mamdani's inference method [8],[29]. Commonly used algorithm for the deffuzication stage is the centre of area algorithm (COA), which converts the fuzzy subsets (duty cycle changes) to real numbers. MPPT fuzzy logic controllers perform well under varying atmospheric conditions. However, their effectiveness depends a lot on system tuning, which achieves an efficient rule base table [31].

2.3.3 MPPT methods for non-uniform radiation

The operating variables of a solar cell such as solar irradiance and cell temperature module changes continuously. Consequently the static resistance varies and in case of partial shading or flexible PV bending, multiple local maxima appear on the P-V characteristic curve of the array. Multiple local peaks set a barrier in locating the global maximum power point as the conventional methods are trapped at local maxima or oscillate around them [33]. These facts set the need for more robust MPPT algorithms that are able to locate and track the global peak in minimum steps, taking into account the rapid changing environmental conditions.

Partial shading and non uniform insolation of PV cell transform the MPPT into a non convex optimization problem that conventional algorithms such as Perturb and Observe or Incremental Conductance cannot handle with. Many approaches which can cope with the non convex space of power-voltage characteristic under either non uniform isolation or partial shading have been proposed so far.

Heuristic algorithms that can extract an optimal solution of NP problems, have been utilized by the research community in order to find approximate solutions to the MPPT problem under partial shading conditions. There are two main categories of heuristic algorithms: Population Based algorithms and Partial Search. These algorithms overcome the multiple peak barrier utilizing swarm intelligence (PSO algorithm), genetic evolution (Differential Evolution) or partial searching (Chaotic search) that fragments the power-voltage characteristic into several parts as Fibonacci or chaotic sequences indicate. The penalties of these techniques are high complexity,requirement for partial knowledge of PV array structure and mainly the algorithms' stochastic nature that cannot guarantee convergence under any operating conditions.

Other techniques involve modified Perturb and Observe algorithm integrated with fuzzy logic controller[34] or open-circuit method[8]. The main concept of these algorithms constitute a steep ascent walk across the power-voltage characteristic with variant duty cycle step, which can discriminate the global best among the locals. In case of[34] fuzzy logic controller outputs a dynamic duty cycle step taking into account the first order derivative of power, current and voltage.

Differential Evolution

Differential evolution algorithm is a member of the genetic algorithm which is a stochastic, population-based optimization algorithm [35]. The optimization process is conducted ike genetic algorithms using similar operators: crossover, mutation and selection. The main difference with Genetic Algorithms is that the latter rely on crossover, while Differential Evolution relies on mutation operation. The algorithm uses mutation operation as a search mechanism and selection operation to direct the prospective regions in the search space.

Mutation The mutation operation of DE applies the vector differentials between the existing population members in order to determine the degree and direction of perturbation applied to the individual subjects of the mutation operation. The mutation process at each generation begins by randomly selecting three individuals r_1,r_2,r_3. The i_{ith} perturbed individual, $V_{i,G+1}$, is generated by adding the weighted difference between the two

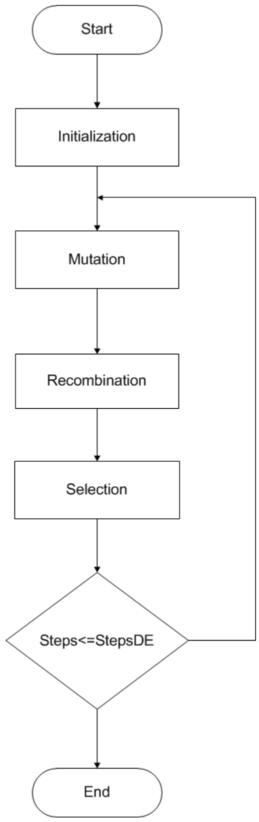

Figure 2.4: Differential Evolution algorithm

vectors to the third vector as follows:

$$V_{i,G+1} = X_{r1,G} + F(X_{r2,G} - X_{r3,G}) \tag{2.9}$$

where F is the mutation scaling factor chosen from the range(0,1] and G is the generation number. Several mutation equations for producing the donor vectors have been proposed so far [36] that are differentiated into the vector to be perturbed, the number of differences vectors considered for perturbation and the type of crossover that is used.

Crossover Once the mutant vector is generated, the perturbed individual, $V_{i,G+1}=(V_{i,i,G+1},...,V_{n,i,G+1})$ and the current population member, $X_{i,G}=(x_{1,i,G},...,x_{n,i,G})$ are then subject to the crossover operation, that finally generates the population of candidates or trial vectors, $U_{i,G+1}=(u_{1,i,G+1},...,u_{n,i,G+1})$ as follows:

$$U_{j,i,G+1} = \begin{cases} V_{j,i,G+1} & \text{if a rand number ;} \\ X_{j,i,G} & \text{otherwise.} \end{cases} \tag{2.10}$$

$$j = 1, 2, ...D, i = 1, 2, ..., Np \tag{2.11}$$

Selection The selection scheme of DE also differs from that of the others EAs. The population for the next generation is selected from the individual in current population and its corresponding trial vector according to the following rule:

$$X_{j,i,G+1} = \begin{cases} U_{j,i,G+1} & f(X_{i,G}) \leq f(U_i, G+1)); \\ X_{j,i,G} & \text{otherwise.} \end{cases} \tag{2.12}$$

Thus, each value is compared with its counterpart and the better value is selected.So if the new trial vector yields an equal or lower value of the objective function, it replaces the corresponding target vector in the next generation: otherwise the target is retained in the population. Consequently, the next generation is equal or better than the current generation and never deteriorates.

Chaotic Partial Search Algorithm

Chaotic Search MPPT Algorithm is a partial search heuristic algorithm that depends on the sequential fragmentation of power-voltage characteristic, utilizing chaotic sequences that are generated by discreet domain maps.

Chaos in general is defined as qualitative changes in behavior and, in extreme cases, even instability that arises in a system due to nonlinear behavior. Nonlinear recursive equations (chaotic map) depend their instability on initial parameters, fluctuating between periodic, stable and disorderly behaviors. In an unstable state, chaotic map exhibit pseudo random behavior. Chaos has the characteristics of long term unpredictability, initial sensitivity, ergodicity and boundedness. Ergodicity refers to the fact that it can reach all the states in a certain domain area non-repeatedly,in a deterministic way and due to unpredictability, it can imitate the randomness. The chaotic search mechanism can prevent premature convergence effectively.

Several recursive equations with chaotic behavior have been proposed in the literature. Every chaotic map signifies a sensitive response to the initial value X_0. Different initial values can evolve into completely different states revealing oscillations and fractal behaviors. A qualitative measure of chaotic maps boundedness and stability consists the bifurcation diagram, which indicates the chaotic maps' behavior according to parameter sweep.In Fig. 2.5is the bifurcation diagram of sine chaotic map indicates the stable solutions of sin recursive equation (2.13):

$$.x_t = \lambda * x_{t-1} * sin(pi * x_{t-1}) \tag{2.13}$$

Sweeping the λ parameter from 1.25 to 1.65. The chaotic behavior happens for λ higher than 1.5. The chaotic maps can generate periodic and ergodic sequences that execute a pseudo random non-repeated deterministic walk as previously mentioned. This stochastic walk constitutes a partial search method, which can handle the non convex shape of power-voltage characteristic in case of non-uniform PV module irradiation. The algorithm proposed in [37] uses sine as well as logistic map representing duty cycle values. After combining and ordering the chaotic sequences, the algorithm calculates the power of each element and find the maximum among the values of current generation. Every next generation, the chaotic domain shrinks around the current peak, consequently after several iterations the global maximum is estimated. This method assures a rapid convergence with the least power calculation steps.

Figs. 2.6 depicts the initial and next iteration search zone where $\mathrm{X_i}$ and $\mathrm{Y_i}$ chaotic maps' products.

As shown in Fig. 2.7 The algorithm firstly initializes and produces both chaotic maps' iterations. Sine as well as Log map are used in order to produce the chaotic sequences $\mathrm{X_i}$ and $\mathrm{Y_i}$ respectively. After the sequences have been combined and ordered to a new vector, the algorithm calculates power for each value and executes a maximum search that looks for peaks higher than their nearest neighbors and stores their indices. The peak with the maximum value among the others is chosen and its closest neighbors are

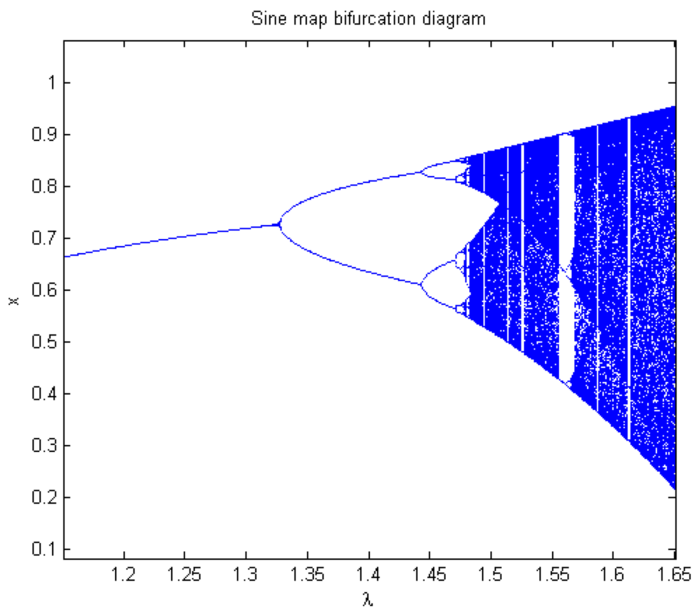

Figure 2.5: Sine Map Bifurcation diagram

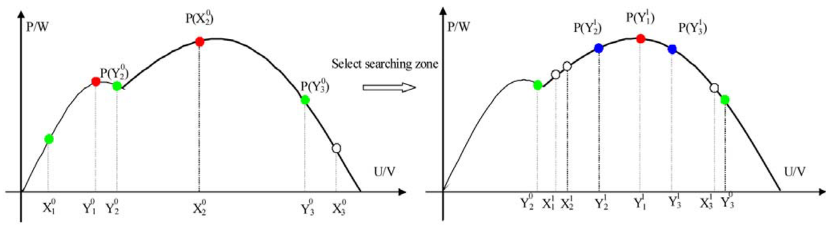

Figure 2.6: Initial and later steps of chaotic partial search.

used to define the bounds of the next iteration search zone. The algorithm termination criterion is estimated by a defined error margin between the power calculated at the peaks and its closest neighbors.

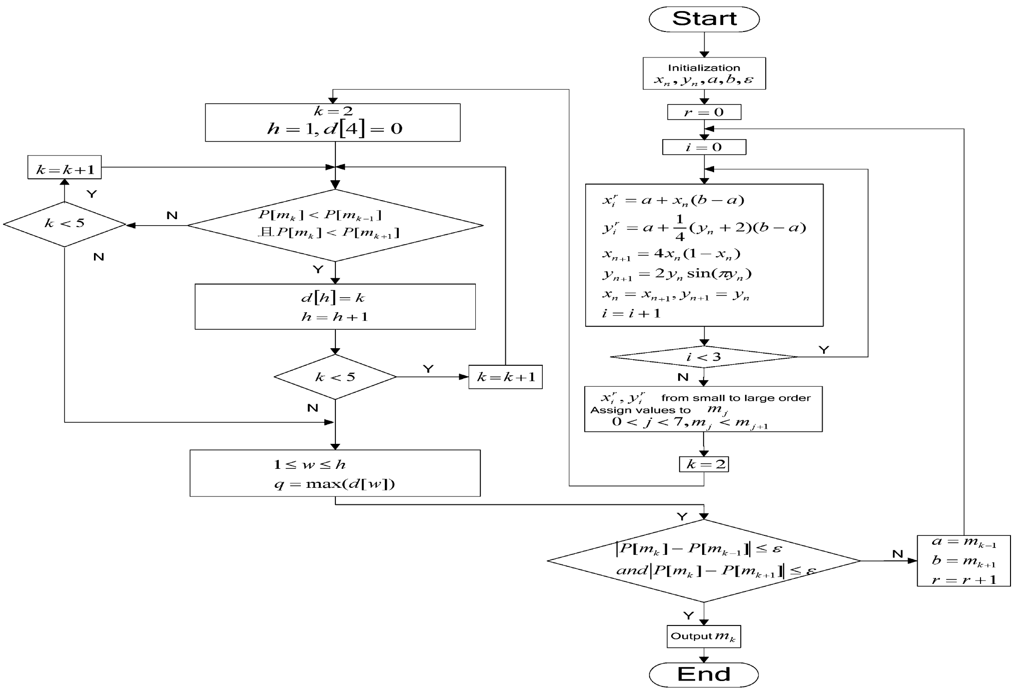

Figure 2.7: A flow chart of chaotic partial search algorithm

Standard Particle Swarm Algorithm

Standard Particle Swarm Optimization [33] method involves a swarm of particles moving in a d-dimensional search-space, involving cooperation in searching for the global maximum on condition that the fitness of the particles can be calculated. Each particle's next movement is influenced by its local best known position in addition with the best known position among the individual best positions of particles. The convergence of particle swarm optimization process has been proven through iterative function system and probabilistic theory in [38].

Each particle has a position represented by a position-vector x_i (i is the index of the particle) and a velocity represented by a velocity-vector v_i. Each particle remembers its own best position so far in a vector $pBest_i$, and its j-th dimensional value is $p_{i,j}$. The best position from the swarm so far is then stored in a vector pGlobal, and its j-th dimensional value is $gBest_{i,j}$. During the iteration time t, the update of the velocity from the previous velocity is determined by (2.14) where r_1 and r_2 are the random numbers, uniformly distributed within the interval [0,1] for the j-th dimension of i- th particle, c_1 positive self recognition coefficient, c_2 social coefficient, w momentum factor, x constriction factor:

$$v_{i,j}(t) = x*(w*v(t-1)+c_1*r_1*(pBest_{i,j}(t-1)-s_{i,j}(t-1))+c_2*r_2*(gBest(t-1)-s_{i,j}(t-1))) \tag{2.14}$$

.Consequently, the new position is determined by the sum of the previous position and the new velocity by (2.15)

$$s_{i,j}(t) = s_{i,j}(t-1) + v_{i,j}(t) \tag{2.15}$$

From 2.14, a particle decides where to move next, considering its own experience, which is the memory of its best past position, and the experience of its most successful particle in the swarm. The PSO algorithm reinitializes the particles with uniformly random positions whenever they are inactive, which is detected:

$$v_{i+1} < -dV \tag{2.16}$$

$$(P(s_{i+1}) - P(s_i))/P(s_i) < dP \tag{2.17}$$

The reinitialization happens two conditions (2.16) and (2.17) are satisfied for N_c consecutive time units. The algorithm updates the pBest position whenever the current position's power is better than the personal best power, as well as updates the global Best power and position when it is necessary required.Figs. 2.8 illustrates the fow chart of the Particle Swarm Optimization algorithm.

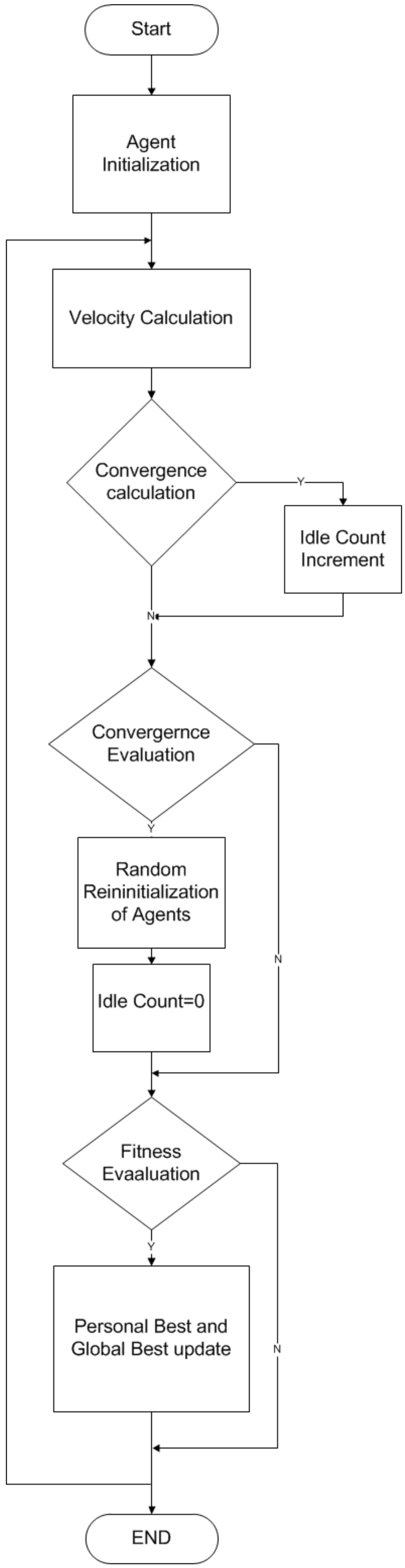

Figure 2.8: Flowchart of Particle Swarm Optimization algorithm

Hybrid Particle Swarm Algorithm with Embedded dual Carrier Chaotic Search

Hybrid Particle Swarm Algorithm with Embedded dual Carrier Chaotic Search is a Hybrid PSO algorithm that uses chaos sequences in order to reinitialize the particles. Some particles become inactive when their location and pBest is close to gBest so their velocity is close to zero. As a consequence other particles approach the inactive particle and as a result the system stalls. However, the random reinitialization of the particles' positions doesn't seem to be effective as the updates of gBest and pBest show their blindness, which affects the speed of convergence adding additional computing time.

The main idea of Hybrid PSO algorithm [39] (Fig.2.9) is that whenever the particles converge and stall, the algorithm uses chaos sequences to escape from local minima and stagnancy. The chaotic sequences, due to their non repeated and ergodic property results in non repeated scattered search as the chaotic maps indicates. However, due to the unlimited number of chaotic iterations that the algorithm presented in [39] proposes, the procedure is missed out in terms of overal speed convergence, taking into account the dual carrier chaotic variables. An alternative approach to [39] is presented in this thesis that restricts the chaotic iterations whenever a particle stalls is by polling a temporal variable posPower that stores the current power during the chaotic walk.

The dual carrier chaotic searching that is proposed uses Sine as well as Logistic chaotic map to produce chaotic variables as follows:

$$y_t = 4 * y_{t-1} * (1 - y_{t-1}) \tag{2.18}$$

$$x_t = 2 * x_{t-1} * sin(pi * x_{t-1}) \tag{2.19}$$

The Sine chaotic map (2.19) offers a near neighborhood of current particle position optimal solution as the Logistic mapping (2.18) executes a scattered search around the current particle position. The centralization and the variance of each map are adjusted by the following equations:

$$yLog_t = particlePosition + (a - b) * (k * y_t - 1)/div_{Log} \tag{2.20}$$

$$xSin_t = particlePosition + (a - b) * (g * x_t + 1)/div_{Sin} \tag{2.21}$$

The initial particles' positions are assigned in correspondence with the Logistic chaotic variables. The $\mathrm{i_{th}}$ particle is located at a position that $\mathrm{i_{th}}$ Logistic power indicates. The parameters a and b set the bounds of chaotic search space and the $\mathrm{div_{Sin}}$ & $\mathrm{div_{Log}}$ factors scale it in case of sin map. The initial particles positions are scattered in accordance to (2.22). The mean value is set at the middle of the voltage range in terms of better efficiency. Parameters k and g refer to the scaling procedure are determined experimentally.

$$InitParticlePosition = floor(middlePosition + variance * (2 * yLog - 1)) \tag{2.22}$$

During the chaotic search process (Fig. 2.10) The posPower variable is initially loaded with the current personal power before the chaotic search. Whenever the Sin map generates a position that is not better in terms of power than the temporal variable posPower (temporary position is updated in every chaotic searching loop), the temporary position is compared with the position that is generated by the logistic map. In case that the temporary position is worse or equal than pBest of the current particle the procedure is repeated. The search that is proposed offers a local and scattered search for a position that is better than the current particle's personal best position without taking account

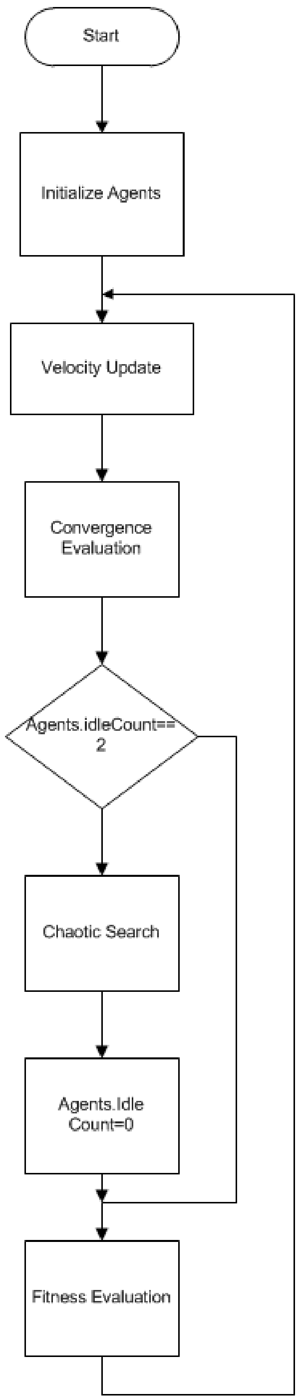

Figure 2.9: A flowchart of the Particle Swarm algorithm with embedded chaotic search.

of the current or best positions of others particles. In this hybrid PSO approach the particles remain concentrated in the searching of better positions without being lost in the power-voltage characteristic. The duty cycle accesses remain low because of the restricted number of iterations searching for a better position than the current one. The chaotic search iterations are limited by Nmax in order to prevent infinite iterations in case that no better positions are found.

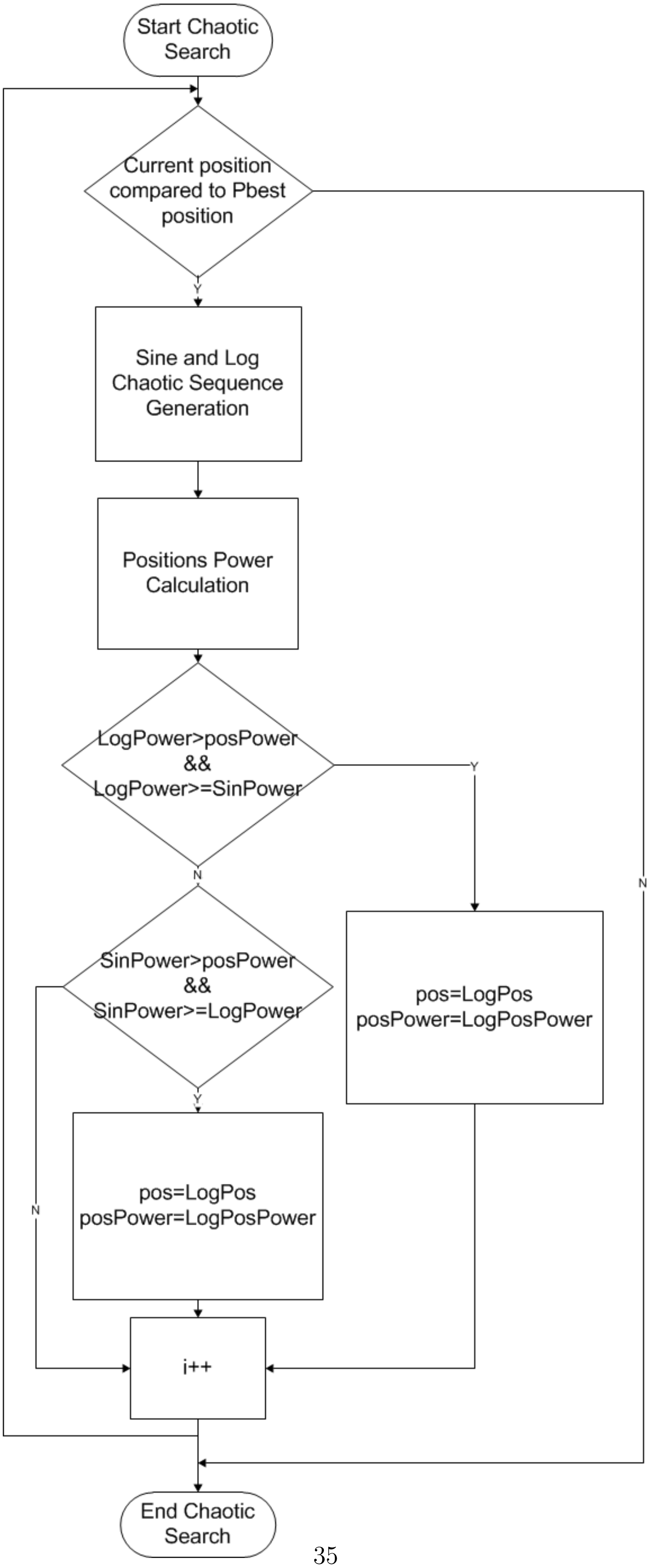

Figure 2.10: A flowchart of the Chaotic Search function

Chapter 3

System Implementation

The purpose of developing the PV system which is presented in this section, is the examination of the power-voltage and power-voltage characteristics of flexible PV module under non-uniform irradiation conditions as well as the evaluation of MPPT algorithms that can handle with the non convex shape of the resulting power-voltage characteristic.

3.1 Hardware

The hardware system requirements are the following:

- flexible PV module with bypass diodes at every cell for complete protection
- power converter that interfaces the PV module generated power and evaluates MPPT algorithms
- capability of connection to a personal computer

3.1.1 Flexible PV module

Due to the requirements of the evaluation concept, the PV module which is chosen is the model PVL-68 manufactured by Uni-Solar, is based on amorphous silicon technology. It includes eleven modules in series connection and bypass diodes in parallel with eachcell.

The characteristics of PV module under Standard Test Conditions are the following:

- Pmax: 68W
- Vmpp: 16.5V
- Impp: 4.13A
- Voc: 23.1V
- Isc: 5.1A

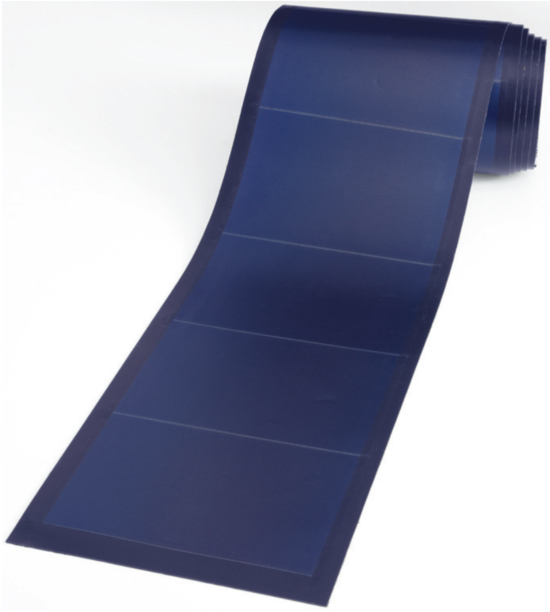

Figure 3.1: Uni-Solar PVL-68 thin-film PV module

3.1.2 Module integrated converter

The MIC topology was chosen in order to interface the PV module generated power and simultaneously reassuring continuous impedance matching between the PV module and converter through the MPPT process implemented. In order to emulate the dc link that connects the node with the central converter and reassure MPPT converter's proper operation, four lead-acid batteries of 12V each were deployed at the converter's output to stabilize the system's output voltage. System's MIC was designed to comply with PV specifications based on simple boost converter design. A buck-type switching regulator circuit has been constructed for components' power supply purposes. In order to prevent overcharging of batteries,a 30 Ohm resistor array is used in parallel connection with the converter's output.

The specifications of the MIC system which was designated are the following:

- 0-24V input voltage,
- 48V output voltage,
- input voltage sensor,
- input current sensor,
- serial port IO
- Atmel Atmega 8535 microcontroller unit

The block diagram of the MIC system which was developed is showing in Fig. ??:

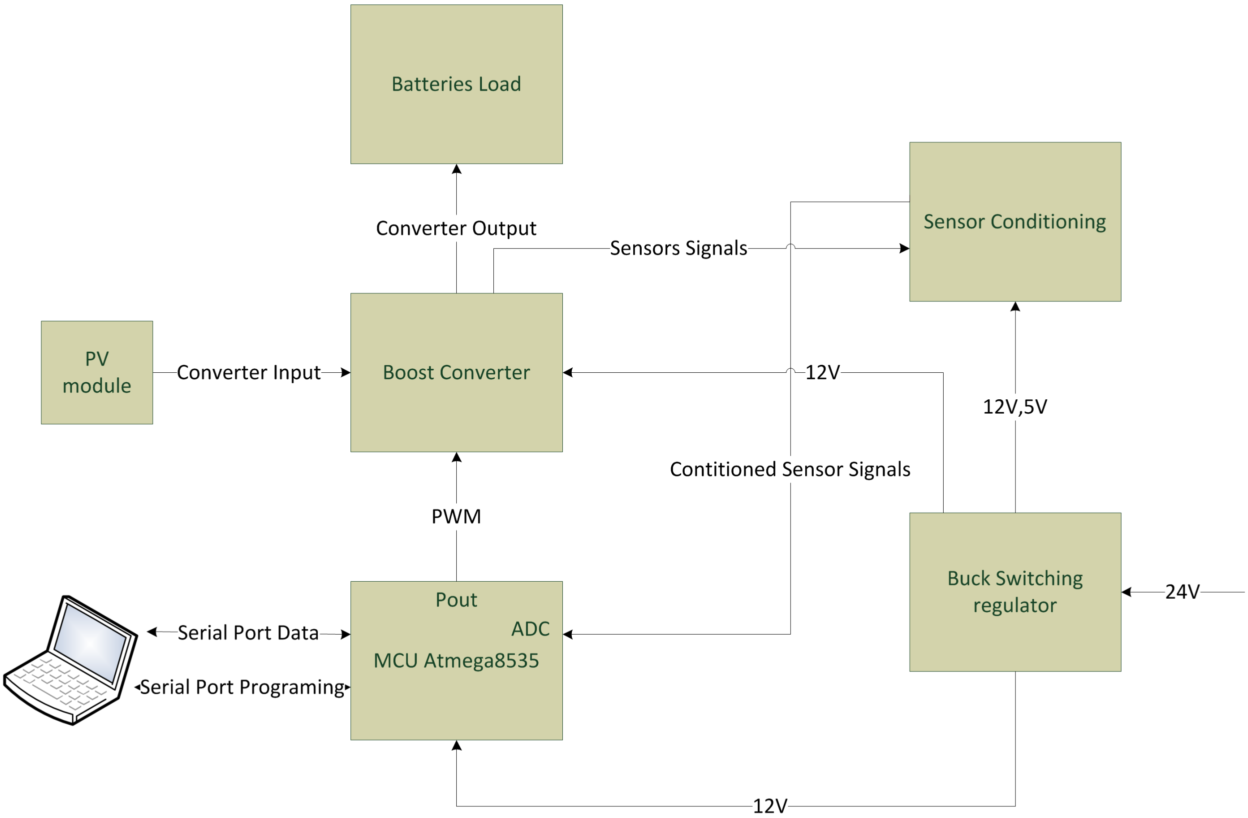

Figure 3.2: The block diagram of the MIC system.

Boost Converter Boost converter circuit was designed to interface the PV module to the battery bank and perform the MPPT operation.

Boost converter characteristics and components employed are the following:

- 39kHz operational frequency
- power mosfet IRFZ44
- mosfet driver ICL7667
- power diode MBR1060
- voltage and current sensor conditioning circuits based on the LM358 dual operational amplifier
- Hall-effect-type current transducer sensor LTSR6-NP with 3 turns wiring

Converter's coil inductance should ensure continuous switching operation over the entire duty cycle range of the MPPT procedure. Equation (3.1) refers to the average inductor current at the boundary condition between the continuous and discontinuous conduction of boost converter [25]:

$$I_L = \frac{T_s * V_o}{2L} * D(1 - D) \tag{3.1}$$

It is derived that with maximum input voltage 24V and 48V output, the boundary condition happens at the converter's duty cycle D= 50%, Ts =1/fs , and I_L average input current. In continuous conduction,the input/output voltage relation is given by:

$$\frac{V_o}{V_{in}} = \frac{1}{1 - D} \tag{3.2}$$

Assuming 39khz converter's switching frequency as well as a minimum input current of about 1.6 A from equation (3.1) is derived that in order to be in continuous conduction, the least converter's inductance should be 100uH. However, because PV module's current is tapering to zero as duty cycle goes to 50%, 160uH inductance is used to ensure continuous conduction until of about 1A input current.

Switching converters show voltage output ripple due to the power Mosfet's switching operation. Equation (3.3) [25] calculates the peak-to-peak ripple of output voltage in continuous mode of operation.

$$\delta V_0 = \frac{\delta Q}{C} = \frac{I_0 D T_s}{C} \tag{3.3}$$

Given a 2% of desired ripple at a duty cycle of 50% and an output current 500mA, from equation (3.3) it is derived that output capacitance should be 330uF.

Signal Conditioning Circuit The signal conditioning circuit manipulates the signals of the input current and voltage in a way that meets the requirements of MCU's ADC. The circuit is based on LM358 dual operational amplifier. The A operational amplifier operates as a differential amplifier by compensating the current transducer signal (2.5V-5V for positive current direction) and upscaling this to the ADC operational level (0V-5V). In case of voltage sense the B operational amplifier of IC LM358 operates as a differential amplifier that sub-quintuples the input voltage. Due to the appearance of white noise, 100nF capacitors were used for noise filtering. In order to prevent overvoltage and undervoltage of ADC input, one diode for each output constrains the maximum output voltage to 5V as well as another diode protects the ADC input from negative voltage. The voltage and current measurements accuracy is about 10 mV and 10mA, respectively. Consequently the power calculation accuracy is about 100mW. The boost and converter and signal conditioning circuit schematic is illustrated in Fig. 3.3.

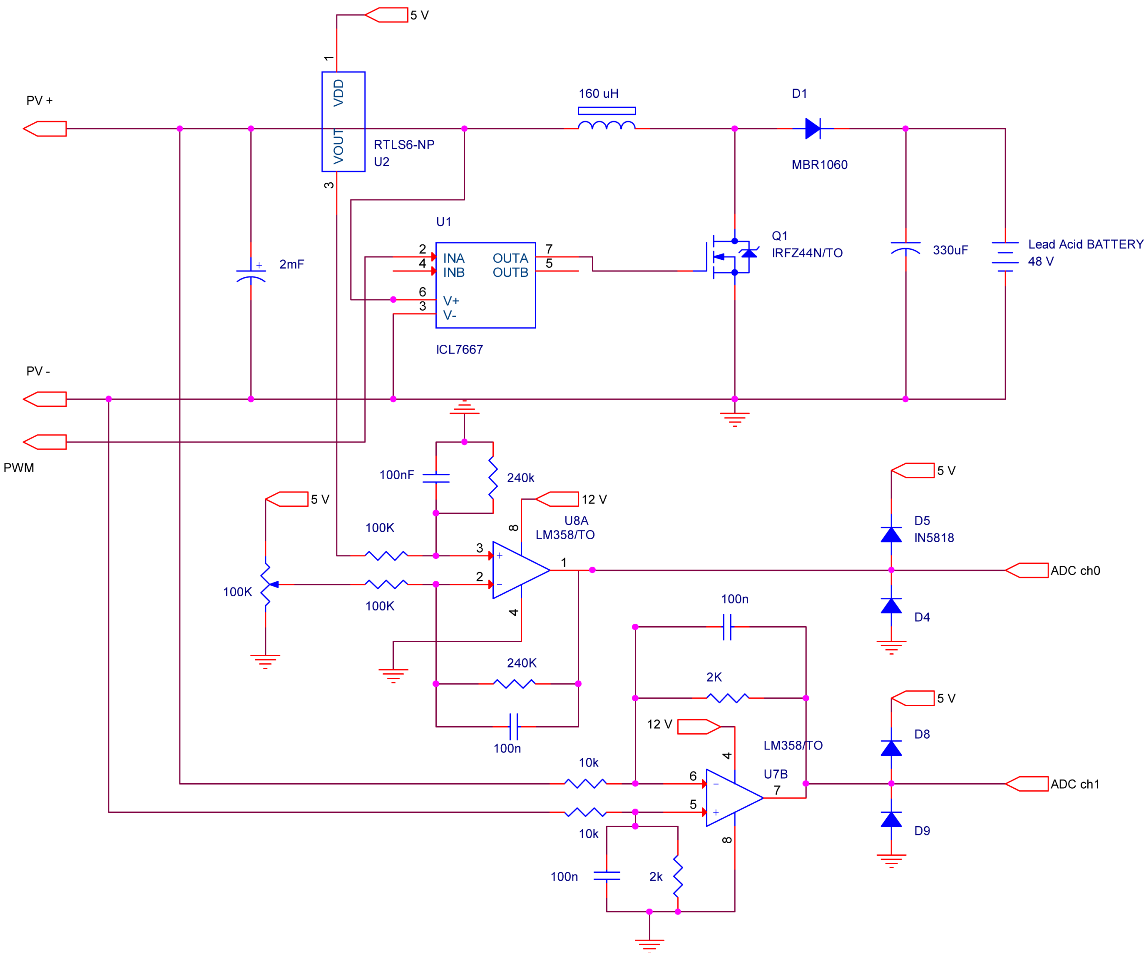

Figure 3.3: Boost converter schematic diagram.

Buck switching voltage regulator The buck switching regulator is based on the ICs LM305 and MC7805. The main circuit regulates the voltage from 24V to 12V in order to supply the LM358 and ICL7667. Linear regulator MC7805 regulates the voltage from 12V to 5V with the purpose to supply the LTSR 6-NP current transducer.Circuit schematic diagram is shown in Fig. 3.4

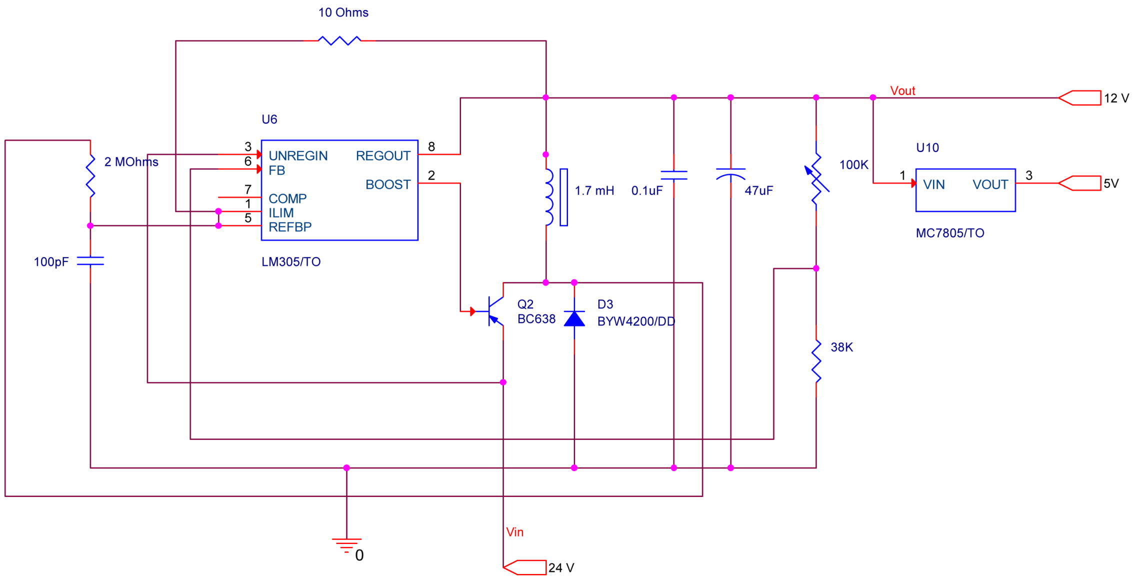

Figure 3.4: Buck switching regulator circuit.

Atmega 8535 The microcontroller unit (MCU) Atmega 8535 supported by the development card STK500 was used. MCU's system clock was supplied by external crystal,clocked at 10 MHZ. MCU's peripherals that were used are the following:

- 2 ADC channels of 10bit resolution,
- PWM signal generation of 8 bit resolution,
- External System clock support,
- External ADC reference voltage AREF supplied by the STK500 board

3.2 Software

The MCU programming as well as the setup of STK500 was achieved by programming suite AVR Studio 5.1.

3.2.1 Switching frequency generation

Converter's switching frequency is generated by PWM signal.

PWM signal Registers:

- OCR2 pwm's duty cycle register
- TCCR2
  BIT 7 : FOC0 Force Output Compare [Not used]
  BIT 6 : WGM20 Wave form generation mode [SET to 1]
  BIT 5 : COM21 Compare Output Mode [SET to 1]
  BIT 4 : COM20 Compare Output Mode [SET to 0]
  BIT 3 : WGM21 Wave form generation mode [SET to 1]
  BIT 2 : CS22 Clock Select [SET to 0]
  BIT 1 : CS21 Clock Select [SET to 0]
  BIT 0 : CS20 Clock Select [SET to 1]

The MCU Atmega 8535 has the ability of either 8-bit or 10-bit PWM generation and in the developed system an 8bit resolution was used. In addition due to the fact that the converter's effective duty cycle was higher than 50%, OCR2 register's values was restricted between 128 and 255.The PWM signal's frequency was set at 39khz.

3.2.2 USART connection

The MCU 8535 has the ability of USART connection.The development kit STK 500 provides a dual USART connection for both communication and programming. The communication is achieved using a terminal console program through the PC serial port.

Setup Baud rate was set at 9600 symbols per second.
Registers:

- UBRRH Set Uart baud rate High Register
- UBRRL Set Uart baud rate Low Register
- UCSRC USART Control and Status Register C
  BIT 7: URSEL Register Select [SET to 1]
  BIT 1: UCSZ0 6-bit Character Size [SET to 1]
- UCSRB USART Control and Status Register B
  BIT 4: RXEN Receiver Enable [SET to 1]
  BIT 3: TXEN Transmitter Enable [SET to 1]

USART interface functions For better USART's interface, global functions were created to push float, integers numbers and arrays of characters into USART connection.

- USART_Transmit() Put character into USART
- USART_Receive() Get character from USART
- USART_Flush() Flush USART
- USARTWriteString() Send a string through USART
- float2String() Convert float number to string
- int2String() Convert integer to string
- printInt() Print integer number
- printFloat() Print float number
- printString() Print String

3.2.3 Sensor Interface

ADC setup Registers:

- ADMUX ADC Multiplexer and selection register
- ADCSRA ADC control and status register
  BIT 7: ADEN ADC enable [SET to 1]
  BIT 6: ADSC ADC start conversion [SET to 1]
  BIT 5: ADIE ADC interrupt enable [SET to 1]
  BIT 2: ADPS2 ADC Prescaler Division Clock factor 64 [SET to 1]
  BIT 1: ADPS1 ADC Prescaler Division Clock factor 64 [SET to 1]
- ADC Selected ADC channel's data

Calibration Due to the 10 bit ADC resolution and the use of a 5V reference voltage the outputs are scaled according to equation (3.4):

$$InputSignalVoltage = ADCData * 5/1024 \tag{3.4}$$

Then, the average value is estimated by taking into account 50 successive values within 1ms interval. The least squares algorithm was used to estimate the sensor input-output characteristic, translating equations (3.5 and 3.6) into input current and voltage units. The LS algorithm calculates the best fit line according to voltage and current observations equations (3.6 & 3.5).

$$CurrentSensorValue = 1.3755 * AverageInputSignalHall + 0.0203 \tag{3.5}$$

$$VoltageSensorValue = 4.9729 * AverageInputSignalVoltage + 0.0794; \tag{3.6}$$

Figures 3.5 and 3.6 depict the best fit lines for the voltage and hall sensor respectively, which were derived from the L.S. algorithm according to the measurements at various operating points.

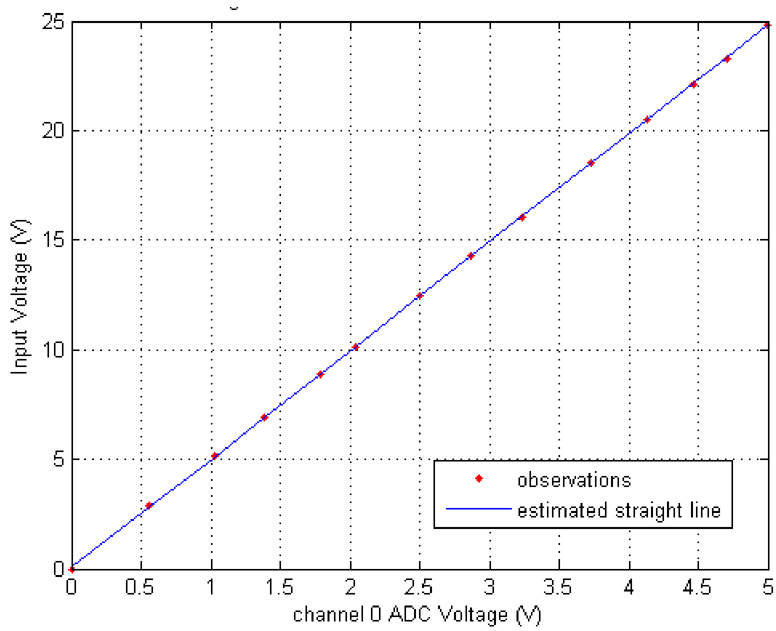

Figure 3.5: Least Squares best fit line of the Input Voltage Sensor

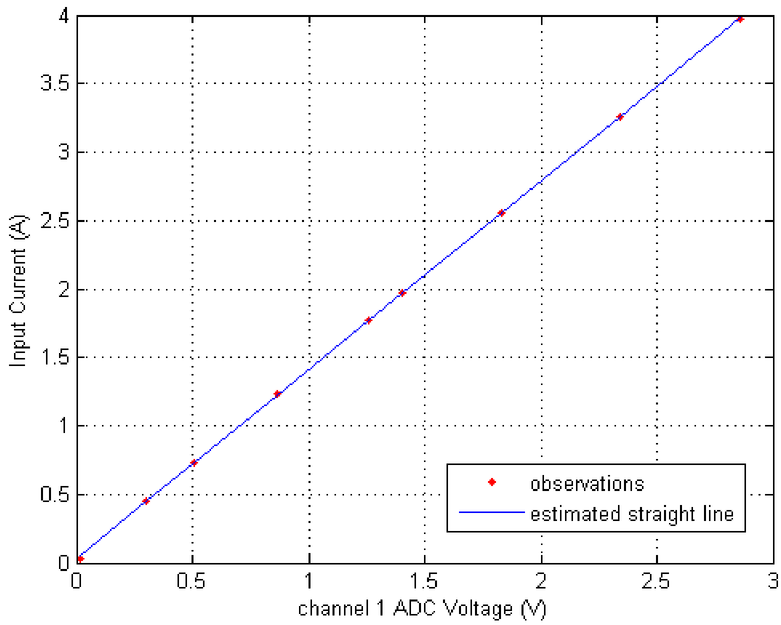

Figure 3.6: Least Squares best fit line of the Hall Sensor

3.3 System Evaluation

The module integrated converter which was designed and constructed was utilized to evaluate the operation of the flexible photovoltaic module under several environmental conditions and different bend shapes. Four MPPT algotithms were evaluated under non-uniform irradiation conditions: Particle Swarm Optimization, Chaotic Particle Swarm Optimization, Differential Evolution and Chaotic algorithm. Every MPPT algorithm was compared with the results obtained using exhaustive search procedure.

In order to simulate the bend shapes that the flexible PV module can form ,an appropriate base was constructed according to the arch shape model that was described in paragraph 1.1.2.

3.3.1 Power-Voltage & Current-Voltage characteristics under non uniform irradiation

The measurements took place all over the day simulating at all possible installation shapes. One measurement per hour from 9 p.m. to 6 a.m. was conducted for all bend shapes with center angles from 0^o to 180^o with 30 degrees step. The power-voltage as well as the current-voltage characteristics of the flexible PV module were measured at each position.

power-voltage characteristics under non uniform conditions Figures 3.7-3.20 depict power-voltage and current-voltage characteristics for every center angle all over the day including information of the corresponding solar irradiation and environment temperature conditions.

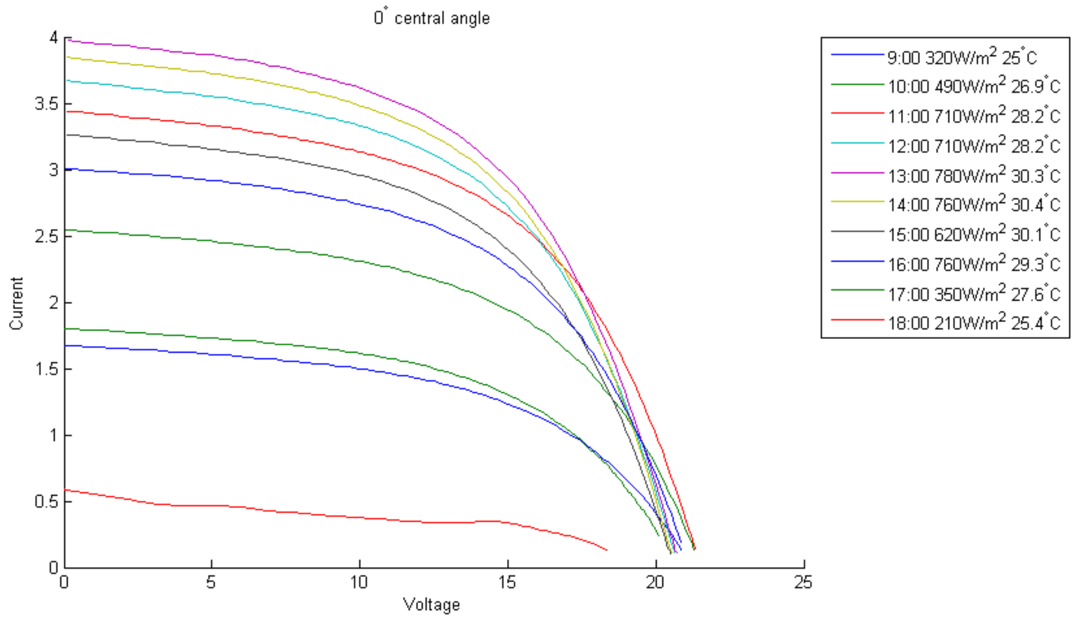

Figure 3.7: Current-voltage characteristics with central angle $\theta = 0^o$

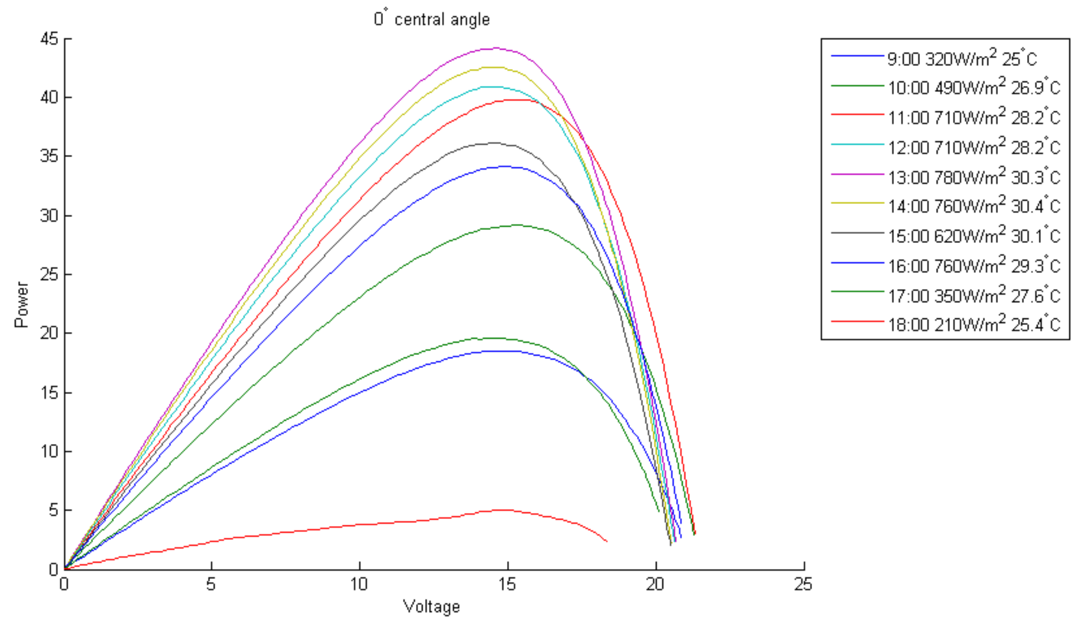

Figure 3.8: Power-voltage characteristics with central angle $\theta = 0^o$

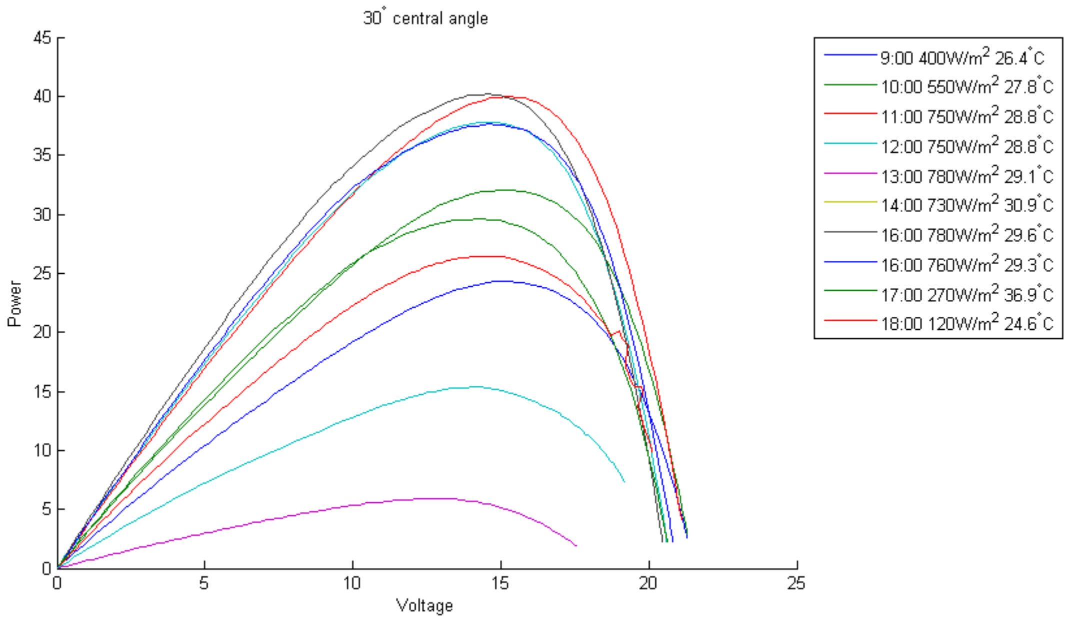

Figure 3.9: Current-voltage characteristics with central angle θ =30°

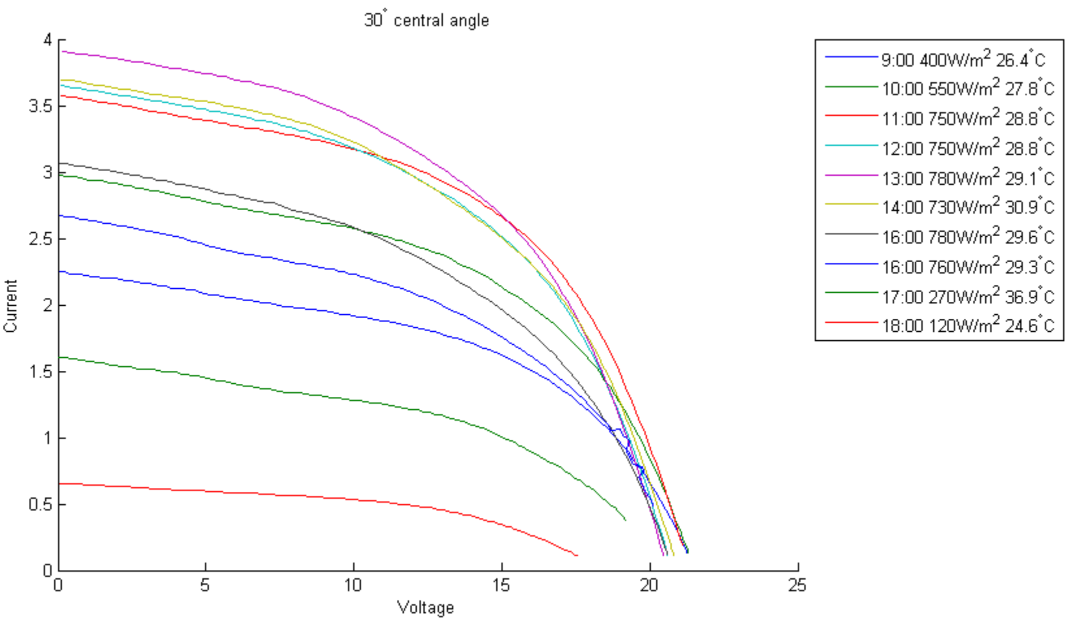

Figure 3.10: Power-voltage characteristics with central angle θ =30°

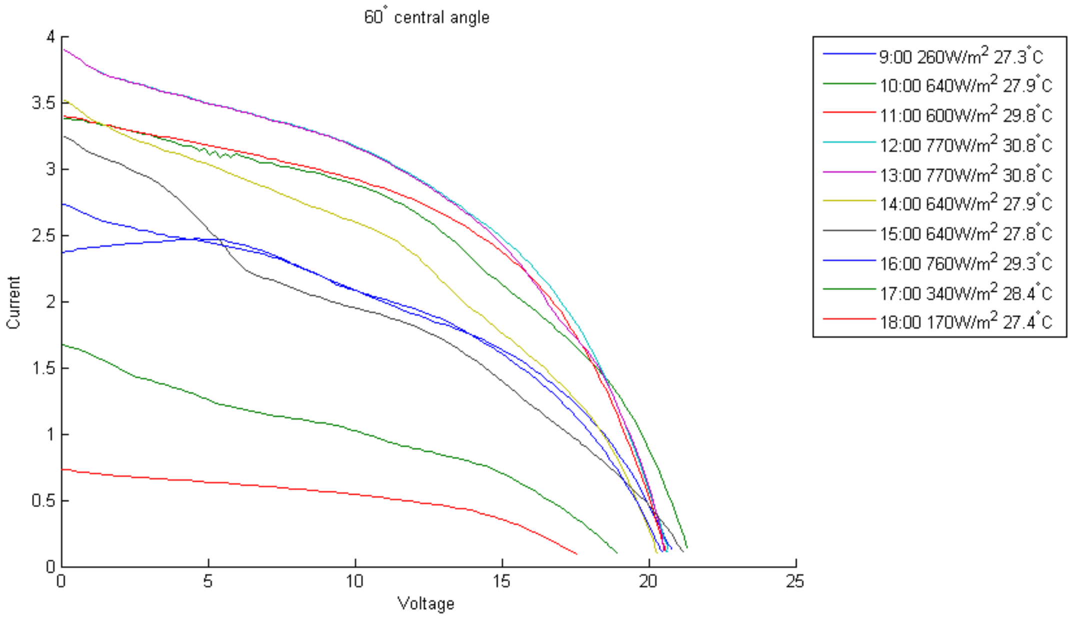

Figure 3.11: Current-voltage characteristics with central angle θ =60°

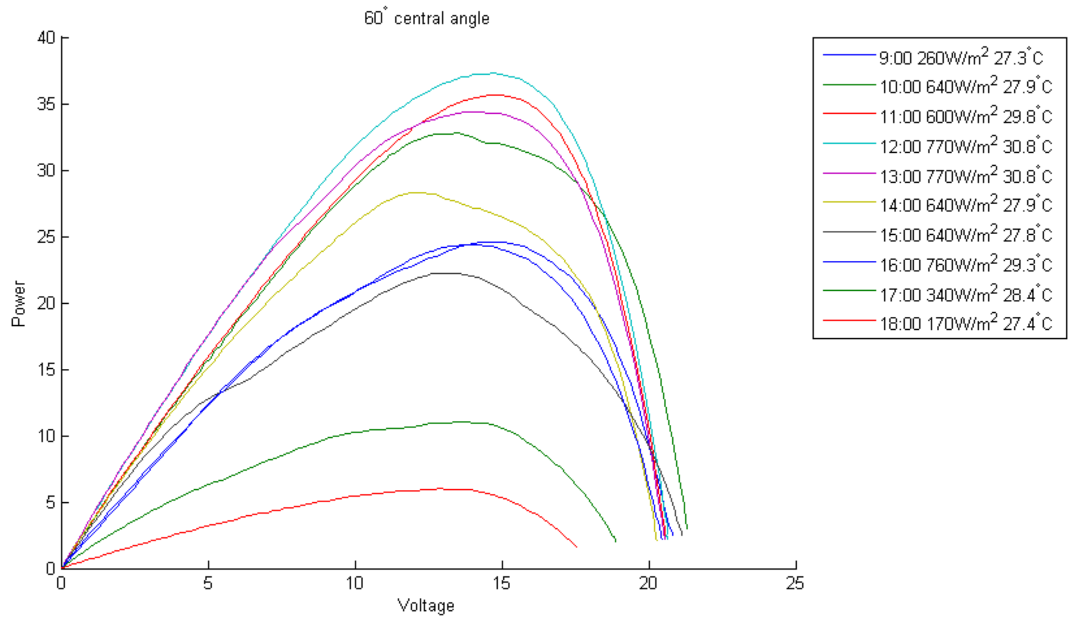

Figure 3.12: Power-voltage characteristics with central angle θ =60°

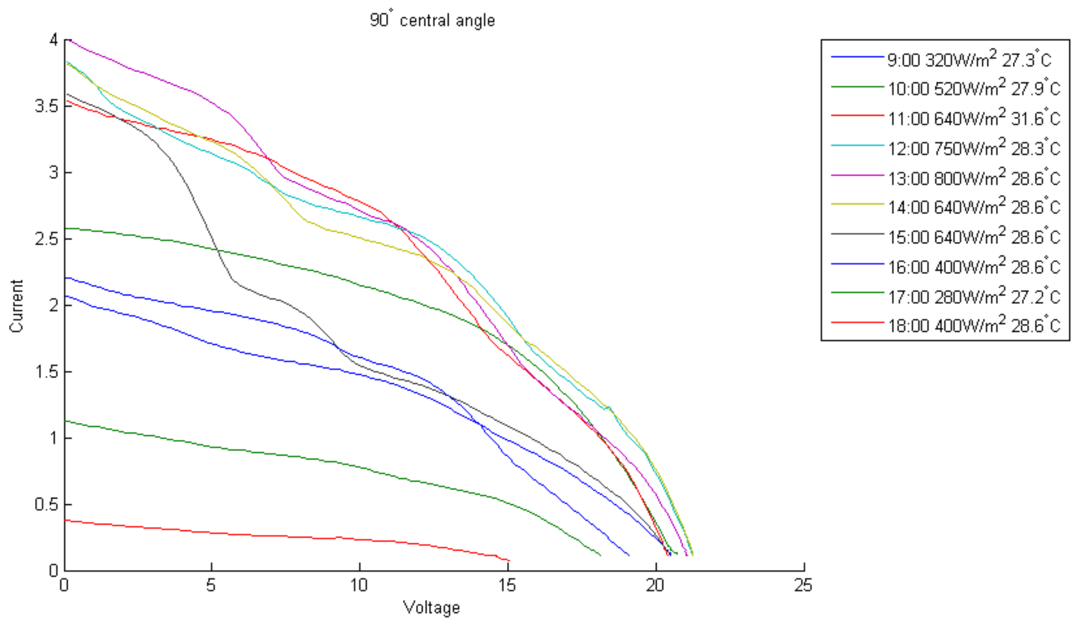

Figure 3.13: Current-voltage characteristics with central angle θ =90°

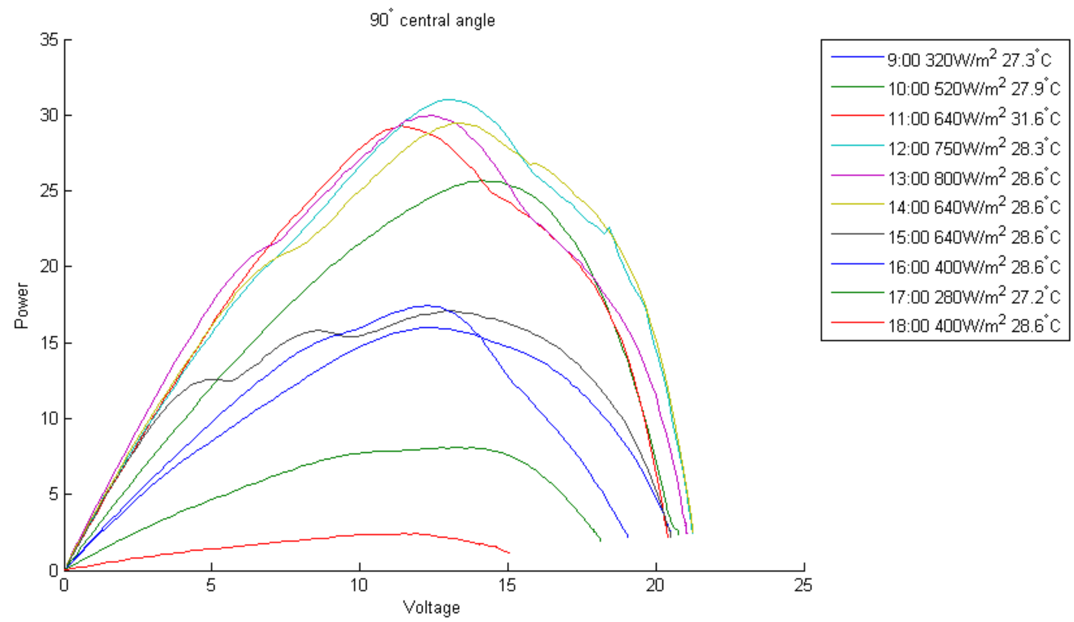

Figure 3.14: Power-voltage characteristics with central angle θ =90°

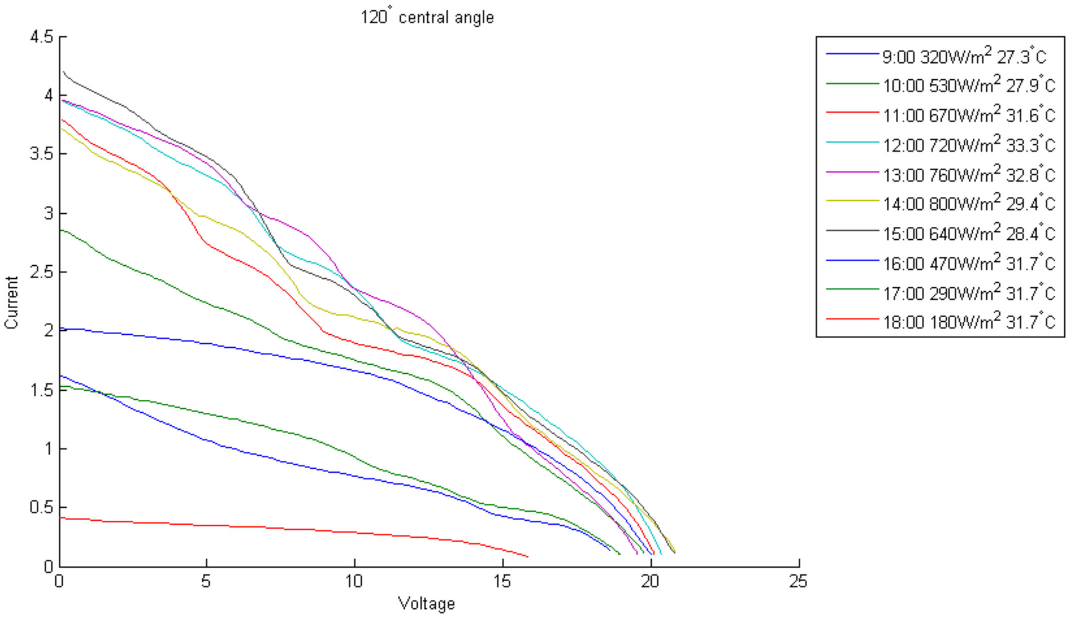

Figure 3.15: Current-voltage characteristics with central angle θ =120°

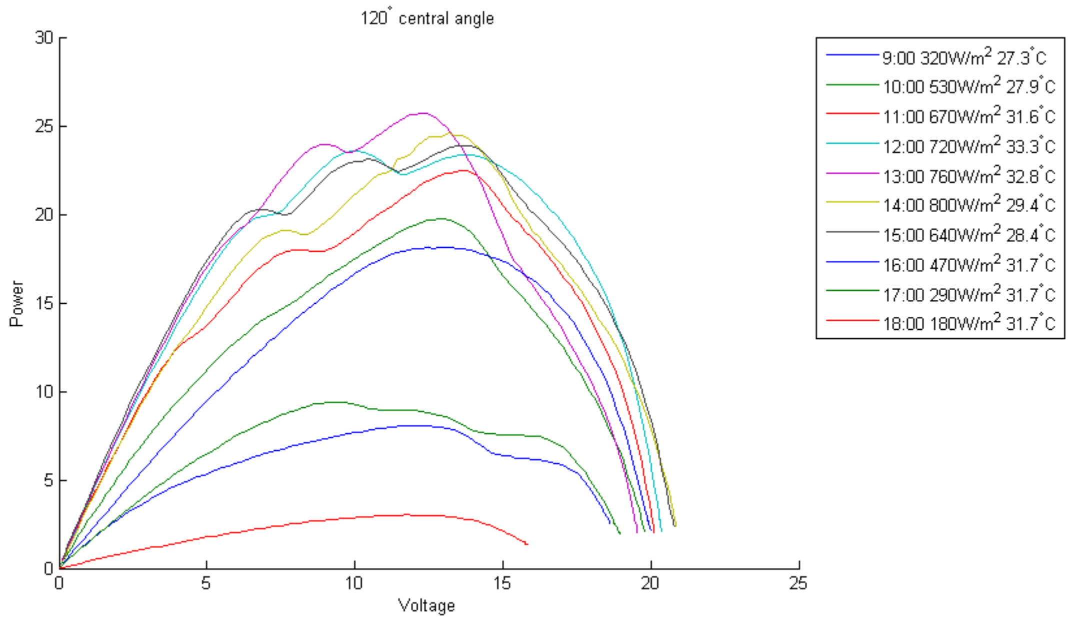

Figure 3.16: Power-voltage characteristics with central angle θ =120°

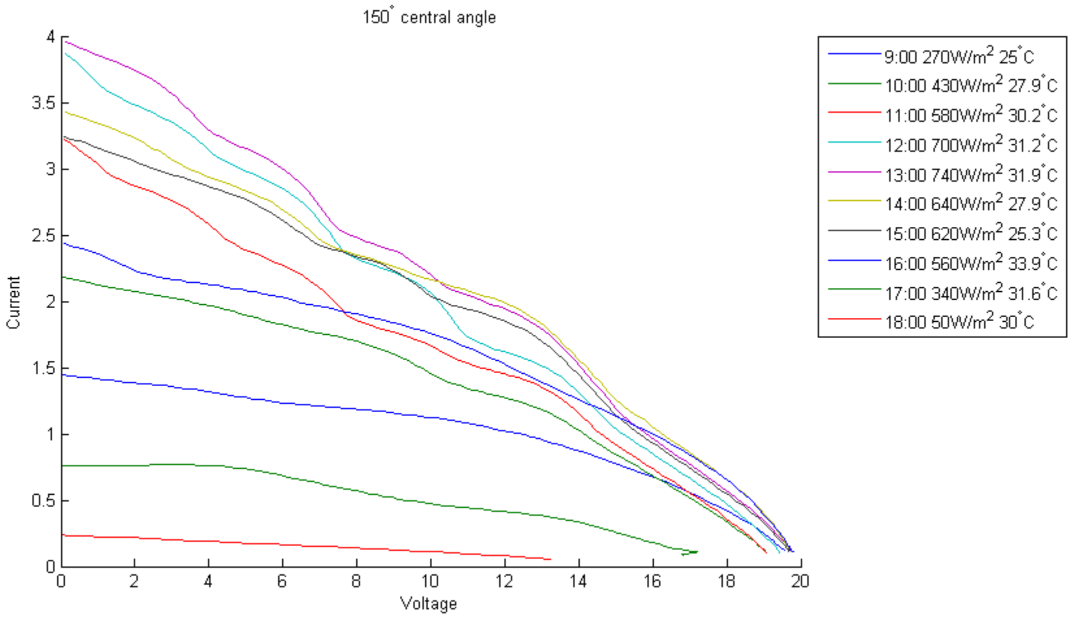

Figure 3.17: Current-voltage characteristics with central angle θ =150°

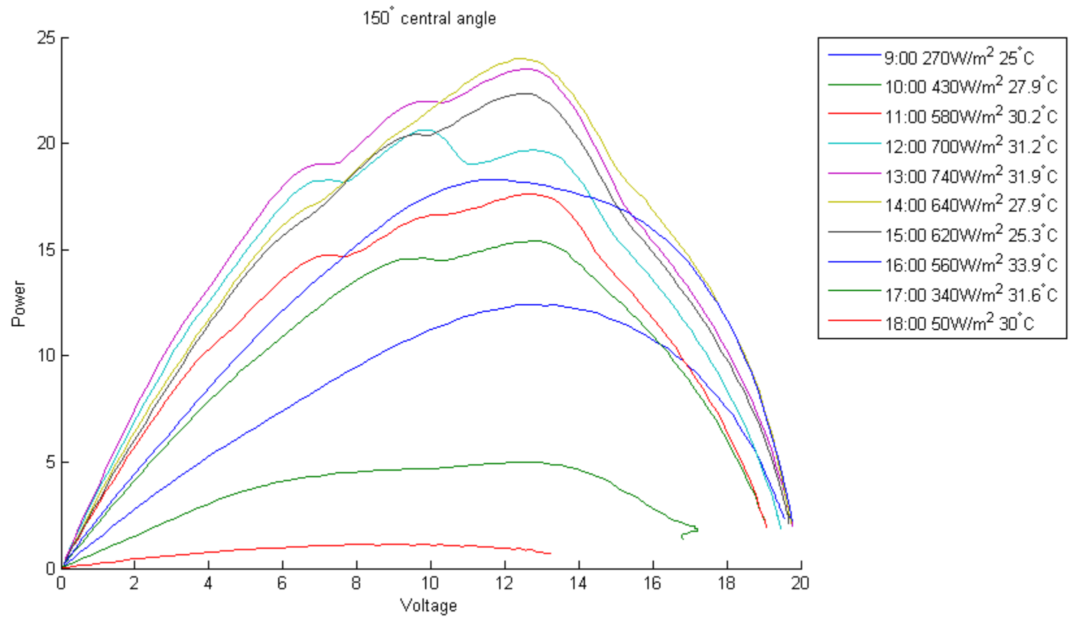

Figure 3.18: Power-voltage characteristics with central angle θ =150°

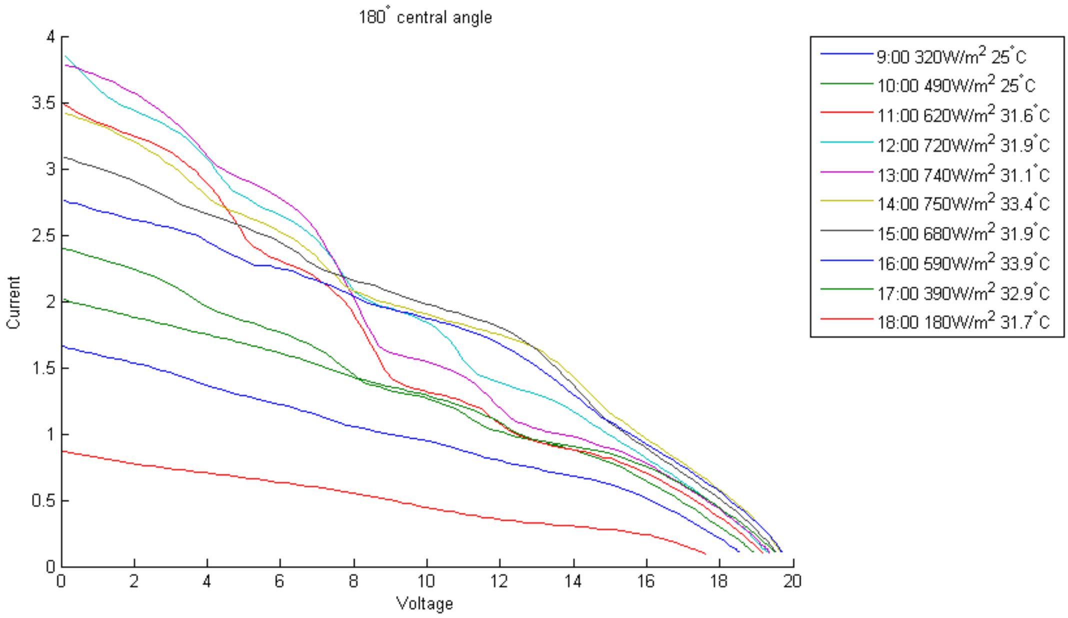

Figure 3.19: Current-voltage characteristics with central angle θ =180°

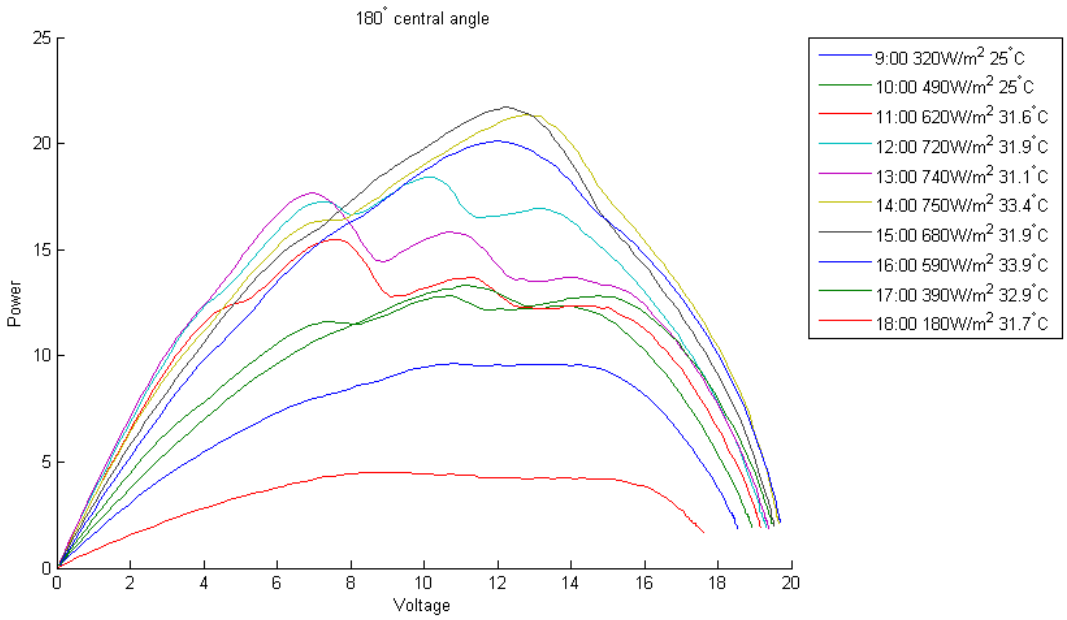

Figure 3.20: Power-voltage characteristics with central angle θ =180°

The characteristics reveal the existence of several local maximum peaks for arc with center angles higher than 60 degrees. In case that the center angle is less or equal than 30 degrees the power-voltage characteristic is convex. However the maximum power point is about 5 watt lower when the center angle augments from 0 ^{o} to 30^{o} degrees. power-voltage characteristics for higher than 60^{o} center angle reveal that the number of the local peaks varies from an hour to another as the phenomenon of non-uniform irradiation across the PV module takes place more noticeable. For example Figs. 3.16 depicts that the local peaks at 12:00 are more than the peaks at 16:00 for the same bend shape of a given center angle. Furthermore as shown from the Fig. 3.20 is clearly illustrated that the operation point's position is changing along the day. As a conclusion, it seems that the sun's position affects the PV module characteristics as the solar angle in combination with the bend shape of the PV module, results in a different incident irradiation on each solar cell.

3.3.2 MPPT Algorithms Evaluation

The number of generations that each MPPT algorithm is executed was defined in order to ensure convergence at straight position with minimum steps. However because PSO as well as the Differential Evolution algorithm execute random procedures to initialize and direct the particles the actual number of steps for convergence is variable. With a view to define an ideal number of generations that ensure convergence at zero bend position the algorithms were executed several times. Every algorithm's result is compared with the global maximum point that is calculated by exhaustive searching. Thus the convergence of every algorithm is evaluated by the distance from the global maximum power. The upper barrier of steps that every method is compared with is 128 steps (The number of steps that the exhaustive search executes). The algorithms' evaluation took place all over the day from 9 p.m to 6 a.m.

The choice of the step as a quantity of measurement of the convergence penalty refers to the changes of the converter's Duty Cycle. In order to evaluate the algorithms this measure was chosen in contrary to the quantity of time because, the duration of each step varies according to the converter's implementation.Thus, the time elapsed to convergence cannot be an objective quantity of measurement.

Algorithms' setup

Particle Swarm Optimization Parameters of PSO method were set to assure an efficient operation of the algorithm. Due to the fact that the characteristics of the PV module under non-uniform irradiation conditions had not been known before, the fine tuning of parameters wasn't feasible, however a setting approach was based on simulation as well as the power-voltage characteristic of the PV module on the horizontal shape.Table 3.1 refers to the basic parameters that the PSO algorithm was set.The PSO algorithm was executed for 2,3,4,5,6 total number of agents.

Chaotic Particle Swarm Optimization Hybrid Chaotic PSO MPPT method as described in paragraph 2.3.3 utilize the same with basic parameters with the PSO algorithm for comparison purposes. The chaos generations in case of particle stagnancy were set to 3 in order to retain balance between the additional steps that the chaotic pseudo-random procedure executes and the searching ability of higher personal best position. The ideal scattering parameters that refer to equations 2.20 and 2.21 were defined after experimentation.Table 3.2 refer to the extra parameters that CPSO uses.The CPSO algorithm was executed for 2,3,4,5,6 total number of agents.The CPSO version that was tested initialize the particles with chaotic sequences that are centralized at the edge of characteristics.

Table 3.1: PSO parameters

w	0.8
c1	1.1
c2	1.3
dV	0.49
dP	0.50
x	0.8
generations	15

Table 3.2: CPSO parameters

div_{Log}	2
div_{Sin}	4
k	1.29
g	0.5
generations	10
Nmax	4
a	255
b	128

Differential Evolution Differential Evolution Method was executed for 10 generations, for 4, 6, 8 total populations of genes.

Chaotic Partial Search Partial search as described in paragraph 2.3.3 terminates in case that its convergence condition is true. The method was executed for 5, 6, 7 and 8 total population numbers.

Results

The algorithms were evaluated under non-uniform irradiation conditions along the day. Tables 3.5- contain the entire set of algorithms' results on various settings for each hour. Every record consists of the distance of the resulting convergent point to the global power point accompanied with the number of steps (i.e. evaluations of the power-voltage characteristic) required to converge. Negative distance values indicate an offset from the global best point to the point of algorithm's convergence. Positive values refer to unpredictable power increase during the algorithm's execution as well as to the measurement error of about 100mW. It is defined that in case of higher than offset 1% of the nominal power of PV module then the result cannot be evaluated as it cannot be assessed that the algorithm converged to the global optimum point or not. Table 3.3 depicts the maximum and minimum offsets of the MPPT methods. Tables 3.15-3.24 refer to the percentage of the difference of steps between of CPSO and the different setups of each method. Table 3.4 indicates the minimum and maximum percentages of the difference of steps between the CPSO and the others algorithms.

	max	min
CPSO	-2.742	2.994
PSO	-8.925	3.499
DE	-8.986	2.246
Chaotic	-7.14	2.974

Table 3.3: Minimum and maximum deviation from the global best for each algorithm.

	PSO	DE	Chaotic
min	0.0	2.1	0.0
max	45.5	736.4	263.6

Table 3.4: Minimum and maximum percentages of the difference between the steps of CPSO and the others algorithms.

Table 3.5: The results of each MPPT algorithm at 9:00.

method	θ =0°	steps	θ =30°	steps	θ =60°	steps	θ =60°	steps	θ =120°	steps	θ =150°	steps	θ =180°	steps
CPSO														
2 agents	-0.9020	26	0.1890	22	0.1950	22	2.8020	22	0.3470	22	0.0230	28	0.0440	22
3 agents	-0.7800	39	0.2390	35	0.1250	41	2.8300	41	0.4030	35	0.1490	41	0.1920	35
4 agents	-0.6770	60	0.2780	48	0.1760	48	2.1910	62	0.3860	48	0.1370	48	0.2240	48
5 agents	-0.4860	59	0.3310	59	0.0780	59	2.7920	59	0.4790	59	0.2310	63	0.2100	61
6 agents	-0.3060	78	0.4340	82	0	84	2.9940	78	0.5370	78	0.3080	78	0.1690	82
PSO														
2 agents	-2.1190	32	-3.1220	32	-2.9840	32	-0.2820	32	-0.0120	32	0.0560	32	-0.3560	32
3 agents	0.1340	48	0.2590	48	0.1530	48	0.0260	48	0.1200	48	0.1080	48	-0.3230	48
4 agents	0.2430	64	0.4460	64	0.1710	64	0.2260	64	0.1660	64	0.1530	64	-0.3020	64
5 agents	0.3810	80	0.5200	80	-0.9830	80	0.3420	80	0.2950	80	0.1590	80	-0.2340	80
6 agents	0.6250	96	0.8210	96	-24370	96	0.4690	96	0.4160	96	-8.9250	96	-0.1520	96
DE														
4 genes	0.0930	69	-0.1870	69	2.2460	92	-3.0380	92	0.1690	92	0.0590	92	0.0980	92
6 genes	0.5060	92	0.5090	92	-6.2000	138	-3.1630	138	0.3350	138	-0.2840	138	-0.1330	138
8 genes	0.6710	115	0.7440	115	-4.7970	184	-2.7630	184	0.4430	184	-2.1260	184	-0.0180	184
Chaotic														
5 agents	-7.1400	50	0.1820	50	-0.0010	50	0.2390	50	0.5050	50	-2.1920	50	-0.4650	50
6 agents	-6.7810	60	0.1870	60	0.0300	60	0.2390	60	0.5710	60	-0.1190	60	-0.3890	60
7 agents	-6.7510	70	0.2050	70	0.0910	70	0.2740	70	0.6330	70	-0.0400	70	-0.3440	70
8 agents	-6.7190	80	0.2670	80	0.0440	80	0.3160	80	0.7000	80	-0.2650	80	-0.3550	80

Table 3.6: The results of each MPPT algorithm at 10:00.

method	θ =0º	steps	θ =30º	steps	θ =60º	steps	θ =60º	steps	θ =120º	steps	θ =150º	steps	θ =180º	steps
CPSO														
2 agents	-0.9020	26	0.1890	22	0.1680	22	0.2170	22	-0.0130	22	-2.6950	22	0.1390	28
3 agents	-0.7800	39	0.2390	35	0.1980	35	0.1070	41	-0.1380	45	-2.7420	35	0.1400	41
4 agents	-0.6770	60	0.2780	48	0.1750	50	0.1990	56	-0.1000	54	0.1790	56	0.1700	50
5 agents	-0.4860	59	0.3310	59	0.2920	57	0.2440	57	-0.0140	61	0.2360	59	0.2510	61
6 agents	-0.3060	78	0.4340	82	0.3240	74	0.0510	84	-0.1190	66	0.2870	82	0.2600	86
PSO														
2 agents	-2.1190	32	-3.1220	32	-0.0950	32	-1.6160	32	-0.1920	32	0.0830	32	0.0800	32
3 agents	0.1340	48	0.2590	48	-0.0050	48	0.2310	48	0.1390	48	0.1180	48	0.0770	48
4 agents	0.2430	64	0.4460	64	-0.0240	64	0.2010	64	0.1730	64	0.1240	64	0.0970	64
5 agents	0.3810	80	0.5200	80	0.1540	80	0.0880	80	0.3510	80	-8.1880	80	0.2090	80
6 agents	0.6250	96	0.8210	96	0.3480	96	-0.2090	96	0.3390	96	0.3260	96	0.2600	96
DE														
4 genes	0.0930	69	-0.1870	69	-0.2580	69	-0.3980	92	-0.0720	92	-0.3690	92	1.0540	92
6 genes	0.5060	92	0.5090	92	-0.5990	92	-0.7420	138	-0.5890	138	-0.3190	138	1.0990	138
8 genes	0.6710	115	0.7440	115	-2.5710	115	-0.3550	184	0.2970	184	-3.1470	184	0.2230	184
Chaotic														
5 agents	-7.1400	50	0.1820	50	0.1410	50	-0.1640	50	-0.1980	50	2.0570	50	0.0640	50
6 agents	-6.7810	60	0.1870	60	0.1990	60	0.2750	60	-0.0660	60	2.9120	60	0.0050	60
7 agents	-6.7510	70	0.2050	70	-0.2300	70	-0.3000	70	-0.1030	70	2.9740	70	0.1700	70
8 agents	-6.7190	80	0.2670	80	0.3450	80	-0.3040	80	-0.0860	80	2.9710	80	0.2240	80

Table 3.7: The results of each MPPT algorithm at 11:00.

method	θ =0º	steps	θ =30º	steps	θ =60º	steps	θ =60º	steps	θ =120º	steps	θ =150º	steps	θ =180º	steps
CPSO														
2 agents	0.3500	22	-0.1150	22	0.0020	22	0.0020	22	0.1520	22	-0.0560	24	0.1190	22
3 agents	0.4050	41	-0.0490	41	0.0180	35	0.0180	35	0.3180	35	-0.0300	39	0.0920	41
4 agents	0.3210	50	-0.0120	48	0.0780	48	0.0780	48	0.2860	48	0.0430	50	0.1210	48
5 agents	0.5260	57	0.0430	63	0.0480	71	0.0480	71	0.3110	59	0.0610	59	0.1780	61
6 agents	0.6010	80	0.1210	78	0.1410	80	0.1410	80	0.4070	78	0.0130	76	0.2390	76
PSO														
2 agents	0.0390	32	-5.7950	32	-1.4730	32	-11660	32	-1.0000	32	-0.1640	32	-0.1090	32
3 agents	0.1610	48	-0.1530	48	0.0590	48	0.0600	48	-0.2360	48	0.0710	48	-0.0220	48
4 agents	0.2630	64	-0.0550	64	0.1180	64	0.0630	64	-3.3110	64	0.1220	64	-0.0290	64
5 agents	0.3580	80	-0.1250	80	0.3090	80	0.2130	80	0.0750	80	0.1040	80	0.0480	80
6 agents	0.3780	96	0.0410	96	0.3880	96	0.3360	96	0.0070	96	0.1810	96	0.1820	96
DE														
4 genes	-1.6990	69	-2.4550	69	-0.1230	92	-0.1100	92	0.1650	92	-0.7060	92	-0.1200	92
6 genes	-0.1310	92	-0.2520	92	-0.6140	138	0.3010	138	-2.8690	138	-0.8490	138	-0.4460	138
8 genes	0.2730	115	0.1160	115	0.3060	184	-2.9760	184	0.1610	184	-7.3180	184	0.1300	184
Chaotic														
5 agents	0.3330	50	-0.7430	50	-0.1890	50	0.1390	50	-0.0840	50	-0.7480	50	-3.2290	50
6 agents	0.5410	60	-0.1380	60	-0.1890	60	-0.6190	60	0.0240	60	0.1500	60	0.1110	60
7 agents	0.5410	70	0.2550	70	-0.0360	70	0.2240	70	0.0640	70	-0.0960	70	0.1600	70
8 agents	0.4640	80	0.2150	80	-0.0670	80	-0.3930	80	0.0750	80	-0.1800	80	-0.0650	80

Table 3.8: The results of each MPPT algorithm at 12:00.

method	θ =0º	steps	θ =30º	steps	θ =60º	steps	θ =60º	steps	θ =120º	steps	θ =150º	steps	θ =180º	steps
CPSO														
2 agents	0.3370	22	0.0750	22	-0.1070	22	-0.1070	22	0.0020	22	-0.1700	28	-0.6470	28
3 agents	0.3890	35	0.1060	37	-0.1850	41	-0.1850	41	-0.1080	41	-0.0620	39	-0.6380	41
4 agents	0.3250	50	0.1200	56	-0.0950	48	-0.0950	48	-0.1860	54	-0.0960	50	0.1270	50
5 agents	0.2430	57	0.2250	57	-0.0310	63	-0.0310	63	0.1880	63	-0.0690	59	0.2080	59
6 agents	0.3840	80	0.2720	88	-0.0420	80	-0.0420	80	0.4560	80	-0.0410	76	0.2250	84
PSO														
2 agents	-1.3670	32	-1.0230	32	0.3910	32	0.3910	32	-0.0140	32	-0.0750	32	0.1140	32
3 agents	-0.2140	48	-0.0560	48	0.4380	48	0.4380	48	-0.0480	48	0.0660	48	-1.7280	48
4 agents	-0.4650	64	-0.0300	64	0.7490	64	0.7490	64	-0.0240	64	0.0290	64	0.0070	64
5 agents	-0.2070	80	0.2130	80	0.6210	80	0.6210	80	0.0960	80	0.1000	80	-0.6150	80
6 agents	-0.0410	96	0.2860	96	0.5470	96	0.5470	96	0.2220	96	0.1670	96	-7.9220	96
DE														
4 genes	-0.3210	92	-0.1340	92	0.1020	92	0.1020	92	-0.1800	92	0.0120	92	-0.0500	92
6 genes	-6.2820	138	-0.0610	138	-0.5800	138	-0.5800	138	0.0680	138	-0.9390	138	0.0740	138
8 genes	0.3050	184	0.1250	184	0.1730	184	0.1730	184	0.1950	184	-0.6490	184	-1.1460	184
Chaotic														
5 agents	-2.0020	50	0.1000	50	-5.4130	50	-1.3580	50	-0.6540	40	0.0080	50	-0.3380	50
6 agents	0.2890	60	0.0810	60	-0.0710	60	-0.0170	60	0.1080	60	0.0450	60	-0.2880	60
7 agents	0.2220	70	0.2150	70	-0.0710	70	0.1250	70	0.1250	70	0.1080	70	-0.2590	70
8 agents	0.3400	80	0.3160	80	-1.0390	80	0.0190	80	-0.0330	80	0.1070	80	-0.2840	80

Table 3.9: The results of each MPPT algorithm at 13:00.

method	θ =0º	steps	θ =30º	steps	θ =60º	steps	θ =60º	steps	θ =120º	steps	θ =150º	steps	θ =180º	steps
CPSO														
2 agents	0.0080	22	0.2900	22	0.1650	22	0.1150	22	-0.0910	22	0.0890	22	-0.0370	24
3 agents	-0.0790	41	0.1450	41	0.2690	35	0.1520	35	-0.0590	39	0.3010	41	0.1450	37
4 agents	-0.1200	50	0.0960	54	0.2230	48	0.0720	48	-0.1620	50	0.2330	44	0.3360	60
5 agents	-0.0020	57	0.4180	57	0.3750	63	0.1470	57	-0.1110	59	0.2970	59	0.2860	61
6 agents	0.1640	82	0.3610	86	0.2230	82	0.1080	78	-0.2170	84	1.3430	72	0.3120	78
PSO														
2 agents	-1.4290	32	-1.2100	32	-0.5440	32	-0.4340	32	-0.1860	32	-0.1850	32	0.1600	32
3 agents	-0.5170	48	-0.1070	48	0.2150	48	0.1440	48	0.0480	48	-0.1950	48	-0.2270	48
4 agents	-0.2940	64	-0.1250	64	-0.2010	64	-0.8500	64	0.1540	64	-0.1120	64	0.1220	64
5 agents	-0.1380	80	-0.1020	80	-0.0790	80	-6.4330	80	0.2660	80	-0.1860	80	-0.2430	80
6 agents	-0.0490	96	-0.1340	96	-0.1310	96	-0.9730	96	0.2210	96	-0.2140	96	0.0290	96
DE														
4 genes	-0.1870	92	-0.0950	92	-0.2400	92	-1.3520	92	0.0520	92	-0.0980	92	0.1000	92
6 genes	-0.3700	138	-0.8590	138	-0.4350	138	-1.6540	132	-0.6270	138	-0.5750	138	0.1160	138
8 genes	0.0570	184	0.0170	184	-0.3680	184	-2.6980	184	-1.1590	184	-0.1330	184	-1.4330	184
Chaotic														
5 agents	-0.9830	50	0.1490	50	-3.0080	40	-3.0870	50	-4.2400	50	0.9750	40	0	50
6 agents	-0.0280	60	0.2860	60	-0.1190	60	0.0920	60	-4.3330	60	0.8810	60	-0.0070	60
7 agents	0.0070	70	0.3560	70	-0.0650	70	-0.2320	70	-4.3620	70	-0.2790	70	-0.0380	70
8 agents	-0.0670	80	0.3770	80	-0.1090	80	0.0070	80	-4.3320	80	0.9490	80	-0.0250	80

Table 3.10: The results of each MPPT algorithm at 14:00.

method	$\theta=0^o$	steps	$\theta=30^o$	steps	$\theta=60^o$	steps	$\theta=60^o$	steps	$\theta=120^o$	steps	$\theta=150^o$	steps	$\theta=180^o$	steps
CPSO														
2 agents	-0.1100	22	0.0480	22	-0.1620	22	-0.3380	22	-0.0560	22	-0.0990	22	-0.4500	28
3 agents	-0.1710	35	-0.0490	43	-0.3460	41	-0.2090	39	-0.0510	39	0.0020	45	-0.4670	41
4 agents	-0.2790	50	0.0560	58	-0.1970	48	-0.0940	52	-0.1890	50	0.0330	48	0.2810	52
5 agents	-0.1060	57	0.0960	57	-0.3830	59	-0.0830	59	-0.1740	59	0.0420	65	0.3090	59
6 agents	-0.1690	80	-0.0960	88	-0.2910	80	-0.1290	82	-0.2210	88	0.0080	86	0.2780	86
PSO														
2 agents	-1.3740	32	-1.0690	32	-0.1050	32	0.3140	32	-1.0320	32	-0.1800	32	0.2020	32
3 agents	-0.1260	48	-0.0950	48	-0.1300	48	0.1910	48	-0.3120	48	-0.1050	48	0.0620	48
4 agents	-0.1830	64	-0.1360	64	-0.1250	64	0.1510	64	-0.2780	64	-0.0520	64	0.1160	64
5 agents	-0.1720	80	-0.2540	80	-0.0200	80	-0.0100	80	-0.2030	80	-0.0850	80	-0.6470	80
6 agents	-0.1390	96	-0.3910	96	-0.1550	96	-1.1610	96	-0.2980	96	-0.1130	96	0.0350	96
DE														
4 genes	-0.3720	92	-0.3350	92	-0.1830	92	-0.9970	92	-5.9320	92	-0.1030	92	-0.0320	92
6 genes	-6.4440	138	-1.3590	138	-0.2110	138	-2.9700	138	-7.1740	138	-1.0330	138	-0.0020	138
8 genes	-0.3970	184	-0.4860	184	-1.3190	184	-3.9400	184	-8.9860	183	-0.5050	184	-0.6100	184
Chaotic														
5 agents	-0.9330	50	-0.5560	50	-3.4140	50	-0.4220	50	-0.7400	50	-0.3070	50	-0.8260	50
6 agents	-0.2760	60	-0.1440	60	0.0500	60	-0.0570	60	-0.1780	60	-0.0210	60	-0.5140	60
7 agents	-0.3460	70	-0.0600	70	0.0760	70	-0.0660	70	-0.1890	70	-0.0230	70	-0.5050	70
8 agents	-0.2590	80	-0.1810	80	-0.0410	80	-0.1190	80	-0.3000	80	-0.2320	80	-0.6470	80

Table 3.11: The results of each MPPT algorithm at 15:00.

method	θ =0°	steps	θ =30°	steps	θ =60°	steps	θ =60°	steps	θ =120°	steps	θ =150°	steps	θ =180°	steps
CPSO														
2 agents	-0.3240	22	-0.4280	22	-0.0750	22	-0.3340	22	-0.2400	22	0.3480	26	-0.0080	28
3 agents	-0.4900	45	-0.4080	39	-0.0140	39	-0.2410	41	-0.1960	37	0.2110	47	-0.0380	41
4 agents	-0.4120	54	-0.2930	56	-0.1310	50	-0.2670	50	-0.2920	46	-0.9560	50	-0.0260	56
5 agents	-0.3560	57	-0.2950	55	-0.1390	59	-0.2080	59	-0.2410	55	-1.2300	65	0.0110	59
6 agents	-0.3260	80	-0.4180	88	-0.1550	76	-0.2220	78	-0.3570	74	-0.6400	86	0.0070	88
PSO														
2 agents	-1.4100	32	-0.8550	32	-0.1570	32	-0.5540	32	-0.2290	32	-0.5890	32	-0.1570	32
3 agents	-0.2750	48	-0.2430	48	-0.1810	48	-0.1650	48	-0.1050	48	-0.1440	48	-0.0530	48
4 agents	-0.2450	64	-0.6240	64	-0.2780	64	-0.0590	64	-0.0810	64	-0.0690	64	-0.0880	64
5 agents	-0.2750	80	-0.6440	80	-0.3830	80	-0.1180	80	-0.1410	80	-0.0760	80	-0.0930	80
6 agents	-0.3600	96	-0.6770	96	-0.5370	96	-0.0870	96	-0.1920	96	0.2170	96	-0.0950	96
DE														
4 genes	-0.1380	92	-0.4230	92	-0.2620	92	-0.1580	92	-0.0970	92	0.0650	92	-0.3460	92
6 genes	-1.4880	138	-0.8300	138	-0.3640	138	-0.3480	138	-0.6170	138	-3.5790	138	-0.8310	138
8 genes	-0.4610	184	-0.5510	184	-0.5690	184	-1.0090	184	-0.2680	184	-0.7710	184	-3.1790	184
Chaotic														
5 agents	-1.0830	50	-0.9830	50	-2.5110	50	-0.1410	50	-0.2800	50	0.9640	50	0.0060	50
6 agents	-0.3000	60	-0.1330	60	-0.0870	60	-0.1850	60	-0.4150	60	0.8580	60	-0.0380	60
7 agents	-0.4120	70	-0.2760	70	-0.1260	70	-0.2750	70	-0.3440	70	0.7510	70	-0.0330	70
8 agents	-0.4660	80	-0.1770	80	-0.2460	80	-0.3370	80	-0.2450	80	-0.7070	80	-0.2370	80

Table 3.12: The results of each MPPT algorithm at 16:00.

method	$\theta = 0^o$	steps	$\theta = 30^o$	steps	$\theta = 60^o$	steps	$\theta = 60^o$	steps	$\theta = 120^o$	steps	$\theta = 150^o$	steps	$\theta = 180^o$	steps
CPSO														
2 agents	-0.1480	22	-0.4090	22	1.3340	22	-0.2110	22	-1.5910	22	0.3480	26	-0.0080	28
3 agents	-0.1020	39	-0.7520	35	1.0060	45	-0.2160	35	-0.1650	41	0.2110	47	-0.0380	41
4 agents	-0.1570	54	-0.7860	64	0.7030	64	-0.7350	60	-0.2010	50	-0.9560	50	-0.0260	56
5 agents	-0.2550	57	-0.4870	63	0.9280	57	-0.6820	57	-0.2480	71	-1.2300	65	0.0110	59
6 agents	-0.1560	88	-0.3770	76	0.1700	98	-0.7850	86	-0.2220	76	-0.6400	86	0.0070	88
PSO														
2 agents	-3.2500	32	-0.4280	32	-0.7000	32	-0.1470	32	-0.3560	32	-0.5890	32	-0.1570	32
3 agents	-0.4260	48	-0.5290	48	-0.2630	48	-0.1750	48	-0.1050	48	-0.1440	48	-0.0530	48
4 agents	-0.5680	64	-0.5420	64	-0.2780	64	-0.2550	64	-0.1480	64	-0.0690	64	-0.0880	64
5 agents	-0.4610	80	-0.6570	80	-0.5050	80	-0.2610	80	-0.1240	80	-0.0760	80	-0.0930	80
6 agents	-0.7630	96	-1.2670	96	-0.1450	96	-0.4780	96	-12.2380	96	0.2170	96	-0.0950	96
DE														
4 genes	-0.4810	92	-0.2750	92	-0.3460	92	-0.1420	92	-0.1380	92	0.0650	92	-0.3460	92
6 genes	-1.3590	138	-1.1730	138	-0.3930	138	-0.9030	138	-0.4050	138	-3.5790	138	-0.8310	138
8 genes	-0.9280	184	-0.9250	176	-0.6750	184	-0.6900	184	-1.0840	184	-0.7710	184	-3.1790	184
Chaotic														
5 agents	-0.6770	50	-0.2740	50	-0.2310	50	-0.1240	50	-0.1450	50	0.9640	50	0.0060	50
6 agents	-0.5670	60	-1.1060	60	-0.6340	60	-0.1250	60	-0.2770	60	0.8580	60	-0.0380	60
7 agents	-0.9360	50	-0.3360	70	-0.2960	70	-0.1290	70	-0.1800	70	0.7510	70	-0.0330	70
8 agents	-0.3820	60	-0.4180	80	-0.3700	80	-0.2360	80	-0.2590	80	-0.7070	80	-0.2370	80

Table 3.13: The results of each MPPT algorithm at 17:00.

method	θ =0°	steps	θ =30°	steps	θ =60°	steps	θ =60°	steps	θ =120°	steps	θ =150°	steps	θ =180°	steps
CPSO														
2 agents	-0.3250	22	-0.2150	22	-0.0390	24	0.0020	22	-0.3770	24	-0.1460	22	-0.1740	22
3 agents	-0.4740	47	-0.2140	41	-0.1210	39	-0.0160	39	-0.6040	47	-0.2140	45	-0.1150	39
4 agents	-0.5180	56	-0.3280	50	-0.0920	46	-0.0660	52	-0.5230	60	-0.1640	50	-0.1870	50
5 agents	-0.4610	57	-0.4500	59	-0.1530	59	-0.1100	59	-0.5870	59	-0.2000	59	-0.1500	59
6 agents	-0.6480	86	-0.5900	82	-0.2270	84	-0.1380	78	-0.6910	76	-0.1090	86	-0.2530	76
PSO														
2 agents	-0.6080	32	0.4370	32	-0.2490	32	-0.2220	32	0	32	-0.4420	32	-0.1130	32
3 agents	-0.8680	48	0.7010	48	-0.0370	48	-0.1250	48	-0.0140	48	-0.1850	48	0.0140	48
4 agents	-0.8120	64	0.6110	64	-0.0770	64	-0.1710	64	-0.1030	64	-0.2310	64	0.0110	64
5 agents	-0.9850	80	0.9260	80	-0.8130	80	-0.1520	80	-0.2880	80	-0.3940	80	-0.7080	80
6 agents	-1.5820	96	0.7170	96	-0.2510	96	-0.3980	96	-0.5770	95	3.4990	80	-3.7190	96
DE														
4 genes	-0.0710	92	-1.1680	92	-0.1540	92	-0.1930	92	-0.6120	92	-0.6670	92	0.3630	92
6 genes	-5.9680	138	-1.1830	138	-0.3530	138	-0.8460	138	-1.2040	138	-0.9740	138	0.2760	138
8 genes	-0.4100	184	-1.8870	184	-0.4160	184	-0.5240	184	-1.0540	184	-1.6010	184	-1.0440	184
Chaotic														
5 agents	-0.5120	50	-0.2800	50	-0.5640	50	-0.1220	50	-0.2930	50	-0.1260	50	-0.1640	50
6 agents	-0.5830	60	-0.3480	60	-0.3230	60	-0.2520	60	-0.1650	60	-0.1630	60	-0.1960	60
7 agents	-0.6370	70	-0.4230	70	-0.3590	70	-0.2240	70	-0.1290	70	-0.1630	70	-0.2150	70
8 agents	-0.6370	80	-0.4630	80	-0.3830	80	-0.3020	80	-0.2450	80	-0.1970	80	-0.2430	80

Table 3.14: The results of each MPPT algorithm at 18:00.

method	θ =0°	steps	θ =30°	steps	θ =60°	steps	θ =60°	steps	θ =120°	steps	θ =150°	steps	θ =180°	steps
CPSO														
2 agents	-0.0840	22	-0.4330	22	-0.3210	24	-0.5110	26	-0.5110	26	-0.1120	22	-0.1600	26
3 agents	-0.1410	45	-0.4990	41	-0.3400	47	-0.3580	39	-0.3580	39	-0.1390	41	-0.1790	35
4 agents	-0.2840	68	-0.5830	66	-0.3650	48	-0.3600	56	-0.3600	56	-0.1800	48	-0.2190	48
5 agents	-0.4380	63	-0.6830	57	-0.4180	59	-0.9920	75	-0.9920	75	-0.3470	67	-0.2510	59
6 agents	-0.7480	94	-0.8180	86	-0.5090	82	-1.1450	74	-1.1450	74	-0.3750	74	-0.3580	82
PSO														
2 agents	-0.9600	32	-0.3890	32	-0.4040	32	-0.1780	32	-0.1780	32	-0.0120	32	0.0730	32
3 agents	-1.2590	48	-0.4730	48	-0.2410	48	-0.1580	48	-0.1580	48	-0.0840	48	0.2980	48
4 agents	-0.9930	64	-0.5780	64	-0.3090	64	-0.2240	64	-0.2240	64	-0.0930	64	0.2300	64
5 agents	-1.3860	80	-0.6340	80	-0.3440	80	-0.3140	80	-0.3140	80	-0.0270	80	0.0250	80
6 agents	-1.2130	96	-0.7460	96	-0.4420	96	-0.4220	96	-0.4220	96	-0.0960	96	-0.3590	96
DE														
4 genes	-0.6760	92	-0.0920	92	-0.2340	92	-0.1880	92	-0.1880	92	-0.0650	92	-0.1280	92
6 genes	-0.3810	138	-0.2590	138	-0.4100	138	-0.3580	138	-0.3580	138	-0.1280	138	0.0250	138
8 genes	-2.0600	184	-0.6330	184	-0.5290	184	-0.6330	184	-0.6330	184	-0.2470	184	-0.2420	184
Chaotic														
5 agents	-0.3430	50	-0.3980	50	-0.2570	50	-0.1420	50	-0.1420	50	-0.1550	50	-0.1120	50
6 agents	-0.3250	60	-0.1930	60	-0.2190	60	-0.1700	60	-0.1700	60	-0.1860	60	-0.1810	60
7 agents	-0.3920	70	-0.3290	70	-0.2420	70	-0.1640	70	-0.1640	70	-0.2280	70	-0.2010	70
8 agents	-0.4700	80	-0.3660	80	-0.2330	80	-0.1950	80	-0.1950	80	-0.2680	80	-0.2280	80

Table 3.15: 9:00 Algorithms' steps of convergence deviation from CPSO at %

method	$\theta=0^o$	$\theta=30^o$	$\theta=60^o$	$\theta=60^o$	$\theta=120^o$	$\theta=150^o$	$\theta=180^o$
PSO							
2 agents CPSO-PSO	23,1	45,5	45,5	45,5	45,5	14,3	45,5
3 agents CPSO-PSO	23,1	37,1	17,1	17,1	37,1	17,1	37,1
4 agents CPSO-PSO	6,7	33,3	33,3	3,2	33,3	33,3	33,3
5 agents CPSO-PSO	35,6	35,6	35,6	35,6	35,6	27,0	31,1
6 agents CPSO-PSO	23,1	17,1	14,3	23,1	23,1	23,1	17,1
DE							
4 genes-2 agents CPSO	165,4	213,6	318,2	318,2	318,2	228,6	318,2
4 genes-3 agents CPSO	76,9	97,1	124,4	124,4	162,9	124,4	162,9
4 genes-4 agents CPSO	15,0	43,8	91,7	48,4	91,7	91,7	91,7
4 genes-5 agents CPSO	16,9	16,9	55,9	55,9	55,9	46,0	50,8
4 genes-6 agents CPSO	11,5	15,9	9,5	17,9	17,9	17,9	12,2
6 genes-2 agents CPSO	253,8	318,2	527,3	527,3	527,3	392,9	527,3
6 genes-3 agents CPSO	135,9	162,9	236,6	236,6	294,3	236,6	294,3
6 genes-4 agents CPSO	53,3	91,7	187,5	122,6	187,5	187,5	187,5
6 genes-5 agents CPSO	55,9	55,9	133,9	133,9	133,9	119,0	126,2
6 genes-6 agents CPSO	17,9	12,2	64,3	76,9	76,9	76,9	68,3
8 genes-2 agents CPSO	342,3	422,7	736,4	736,4	736,4	557,1	736,4
8 genes-3 agents CPSO	194,9	228,6	348,8	348,8	425,7	348,8	425,7
8 genes-4 agents CPSO	91,7	139,6	283,3	196,8	283,3	283,3	283,3
8 genes-5 agents CPSO	94,9	94,9	211,9	211,9	211,9	192,1	201,6
8 genes-6 agents CPSO	47,4	40,2	119,0	135,9	135,9	135,9	124,4
Chaotic							
5 agents-2 agents CPSO	92,3	127,3	127,3	127,3	127,3	78,6	127,3
5 agents-3 agents CPSO	28,2	42,9	22,0	22,0	42,9	22,0	42,9
5 agents-4 agents CPSO	16,7	4,2	4,2	19,4	4,2	4,2	4,2
5 agents-5 agents CPSO	15,3	15,3	15,3	15,3	15,3	20,6	18,0
5 agents-6 agents CPSO	35,9	39,0	40,5	35,9	35,9	35,9	39,0
6 agents-2 agents CPSO	130,8	172,7	172,7	172,7	172,7	114,3	172,7
6 agents-3 agents CPSO	53,8	71,4	46,3	46,3	71,4	46,3	71,4
6 agents-4 agents CPSO	0,0	25,0	25,0	3,2	25,0	25,0	25,0
6 agents-5 agents CPSO	1,7	1,7	1,7	1,7	1,7	4,8	1,6
6 agents-6 agents CPSO	23,1	26,8	28,6	23,1	23,1	23,1	26,8
7 agents-2 agents CPSO	169,2	218,2	218,2	218,2	218,2	150,0	218,2
7 agents-3 agents CPSO	79,5	100,0	70,7	70,7	100,0	70,7	100,0
7 agents-4 agents CPSO	16,7	45,8	45,8	12,9	45,8	45,8	45,8
7 agents-5 agents CPSO	18,6	18,6	18,6	18,6	18,6	11,1	14,8
7 agents-6 agents CPSO	10,3	14,6	16,7	10,3	10,3	10,3	14,6
8 agents-2 agents CPSO	207,7	263,6	263,6	263,6	263,6	185,7	263,6
8 agents-3 agents CPSO	105,1	128,6	95,1	95,1	128,6	95,1	128,6
8 agents-4 agents CPSO	33,3	66,7	66,7	29,0	66,7	66,7	66,7
8 agents-5 agents CPSO	35,6	35,6	35,6	35,6	35,6	27,0	31,1
8 agents-6 agents CPSO	2,6	2,4	4,8	2,6	2,6	2,6	2,4

Table 3.16: 10:00 Algorithms' steps of convergence deviation from CPSO at %

method	θ =0º	θ =30º	θ =60º	θ =60º	θ =120º	θ =150º	θ =180º
PSO							
2 agents CPSO-PSO	23,1	45,5	45,5	45,5	45,5	45,5	14,3
3 agents CPSO-PSO	23,1	37,1	37,1	17,1	6,7	37,1	17,1
4 agents CPSO-PSO	6,7	33,3	28,0	14,3	18,5	14,3	28,0
5 agents CPSO-PSO	35,6	35,6	40,4	40,4	31,1	35,6	31,1
6 agents CPSO-PSO	23,1	17,1	29,7	14,3	45,5	17,1	11,6
DE							
4 genes-2 agents CPSO	165,4	213,6	213,6	318,2	318,2	318,2	228,6
4 genes-3 agents CPSO	76,9	97,1	97,1	124,4	104,4	162,9	124,4
4 genes-4 agents CPSO	15,0	43,8	38,0	64,3	70,4	64,3	84,0
4 genes-5 agents CPSO	16,9	16,9	21,1	61,4	50,8	55,9	50,8
4 genes-6 agents CPSO	11,5	15,9	6,8	9,5	39,4	12,2	7,0
6 genes-2 agents CPSO	253,8	318,2	318,2	527,3	527,3	527,3	392,9
6 genes-3 agents CPSO	135,9	162,9	162,9	236,6	206,7	294,3	236,6
6 genes-4 agents CPSO	53,3	91,7	84,0	146,4	155,6	146,4	176,0
6 genes-5 agents CPSO	55,9	55,9	61,4	142,1	126,2	133,9	126,2
6 genes-6 agents CPSO	17,9	12,2	24,3	64,3	109,1	68,3	60,5
8 genes-2 agents CPSO	342,3	422,7	422,7	736,4	736,4	736,4	557,1
8 genes-3 agents CPSO	194,9	228,6	228,6	348,8	308,9	425,7	348,8
8 genes-4 agents CPSO	91,7	139,6	130,0	228,6	240,7	228,6	268,0
8 genes-5 agents CPSO	94,9	94,9	101,8	222,8	201,6	211,9	201,6
8 genes-6 agents CPSO	47,4	40,2	55,4	119,0	178,8	124,4	114,0
Chaotic							
5 agents-2 agents CPSO	92,3	127,3	127,3	127,3	127,3	127,3	78,6
5 agents-3 agents CPSO	28,2	42,9	42,9	22,0	11,1	42,9	22,0
5 agents-4 agents CPSO	16,7	4,2	0,0	10,7	7,4	10,7	0,0
5 agents-5 agents CPSO	15,3	15,3	12,3	12,3	18,0	15,3	18,0
5 agents-6 agents CPSO	35,9	39,0	32,4	40,5	24,2	39,0	41,9
6 agents-2 agents CPSO	130,8	172,7	172,7	172,7	172,7	172,7	114,3
6 agents-3 agents CPSO	53,8	71,4	71,4	46,3	33,3	71,4	46,3
6 agents-4 agents CPSO	0,0	25,0	20,0	7,1	11,1	7,1	20,0
6 agents-5 agents CPSO	1,7	1,7	5,3	5,3	1,6	1,7	1,6
6 agents-6 agents CPSO	23,1	26,8	18,9	28,6	9,1	26,8	30,2
7 agents-2 agents CPSO	169,2	218,2	218,2	218,2	218,2	218,2	150,0
7 agents-3 agents CPSO	79,5	100,0	100,0	70,7	55,6	100,0	70,7
7 agents-4 agents CPSO	16,7	45,8	40,0	25,0	29,6	25,0	40,0
7 agents-5 agents CPSO	18,6	18,6	22,8	22,8	14,8	18,6	14,8
7 agents-6 agents CPSO	10,3	14,6	5,4	16,7	6,1	14,6	18,6
8 agents-2 agents CPSO	207,7	263,6	263,6	263,6	263,6	263,6	185,7
8 agents-3 agents CPSO	105,1	128,6	128,6	95,1	77,8	128,6	95,1
8 agents-4 agents CPSO	33,3	66,7	60,0	42,9	48,1	42,9	60,0
8 agents-5 agents CPSO	35,6	35,6	40,4	40,4	31,1	35,6	31,1
8 agents-6 agents CPSO	2,6	2,4	8,1	4,8	21,2	2,4	7,0

Table 3.17: 11:00 Algorithms' steps convergence deviation from CPSO at %

method	θ =0°	θ =30°	θ =60°	θ =60°	θ =120°	θ =150°	θ =180°
PSO							
2 agents CPSO-PSO	45,5	45,5	45,5	45,5	45,5	33,3	45,5
3 agents CPSO-PSO	17,1	17,1	37,1	37,1	37,1	23,1	17,1
4 agents CPSO-PSO	28,0	33,3	33,3	33,3	33,3	28,0	33,3
5 agents CPSO-PSO	40,4	27,0	12,7	12,7	35,6	35,6	31,1
6 agents CPSO-PSO	20,0	23,1	20,0	20,0	23,1	26,3	26,3
DE							
4 genes-2 agents CPSO	213,6	213,6	318,2	318,2	318,2	283,3	318,2
4 genes-3 agents CPSO	68,3	68,3	162,9	162,9	162,9	135,9	124,4
4 genes-4 agents CPSO	38,0	43,8	91,7	91,7	91,7	84,0	91,7
4 genes-5 agents CPSO	21,1	9,5	29,6	29,6	55,9	55,9	50,8
4 genes-6 agents CPSO	13,8	11,5	15,0	15,0	17,9	21,1	21,1
6 genes-2 agents CPSO	318,2	318,2	527,3	527,3	527,3	475,0	527,3
6 genes-3 agents CPSO	124,4	124,4	294,3	294,3	294,3	253,8	236,6
6 genes-4 agents CPSO	84,0	91,7	187,5	187,5	187,5	176,0	187,5
6 genes-5 agents CPSO	61,4	46,0	94,4	94,4	133,9	133,9	126,2
6 genes-6 agents CPSO	15,0	17,9	72,5	72,5	76,9	81,6	81,6
8 genes-2 agents CPSO	422,7	422,7	736,4	736,4	736,4	666,7	736,4
8 genes-3 agents CPSO	180,5	180,5	425,7	425,7	425,7	371,8	348,8
8 genes-4 agents CPSO	130,0	139,6	283,3	283,3	283,3	268,0	283,3
8 genes-5 agents CPSO	101,8	82,5	159,2	159,2	211,9	211,9	201,6
8 genes-6 agents CPSO	43,8	47,4	130,0	130,0	135,9	142,1	142,1
Chaotic							
5 agents-2 agents CPSO	127,3	127,3	127,3	127,3	127,3	108,3	127,3
5 agents-3 agents CPSO	22,0	22,0	42,9	42,9	42,9	28,2	22,0
5 agents-4 agents CPSO	0,0	4,2	4,2	4,2	4,2	0,0	4,2
5 agents-5 agents CPSO	12,3	20,6	29,6	29,6	15,3	15,3	18,0
5 agents-6 agents CPSO	37,5	35,9	37,5	37,5	35,9	34,2	34,2
6 agents-2 agents CPSO	172,7	172,7	172,7	172,7	172,7	150,0	172,7
6 agents-3 agents CPSO	46,3	46,3	71,4	71,4	71,4	53,8	46,3
6 agents-4 agents CPSO	20,0	25,0	25,0	25,0	25,0	20,0	25,0
6 agents-5 agents CPSO	5,3	4,8	15,5	15,5	1,7	1,7	1,6
6 agents-6 agents CPSO	25,0	23,1	25,0	25,0	23,1	21,1	21,1
7 agents-2 agents CPSO	218,2	218,2	218,2	218,2	218,2	191,7	218,2
7 agents-3 agents CPSO	70,7	70,7	100,0	100,0	100,0	79,5	70,7
7 agents-4 agents CPSO	40,0	45,8	45,8	45,8	45,8	40,0	45,8
7 agents-5 agents CPSO	22,8	11,1	1,4	1,4	18,6	18,6	14,8
7 agents-6 agents CPSO	12,5	10,3	12,5	12,5	10,3	7,9	7,9
8 agents-2 agents CPSO	263,6	263,6	263,6	263,6	263,6	233,3	263,6
8 agents-3 agents CPSO	95,1	95,1	128,6	128,6	128,6	105,1	95,1
8 agents-4 agents CPSO	60,0	66,7	66,7	66,7	66,7	60,0	66,7
8 agents-5 agents CPSO	40,4	27,0	12,7	12,7	35,6	35,6	31,1
8 agents-6 agents CPSO	0,0	2,6	0,0	0,0	2,6	5,3	5,3

Table 3.18: 12:00 Algorithms' steps of convergence deviation from CPSO at %

method	$\theta = 0^o$	$\theta = 30^o$	$\theta = 60^o$	$\theta = 60^o$	$\theta = 120^o$	$\theta = 150^o$	$\theta = 180^o$
PSO							
2 agents CPSO-PSO	45,5	45,5	45,5	45,5	45,5	14,3	14,3
3 agents CPSO-PSO	37,1	29,7	17,1	17,1	17,1	23,1	17,1
4 agents CPSO-PSO	28,0	14,3	33,3	33,3	18,5	28,0	28,0
5 agents CPSO-PSO	40,4	40,4	27,0	27,0	27,0	35,6	35,6
6 agents CPSO-PSO	20,0	9,1	20,0	20,0	20,0	26,3	14,3
DE							
4 genes-2 agents CPSO	318,2	318,2	318,2	318,2	318,2	228,6	228,6
4 genes-3 agents CPSO	162,9	148,6	124,4	124,4	124,4	135,9	124,4
4 genes-4 agents CPSO	84,0	64,3	91,7	91,7	70,4	84,0	84,0
4 genes-5 agents CPSO	61,4	61,4	46,0	46,0	46,0	55,9	55,9
4 genes-6 agents CPSO	15,0	4,5	15,0	15,0	15,0	21,1	9,5
6 genes-2 agents CPSO	527,3	527,3	527,3	527,3	527,3	392,9	392,9
6 genes-3 agents CPSO	294,3	273,0	236,6	236,6	236,6	253,8	236,6
6 genes-4 agents CPSO	176,0	146,4	187,5	187,5	155,6	176,0	176,0
6 genes-5 agents CPSO	142,1	142,1	119,0	119,0	119,0	133,9	133,9
6 genes-6 agents CPSO	72,5	56,8	72,5	72,5	72,5	81,6	64,3
8 genes-2 agents CPSO	736,4	736,4	736,4	736,4	736,4	557,1	557,1
8 genes-3 agents CPSO	425,7	397,3	348,8	348,8	348,8	371,8	348,8
8 genes-4 agents CPSO	268,0	228,6	283,3	283,3	240,7	268,0	268,0
8 genes-5 agents CPSO	222,8	222,8	192,1	192,1	192,1	211,9	211,9
8 genes-6 agents CPSO	130,0	109,1	130,0	130,0	130,0	142,1	119,0
Chaotic							
5 agents-2 agents CPSO	127,3	127,3	127,3	127,3	81,8	78,6	78,6
5 agents-3 agents CPSO	42,9	35,1	22,0	22,0	2,4	28,2	22,0
5 agents-4 agents CPSO	0,0	10,7	4,2	4,2	25,9	0,0	0,0
5 agents-5 agents CPSO	12,3	12,3	20,6	20,6	36,5	15,3	15,3
5 agents-6 agents CPSO	37,5	43,2	37,5	37,5	50,0	34,2	40,5
6 agents-2 agents CPSO	172,7	172,7	172,7	172,7	172,7	114,3	114,3
6 agents-3 agents CPSO	71,4	62,2	46,3	46,3	46,3	53,8	46,3
6 agents-4 agents CPSO	20,0	7,1	25,0	25,0	11,1	20,0	20,0
6 agents-5 agents CPSO	5,3	5,3	4,8	4,8	4,8	1,7	1,7
6 agents-6 agents CPSO	25,0	31,8	25,0	25,0	25,0	21,1	28,6
7 agents-2 agents CPSO	218,2	218,2	218,2	218,2	218,2	150,0	150,0
7 agents-3 agents CPSO	100,0	89,2	70,7	70,7	70,7	79,5	70,7
7 agents-4 agents CPSO	40,0	25,0	45,8	45,8	29,6	40,0	40,0
7 agents-5 agents CPSO	22,8	22,8	11,1	11,1	11,1	18,6	18,6
7 agents-6 agents CPSO	12,5	20,5	12,5	12,5	12,5	7,9	16,7
8 agents-2 agents CPSO	263,6	263,6	263,6	263,6	263,6	185,7	185,7
8 agents-3 agents CPSO	128,6	116,2	95,1	95,1	95,1	105,1	95,1
8 agents-4 agents CPSO	60,0	42,9	66,7	66,7	48,1	60,0	60,0
8 agents-5 agents CPSO	40,4	40,4	27,0	27,0	27,0	35,6	35,6
8 agents-6 agents CPSO	0,0	9,1	0,0	0,0	0,0	5,3	4,8

Table 3.19: 13:00 Algorithms' steps of convergence deviation from CPSO at %

method	$\theta = 0^o$	$\theta = 30^o$	$\theta = 60^o$	$\theta = 60^o$	$\theta = 120^o$	$\theta = 150^o$	$\theta = 180^o$
PSO							
2 agents CPSO-PSO	45,5	45,5	45,5	45,5	45,5	45,5	33,3
3 agents CPSO-PSO	17,1	17,1	37,1	37,1	23,1	17,1	29,7
4 agents CPSO-PSO	28,0	18,5	33,3	33,3	28,0	45,5	6,7
5 agents CPSO-PSO	40,4	40,4	27,0	40,4	35,6	35,6	31,1
6 agents CPSO-PSO	17,1	11,6	17,1	23,1	14,3	33,3	23,1
DE							
4 genes-2 agents CPSO	318,2	318,2	318,2	318,2	318,2	318,2	283,3
4 genes-3 agents CPSO	124,4	124,4	162,9	162,9	135,9	124,4	148,6
4 genes-4 agents CPSO	84,0	70,4	91,7	91,7	84,0	109,1	53,3
4 genes-5 agents CPSO	61,4	61,4	46,0	61,4	55,9	55,9	50,8
4 genes-6 agents CPSO	12,2	7,0	12,2	17,9	9,5	27,8	17,9
6 genes-2 agents CPSO	527,3	527,3	527,3	500,0	527,3	527,3	475,0
6 genes-3 agents CPSO	236,6	236,6	294,3	277,1	253,8	236,6	273,0
6 genes-4 agents CPSO	176,0	155,6	187,5	175,0	176,0	213,6	130,0
6 genes-5 agents CPSO	142,1	142,1	119,0	131,6	133,9	133,9	126,2
6 genes-6 agents CPSO	68,3	60,5	68,3	69,2	64,3	91,7	76,9
8 genes-2 agents CPSO	736,4	736,4	736,4	736,4	736,4	736,4	666,7
8 genes-3 agents CPSO	348,8	348,8	425,7	425,7	371,8	348,8	397,3
8 genes-4 agents CPSO	268,0	240,7	283,3	283,3	268,0	318,2	206,7
8 genes-5 agents CPSO	222,8	222,8	192,1	222,8	211,9	211,9	201,6
8 genes-6 agents CPSO	124,4	114,0	124,4	135,9	119,0	155,6	135,9
Chaotic							
5 agents-2 agents CPSO	127,3	127,3	81,8	127,3	127,3	81,8	108,3
5 agents-3 agents CPSO	22,0	22,0	14,3	42,9	28,2	2,4	35,1
5 agents-4 agents CPSO	0,0	7,4	16,7	4,2	0,0	9,1	16,7
5 agents-5 agents CPSO	12,3	12,3	36,5	12,3	15,3	32,2	18,0
5 agents-6 agents CPSO	39,0	41,9	51,2	35,9	40,5	44,4	35,9
6 agents-2 agents CPSO	172,7	172,7	172,7	172,7	172,7	172,7	150,0
6 agents-3 agents CPSO	46,3	46,3	71,4	71,4	53,8	46,3	62,2
6 agents-4 agents CPSO	20,0	11,1	25,0	25,0	20,0	36,4	0,0
6 agents-5 agents CPSO	5,3	5,3	4,8	5,3	1,7	1,7	1,6
6 agents-6 agents CPSO	26,8	30,2	26,8	23,1	28,6	16,7	23,1
7 agents-2 agents CPSO	218,2	218,2	218,2	218,2	218,2	218,2	191,7
7 agents-3 agents CPSO	70,7	70,7	100,0	100,0	79,5	70,7	89,2
7 agents-4 agents CPSO	40,0	29,6	45,8	45,8	40,0	59,1	16,7
7 agents-5 agents CPSO	22,8	22,8	11,1	22,8	18,6	18,6	14,8
7 agents-6 agents CPSO	14,6	18,6	14,6	10,3	16,7	2,8	10,3
8 agents-2 agents CPSO	263,6	263,6	263,6	263,6	263,6	263,6	233,3
8 agents-3 agents CPSO	95,1	95,1	128,6	128,6	105,1	95,1	116,2
8 agents-4 agents CPSO	60,0	48,1	66,7	66,7	60,0	81,8	33,3
8 agents-5 agents CPSO	40,4	40,4	27,0	40,4	35,6	35,6	31,1
8 agents-6 agents CPSO	2,4	7,0	2,4	2,6	4,8	11,1	2,6

Table 3.20: 14:00 Algorithms' steps of convergence deviation from CPSO at %

method	θ =0°	θ =30°	θ =60°	θ =60°	θ =120°	θ =150°	θ =180°
PSO							
2 agents CPSO-PSO	45,5	45,5	45,5	45,5	45,5	45,5	14,3
3 agents CPSO-PSO	37,1	11,6	17,1	23,1	23,1	6,7	17,1
4 agents CPSO-PSO	28,0	10,3	33,3	23,1	28,0	33,3	23,1
5 agents CPSO-PSO	40,4	40,4	35,6	35,6	35,6	23,1	35,6
6 agents CPSO-PSO	20,0	9,1	20,0	17,1	9,1	11,6	11,6
DE							
4 genes-2 agents CPSO	318,2	318,2	318,2	318,2	318,2	318,2	228,6
4 genes-3 agents CPSO	162,9	114,0	124,4	135,9	135,9	104,4	124,4
4 genes-4 agents CPSO	84,0	58,6	91,7	76,9	84,0	91,7	76,9
4 genes-5 agents CPSO	61,4	61,4	55,9	55,9	55,9	41,5	55,9
4 genes-6 agents CPSO	15,0	4,5	15,0	12,2	4,5	7,0	7,0
6 genes-2 agents CPSO	527,3	527,3	527,3	527,3	527,3	527,3	392,9
6 genes-3 agents CPSO	294,3	220,9	236,6	253,8	253,8	206,7	236,6
6 genes-4 agents CPSO	176,0	137,9	187,5	165,4	176,0	187,5	165,4
6 genes-5 agents CPSO	142,1	142,1	133,9	133,9	133,9	112,3	133,9
6 genes-6 agents CPSO	72,5	56,8	72,5	68,3	56,8	60,5	60,5
8 genes-2 agents CPSO	736,4	736,4	736,4	736,4	731,8	736,4	557,1
8 genes-3 agents CPSO	425,7	327,9	348,8	371,8	369,2	308,9	348,8
8 genes-4 agents CPSO	268,0	217,2	283,3	253,8	266,0	283,3	253,8
8 genes-5 agents CPSO	222,8	222,8	211,9	211,9	210,2	183,1	211,9
8 genes-6 agents CPSO	130,0	109,1	130,0	124,4	108,0	114,0	114,0
Chaotic							
5 agents-2 agents CPSO	127,3	127,3	127,3	127,3	127,3	127,3	78,6
5 agents-3 agents CPSO	42,9	16,3	22,0	28,2	28,2	11,1	22,0
5 agents-4 agents CPSO	0,0	13,8	4,2	3,8	0,0	4,2	3,8
5 agents-5 agents CPSO	12,3	12,3	15,3	15,3	15,3	23,1	15,3
5 agents-6 agents CPSO	37,5	43,2	37,5	39,0	43,2	41,9	41,9
6 agents-2 agents CPSO	172,7	172,7	172,7	172,7	172,7	172,7	114,3
6 agents-3 agents CPSO	71,4	39,5	46,3	53,8	53,8	33,3	46,3
6 agents-4 agents CPSO	20,0	3,4	25,0	15,4	20,0	25,0	15,4
6 agents-5 agents CPSO	5,3	5,3	1,7	1,7	1,7	7,7	1,7
6 agents-6 agents CPSO	25,0	31,8	25,0	26,8	31,8	30,2	30,2
7 agents-2 agents CPSO	218,2	218,2	218,2	218,2	218,2	218,2	150,0
7 agents-3 agents CPSO	100,0	62,8	70,7	79,5	79,5	55,6	70,7
7 agents-4 agents CPSO	40,0	20,7	45,8	34,6	40,0	45,8	34,6
7 agents-5 agents CPSO	22,8	22,8	18,6	18,6	18,6	7,7	18,6
7 agents-6 agents CPSO	12,5	20,5	12,5	14,6	20,5	18,6	18,6
8 agents-2 agents CPSO	263,6	263,6	263,6	263,6	263,6	263,6	185,7
8 agents-3 agents CPSO	128,6	86,0	95,1	105,1	105,1	77,8	95,1
8 agents-4 agents CPSO	60,0	37,9	66,7	53,8	60,0	66,7	53,8
8 agents-5 agents CPSO	40,4	40,4	35,6	35,6	35,6	23,1	35,6
8 agents-6 agents CPSO	0,0	9,1	0,0	2,4	9,1	7,0	7,0

Table 3.21: 15:00 Algorithms' convergence deviation from CPSO at %

method	θ =0°	θ =30°	θ =60°	θ =60°	θ =120°	θ =150°	θ =180°
PSO							
2 agents CPSO-PSO	45,5	45,5	45,5	45,5	45,5	23,1	14,3
3 agents CPSO-PSO	6,7	23,1	23,1	17,1	29,7	2,1	17,1
4 agents CPSO-PSO	18,5	14,3	28,0	28,0	39,1	28,0	14,3
5 agents CPSO-PSO	40,4	45,5	35,6	35,6	45,5	23,1	35,6
6 agents CPSO-PSO	20,0	9,1	26,3	23,1	29,7	11,6	9,1
DE							
4 genes-2 agents CPSO	318,2	318,2	318,2	318,2	318,2	253,8	228,6
4 genes-3 agents CPSO	104,4	135,9	135,9	124,4	148,6	95,7	124,4
4 genes-4 agents CPSO	70,4	64,3	84,0	84,0	100,0	84,0	64,3
4 genes-5 agents CPSO	61,4	67,3	55,9	55,9	67,3	41,5	55,9
4 genes-6 agents CPSO	15,0	4,5	21,1	17,9	24,3	7,0	4,5
6 genes-2 agents CPSO	527,3	527,3	527,3	527,3	527,3	430,8	392,9
6 genes-3 agents CPSO	206,7	253,8	253,8	236,6	273,0	193,6	236,6
6 genes-4 agents CPSO	155,6	146,4	176,0	176,0	200,0	176,0	146,4
6 genes-5 agents CPSO	142,1	150,9	133,9	133,9	150,9	112,3	133,9
6 genes-6 agents CPSO	72,5	56,8	81,6	76,9	86,5	60,5	56,8
8 genes-2 agents CPSO	736,4	736,4	736,4	736,4	736,4	607,7	557,1
8 genes-3 agents CPSO	308,9	371,8	371,8	348,8	397,3	291,5	348,8
8 genes-4 agents CPSO	240,7	228,6	268,0	268,0	300,0	268,0	228,6
8 genes-5 agents CPSO	222,8	234,5	211,9	211,9	234,5	183,1	211,9
8 genes-6 agents CPSO	130,0	109,1	142,1	135,9	148,6	114,0	109,1
Chaotic							
5 agents-2 agents CPSO	127,3	127,3	127,3	127,3	127,3	92,3	78,6
5 agents-3 agents CPSO	11,1	28,2	28,2	22,0	35,1	6,4	22,0
5 agents-4 agents CPSO	7,4	10,7	0,0	0,0	8,7	0,0	10,7
5 agents-5 agents CPSO	12,3	9,1	15,3	15,3	9,1	23,1	15,3
5 agents-6 agents CPSO	37,5	43,2	34,2	35,9	32,4	41,9	43,2
6 agents-2 agents CPSO	172,7	172,7	172,7	172,7	172,7	130,8	114,3
6 agents-3 agents CPSO	33,3	53,8	53,8	46,3	62,2	27,7	46,3
6 agents-4 agents CPSO	11,1	7,1	20,0	20,0	30,4	20,0	7,1
6 agents-5 agents CPSO	5,3	9,1	1,7	1,7	9,1	7,7	1,7
6 agents-6 agents CPSO	25,0	31,8	21,1	23,1	18,9	30,2	31,8
7 agents-2 agents CPSO	218,2	218,2	218,2	218,2	218,2	169,2	150,0
7 agents-3 agents CPSO	55,6	79,5	79,5	70,7	89,2	48,9	70,7
7 agents-4 agents CPSO	29,6	25,0	40,0	40,0	52,2	40,0	25,0
7 agents-5 agents CPSO	22,8	27,3	18,6	18,6	27,3	7,7	18,6
7 agents-6 agents CPSO	12,5	20,5	7,9	10,3	5,4	18,6	20,5
8 agents-2 agents CPSO	263,6	263,6	263,6	263,6	263,6	207,7	185,7
8 agents-3 agents CPSO	77,8	105,1	105,1	95,1	116,2	70,2	95,1
8 agents-4 agents CPSO	48,1	42,9	60,0	60,0	73,9	60,0	42,9
8 agents-5 agents CPSO	40,4	45,5	35,6	35,6	45,5	23,1	35,6
8 agents-6 agents CPSO	0,0	9,1	5,3	2,6	8,1	7,0	9,1

Table 3.22: 16:00 Algorithms' convergence deviation from CPSO at %

method	θ =0°	θ =30°	θ =60°	θ =60°	θ =120°	θ =150°	θ =180°
PSO							
2 agents CPSO-PSO	45,5	45,5	45,5	45,5	45,5	23,1	14,3
3 agents CPSO-PSO	23,1	37,1	6,7	37,1	17,1	2,1	17,1
4 agents CPSO-PSO	18,5	0,0	0,0	6,7	28,0	28,0	14,3
5 agents CPSO-PSO	40,4	27,0	40,4	40,4	12,7	23,1	35,6
6 agents CPSO-PSO	9,1	26,3	2,0	11,6	26,3	11,6	9,1
DE							
4 genes-2 agents CPSO	318,2	318,2	318,2	318,2	318,2	253,8	228,6
4 genes-3 agents CPSO	135,9	162,9	104,4	162,9	124,4	95,7	124,4
4 genes-4 agents CPSO	70,4	43,8	43,8	53,3	84,0	84,0	64,3
4 genes-5 agents CPSO	61,4	46,0	61,4	61,4	29,6	41,5	55,9
4 genes-6 agents CPSO	4,5	21,1	6,1	7,0	21,1	7,0	4,5
6 genes-2 agents CPSO	527,3	527,3	527,3	527,3	527,3	430,8	392,9
6 genes-3 agents CPSO	253,8	294,3	206,7	294,3	236,6	193,6	236,6
6 genes-4 agents CPSO	155,6	115,6	115,6	130,0	176,0	176,0	146,4
6 genes-5 agents CPSO	142,1	119,0	142,1	142,1	94,4	112,3	133,9
6 genes-6 agents CPSO	56,8	81,6	40,8	60,5	81,6	60,5	56,8
8 genes-2 agents CPSO	736,4	700,0	736,4	736,4	736,4	607,7	557,1
8 genes-3 agents CPSO	371,8	402,9	308,9	425,7	348,8	291,5	348,8
8 genes-4 agents CPSO	240,7	175,0	187,5	206,7	268,0	268,0	228,6
8 genes-5 agents CPSO	222,8	179,4	222,8	222,8	159,2	183,1	211,9
8 genes-6 agents CPSO	109,1	131,6	87,8	114,0	142,1	114,0	109,1
Chaotic							
5 agents-2 agents CPSO	127,3	127,3	127,3	127,3	127,3	92,3	78,6
5 agents-3 agents CPSO	28,2	42,9	11,1	42,9	22,0	6,4	22,0
5 agents-4 agents CPSO	7,4	21,9	21,9	16,7	0,0	0,0	10,7
5 agents-5 agents CPSO	12,3	20,6	12,3	12,3	29,6	23,1	15,3
5 agents-6 agents CPSO	43,2	34,2	49,0	41,9	34,2	41,9	43,2
6 agents-2 agents CPSO	172,7	172,7	172,7	172,7	172,7	130,8	114,3
6 agents-3 agents CPSO	53,8	71,4	33,3	71,4	46,3	27,7	46,3
6 agents-4 agents CPSO	11,1	6,3	6,3	0,0	20,0	20,0	7,1
6 agents-5 agents CPSO	5,3	4,8	5,3	5,3	15,5	7,7	1,7
6 agents-6 agents CPSO	31,8	21,1	38,8	30,2	21,1	30,2	31,8
7 agents-2 agents CPSO	127,3	218,2	218,2	218,2	218,2	169,2	150,0
7 agents-3 agents CPSO	28,2	100,0	55,6	100,0	70,7	48,9	70,7
7 agents-4 agents CPSO	7,4	9,4	9,4	16,7	40,0	40,0	25,0
7 agents-5 agents CPSO	12,3	11,1	22,8	22,8	1,4	7,7	18,6
7 agents-6 agents CPSO	43,2	7,9	28,6	18,6	7,9	18,6	20,5
8 agents-2 agents CPSO	172,7	263,6	263,6	263,6	263,6	207,7	185,7
8 agents-3 agents CPSO	53,8	128,6	77,8	128,6	95,1	70,2	95,1
8 agents-4 agents CPSO	11,1	25,0	25,0	33,3	60,0	60,0	42,9
8 agents-5 agents CPSO	5,3	27,0	40,4	40,4	12,7	23,1	35,6
8 agents-6 agents CPSO	31,8	5,3	18,4	7,0	5,3	7,0	9,1

Table 3.23: 17:00 Algorithms' convergence deviation from CPSO at %

method	θ =0°	θ =30°	θ =60°	θ =60°	θ =120°	θ =150°	θ =180°
PSO							
2 agents CPSO-PSO	45,5	45,5	33,3	45,5	33,3	45,5	45,5
3 agents CPSO-PSO	2,1	17,1	23,1	23,1	2,1	6,7	23,1
4 agents CPSO-PSO	14,3	28,0	39,1	23,1	6,7	28,0	28,0
5 agents CPSO-PSO	40,4	35,6	35,6	35,6	35,6	35,6	35,6
6 agents CPSO-PSO	11,6	17,1	14,3	23,1	25,0	7,0	26,3
DE							
4 genes-2 agents CPSO	318,2	318,2	283,3	318,2	283,3	318,2	318,2
4 genes-3 agents CPSO	95,7	124,4	135,9	135,9	95,7	104,4	135,9
4 genes-4 agents CPSO	64,3	84,0	100,0	76,9	53,3	84,0	84,0
4 genes-5 agents CPSO	61,4	55,9	55,9	55,9	55,9	55,9	55,9
4 genes-6 agents CPSO	7,0	12,2	9,5	17,9	21,1	7,0	21,1
6 genes-2 agents CPSO	527,3	527,3	475,0	527,3	475,0	527,3	527,3
6 genes-3 agents CPSO	193,6	236,6	253,8	253,8	193,6	206,7	253,8
6 genes-4 agents CPSO	146,4	176,0	200,0	165,4	130,0	176,0	176,0
6 genes-5 agents CPSO	142,1	133,9	133,9	133,9	133,9	133,9	133,9
6 genes-6 agents CPSO	60,5	68,3	64,3	76,9	81,6	60,5	81,6
8 genes-2 agents CPSO	736,4	736,4	666,7	736,4	666,7	736,4	736,4
8 genes-3 agents CPSO	291,5	348,8	371,8	371,8	291,5	308,9	371,8
8 genes-4 agents CPSO	228,6	268,0	300,0	253,8	206,7	268,0	268,0
8 genes-5 agents CPSO	222,8	211,9	211,9	211,9	211,9	211,9	211,9
8 genes-6 agents CPSO	114,0	124,4	119,0	135,9	142,1	114,0	142,1
Chaotic							
5 agents-2 agents CPSO	127,3	127,3	108,3	127,3	108,3	127,3	127,3
5 agents-3 agents CPSO	6,4	22,0	28,2	28,2	6,4	11,1	28,2
5 agents-4 agents CPSO	10,7	0,0	8,7	3,8	16,7	0,0	0,0
5 agents-5 agents CPSO	12,3	15,3	15,3	15,3	15,3	15,3	15,3
5 agents-6 agents CPSO	41,9	39,0	40,5	35,9	34,2	41,9	34,2
6 agents-2 agents CPSO	172,7	172,7	150,0	172,7	150,0	172,7	172,7
6 agents-3 agents CPSO	27,7	46,3	53,8	53,8	27,7	33,3	53,8
6 agents-4 agents CPSO	7,1	20,0	30,4	15,4	0,0	20,0	20,0
6 agents-5 agents CPSO	5,3	1,7	1,7	1,7	1,7	1,7	1,7
6 agents-6 agents CPSO	30,2	26,8	28,6	23,1	21,1	30,2	21,1
7 agents-2 agents CPSO	218,2	218,2	191,7	218,2	191,7	218,2	218,2
7 agents-3 agents CPSO	48,9	70,7	79,5	79,5	48,9	55,6	79,5
7 agents-4 agents CPSO	25,0	40,0	52,2	34,6	16,7	40,0	40,0
7 agents-5 agents CPSO	22,8	18,6	18,6	18,6	18,6	18,6	18,6
7 agents-6 agents CPSO	18,6	14,6	16,7	10,3	7,9	18,6	7,9
8 agents-2 agents CPSO	263,6	263,6	233,3	263,6	233,3	263,6	263,6
8 agents-3 agents CPSO	70,2	95,1	105,1	105,1	70,2	77,8	105,1
8 agents-4 agents CPSO	42,9	60,0	73,9	53,8	33,3	60,0	60,0
8 agents-5 agents CPSO	40,4	35,6	35,6	35,6	35,6	35,6	35,6
8 agents-6 agents CPSO	7,0	2,4	4,8	2,6	5,3	7,0	5,3

Table 3.24: 18:00 Algorithms' convergence deviation from CPSO at %

method	θ =0^o	θ =30^o	θ =60^o	θ =60^o	θ =120^o	θ =150^o	θ =180^o
PSO							
2 agents CPSO-PSO	45,5	45,5	33,3	23,1	23,1	45,5	23,1
3 agents CPSO-PSO	6,7	17,1	2,1	23,1	23,1	17,1	37,1
4 agents CPSO-PSO	5,9	3,0	33,3	14,3	14,3	33,3	33,3
5 agents CPSO-PSO	27,0	40,4	35,6	6,7	6,7	19,4	35,6
6 agents CPSO-PSO	2,1	11,6	17,1	29,7	29,7	29,7	17,1
DE							
4 genes-2 agents CPSO	318,2	318,2	283,3	253,8	253,8	318,2	253,8
4 genes-3 agents CPSO	104,4	124,4	95,7	135,9	135,9	124,4	162,9
4 genes-4 agents CPSO	35,3	39,4	91,7	64,3	64,3	91,7	91,7
4 genes-5 agents CPSO	46,0	61,4	55,9	22,7	22,7	37,3	55,9
4 genes-6 agents CPSO	2,1	7,0	12,2	24,3	24,3	24,3	12,2
6 genes-2 agents CPSO	527,3	527,3	475,0	430,8	430,8	527,3	430,8
6 genes-3 agents CPSO	206,7	236,6	193,6	253,8	253,8	236,6	294,3
6 genes-4 agents CPSO	102,9	109,1	187,5	146,4	146,4	187,5	187,5
6 genes-5 agents CPSO	119,0	142,1	133,9	84,0	84,0	106,0	133,9
6 genes-6 agents CPSO	46,8	60,5	68,3	86,5	86,5	86,5	68,3
8 genes-2 agents CPSO	736,4	736,4	666,7	607,7	607,7	736,4	607,7
8 genes-3 agents CPSO	308,9	348,8	291,5	371,8	371,8	348,8	425,7
8 genes-4 agents CPSO	170,6	178,8	283,3	228,6	228,6	283,3	283,3
8 genes-5 agents CPSO	192,1	222,8	211,9	145,3	145,3	174,6	211,9
8 genes-6 agents CPSO	95,7	114,0	124,4	148,6	148,6	148,6	124,4
Chaotic							
5 agents-2 agents CPSO	127,3	127,3	108,3	92,3	92,3	127,3	92,3
5 agents-3 agents CPSO	11,1	22,0	6,4	28,2	28,2	22,0	42,9
5 agents-4 agents CPSO	26,5	24,2	4,2	10,7	10,7	4,2	4,2
5 agents-5 agents CPSO	20,6	12,3	15,3	33,3	33,3	25,4	15,3
5 agents-6 agents CPSO	46,8	41,9	39,0	32,4	32,4	32,4	39,0
6 agents-2 agents CPSO	172,7	172,7	150,0	130,8	130,8	172,7	130,8
6 agents-3 agents CPSO	33,3	46,3	27,7	53,8	53,8	46,3	71,4
6 agents-4 agents CPSO	11,8	9,1	25,0	7,1	7,1	25,0	25,0
6 agents-5 agents CPSO	4,8	5,3	1,7	20,0	20,0	10,4	1,7
6 agents-6 agents CPSO	36,2	30,2	26,8	18,9	18,9	18,9	26,8
7 agents-2 agents CPSO	218,2	218,2	191,7	169,2	169,2	218,2	169,2
7 agents-3 agents CPSO	55,6	70,7	48,9	79,5	79,5	70,7	100,0
7 agents-4 agents CPSO	2,9	6,1	45,8	25,0	25,0	45,8	45,8
7 agents-5 agents CPSO	11,1	22,8	18,6	6,7	6,7	4,5	18,6
7 agents-6 agents CPSO	25,5	18,6	14,6	5,4	5,4	5,4	14,6
8 agents-2 agents CPSO	263,6	263,6	233,3	207,7	207,7	263,6	207,7
8 agents-3 agents CPSO	77,8	95,1	70,2	105,1	105,1	95,1	128,6
8 agents-4 agents CPSO	17,6	21,2	66,7	42,9	42,9	66,7	66,7
8 agents-5 agents CPSO	27,0	40,4	35,6	6,7	6,7	19,4	35,6
8 agents-6 agents CPSO	14,9	7,0	2,4	8,1	8,1	8,1	2,4

Case of convex characteristic The hybrid PSO method is based on the PSO convergence mechanism. However, CPSO method does not execute random procedures to initialize and reinitialize the agents in case of stagnancy. As a result the procedure of convergence depends less in randomness. As the method shares the same basic operational parameters with the conventional PSO method, the way that converge when the power-voltage characteristic remains strictly convex is the same, the particles of the algorithms hardly go stagnant. Consequently neither PSO nor CPSO methods reinitialize the particles with the randomization and chaotic search respectively. However, CPSO method converges more accurately in less steps than PSO, as the particles' chaotic initialization distributes the particle in a more efficient way than the random initialization does. As an example the case of 2 agents at 13:00 and arch with central angle $\hat{\theta}$ 0° is shown in Fig. 3.21.

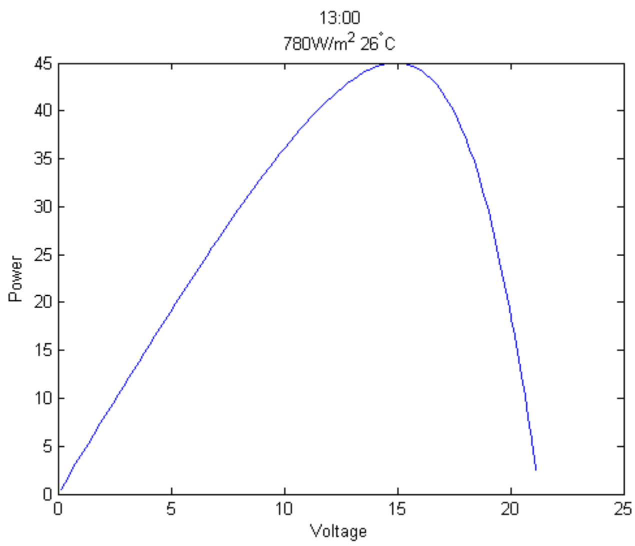

Figure 3.21: power-voltage characteristic

CPSO	offset	steps
2 agents	0.0080	22
3 agents	-0.0790	41
4 agents	-0.1200	50
5 agents	-0.0020	57
6 agents	0.1640	82
PSO		
2 agents	-1.4290	32
3 agents	-0.5170	48
4 agents	-0.2940	64
5 agents	-0.1380	80
6 agents	-0.0490	96
DE		
4 genes	-0.1870	92
6 genes	-0.3700	138
8 genes	0.0570	184
Chaotic		
5 agents	-0.9830	50
6 agents	-0.0280	60
7 agents	0.0070	70
8 agents	-0.0670	80

Figure 3.22: The results of each MPPT method

It is observed that the CPSO method converge at distance of 0.0080 from the global optimum point at 22 steps in contrast to PSO algorithm that converge at distance of 1.4290. As previously mentioned negative values indicates the offset from the global optimum as the global optimum is bigger than the convergent point. In other case the positive distance of CPSO's convergent point that is quite below the barrier of 0.6mW insists an accurate convergence. On the other hand the Differential Evolution as well as the Chaotic Partial Search MPP method converges at 92 steps (4 genes) with offset -0.1870 and 50 steps (5 agents) at offset-0.9830 respectively. The method CPSO with 2 agents is an efficient choice that out performs the other MPP methods in case of convex characteristics.

Case of non convex characteristic The solar PV module under non uniform solar irradiation provokes several local maximum points at the characteristic as the arc's center angle augments from 30° to 180°. The amount as well as the intensity of the phenomenon varies across the day as the solar angle changes. However, 2 basic forms of PV's characteristic under non uniform irradiation are distinguished among all the possible configurations along the day: the cases depicted in Figs. 3.30 and 3.23 that are quite different each other. In the first case, the top of the characteristic reveals several small local maximum points and in the second case, the power-voltage characteristic is deformed by intense local maximum peaks. As a consequence, the global maximum peak is shifted away from any possible prediction. The existence of local maximum points that are emerged without any prediction set a barrier on the use of conventional MPPT methods. Fig. 3.24 and 3.31 depict each methods' results for these cases.

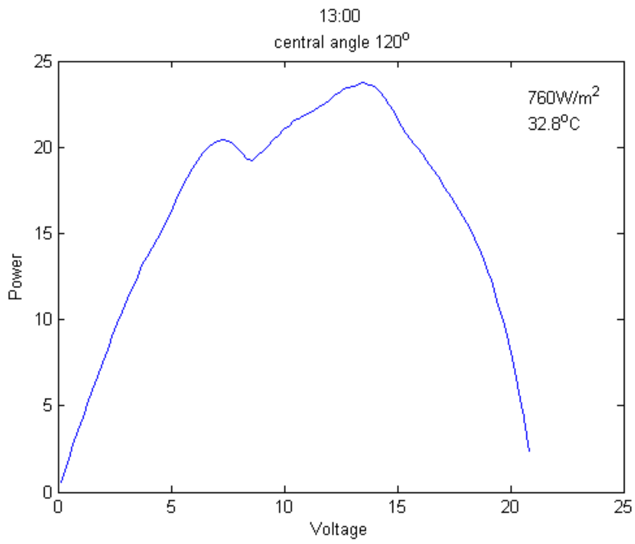

Figure 3.23: Power-voltage characteristic in case of arc with central angle θ =120°

CPSO	offset	steps
2 agents	-0.0910	22
3 agents	-0.0590	39
4 agents	-0.1620	50
5 agents	-0.1110	59
6 agents	-0.2170	84
PSO		
2 agents	-0.1860	32
3 agents	0.0480	48
4 agents	0.1540	64
5 agents	0.2660	80
6 agents	0.2210	96
DE		
4 genes	0.0520	92
6 genes	-0.6270	138
8 genes	-1.1590	184
Chaotic		
5 agents	-4.2400	50
6 agents	-4.3330	60
7 agents	-4.3620	70
8 agents	-4.3320	80

Figure 3.24: The results of each MPPT method at arc with central angle θ =120°

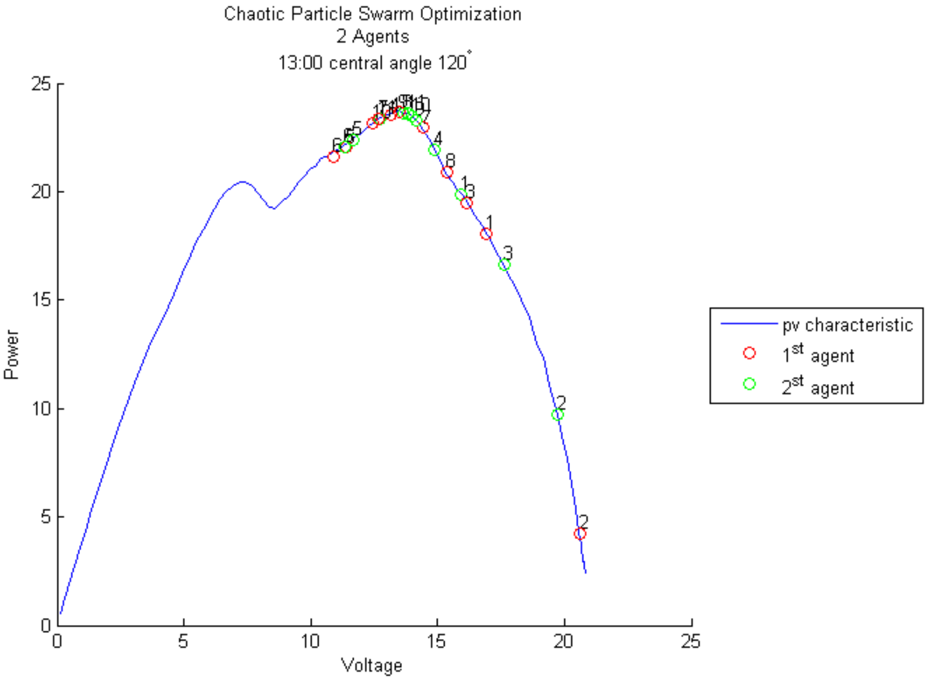

Figure 3.25: Chaotic Particle Swarm Optimization 2 agents central angle θ =120°

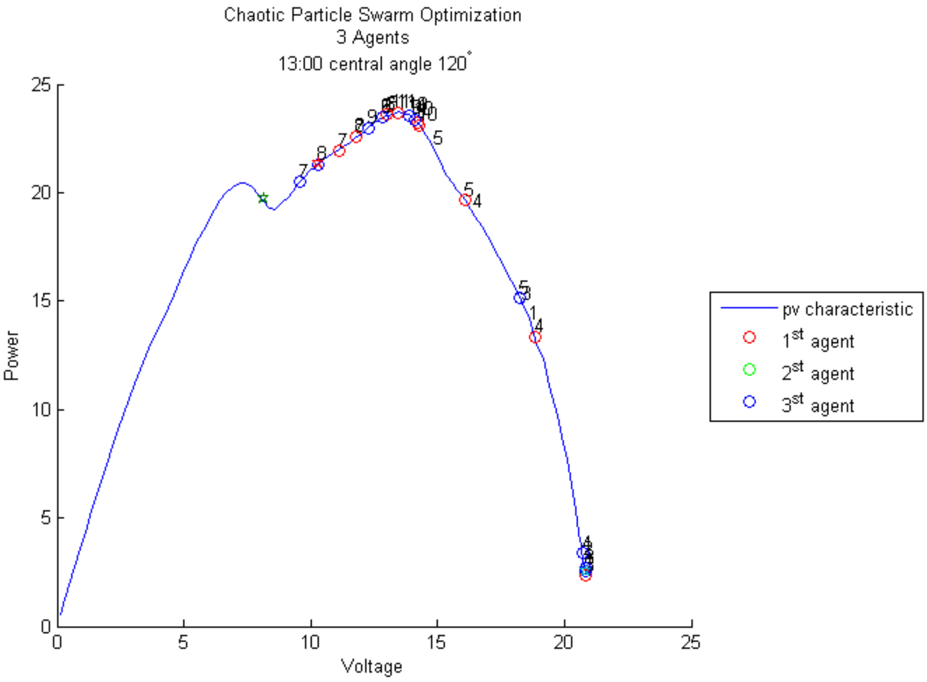

Figure 3.26: Chaotic Particle Swarm Optimization 3 agents central angle θ =180°

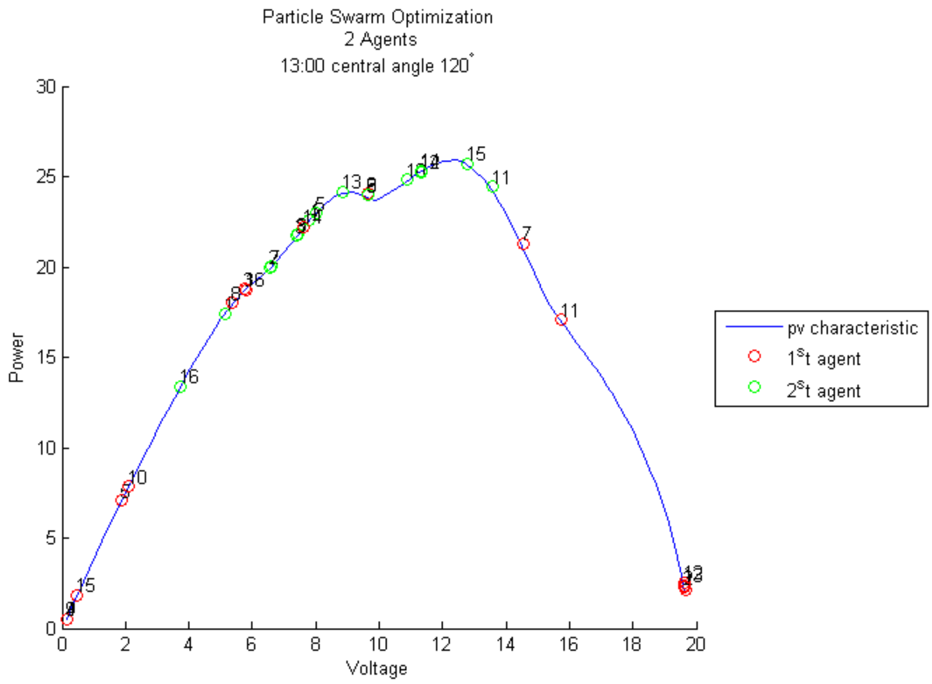

Figure 3.27: Particle Swarm Optimization 2 agents central angle θ =180°

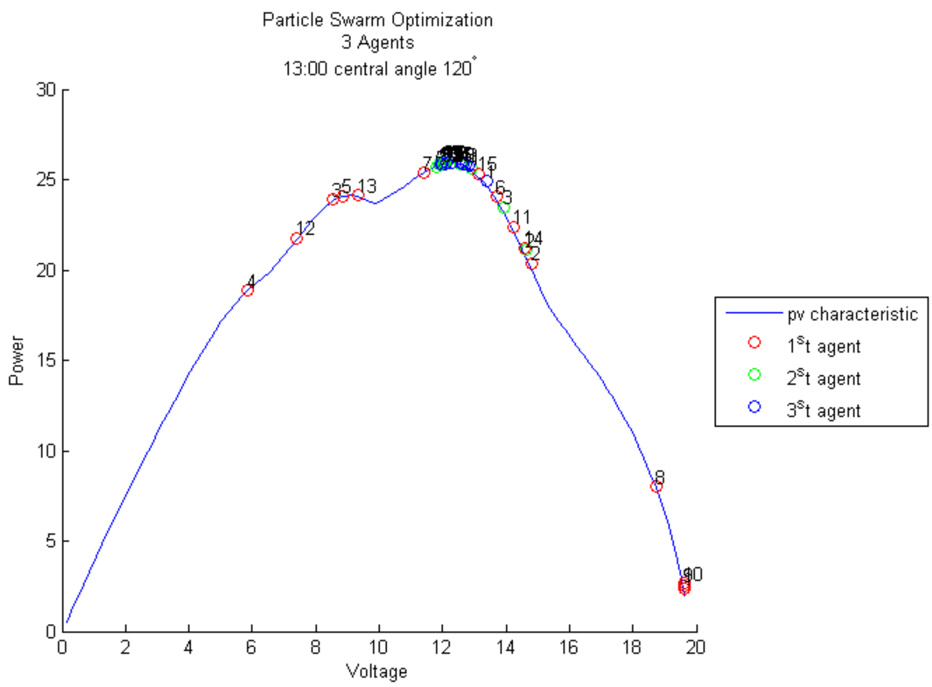

Figure 3.28: Particle Swarm Optimization 3 agents central angle θ =120°

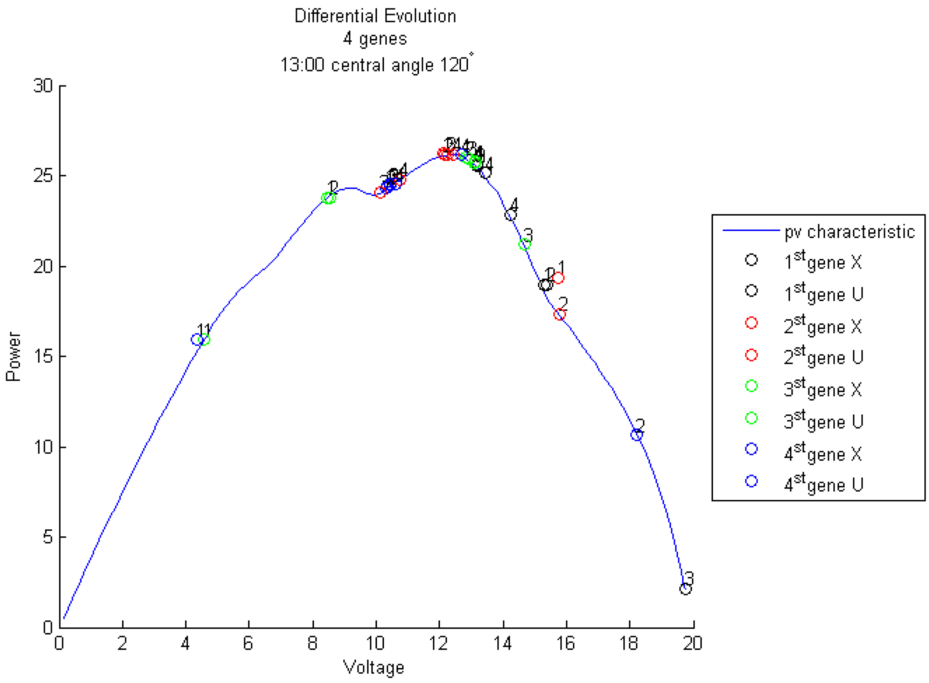

Figure 3.29: Differential Evolution 5 agents central angle θ =120°

In this case the CPSO MPPT method converges at 22 steps with better accuracy than the conventional PSO method which converges at 32 steps both being configured with 2 agents. However, for more agents the PSO algorithm converges more accurate at more steps than the CPSO. The Differential Evolution method converges as accurately as the PSO and CPSO do but it requires a lot more steps than them. This behavior is justified because for every gene of DE 2 steps are executed in the same generation. In case of Chaotic method seems that it failed to locate the MPP as the offset of the convergent point is about -4.000 for all configurations.Figs. 3.25-?? depict the algorithms' steps of convergence at 13:00 configured at central angle of θ=120°.

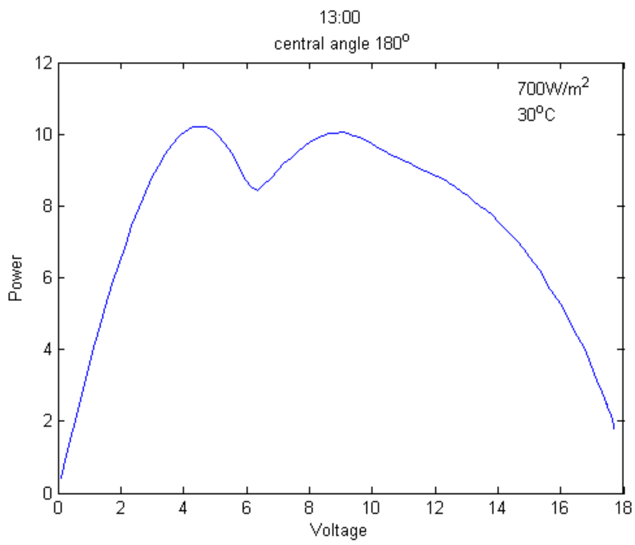

Figure 3.30: arch with central angle θ=180°

CPSO	offset	steps
2 agents	-0.0370	24
3 agents	0.1450	37
4 agents	0.3360	60
5 agents	0.2860	61
6 agents	0.3120	78
PSO		
2 agents	0.1600	32
3 agents	-0.2270	48
4 agents	0.1220	64
5 agents	-0.2430	80
6 agents	0.0290	96
DE		
4 genes	0.1000	92
6 genes	0.1160	138
8 genes	-1.4330	184
Chaotic		
5 agents	0	50
6 agents	-0.0070	60
7 agents	-0.0380	70
8 agents	-0.0250	80

Figure 3.31: Methods' results at arch with central angle θ =180°

The Figs. 3.30 depicts the power-voltage characteristic at 13:00 configured at central angle of θ=180°. In case of 2 agents, the CPSO method is worse than the PSO, since the CPSO didn't converged at the global optimum as shown from the Fig. 3.32. Better performance is expected in this case by initializing the particles with chaotic sequences centralized in the middle of the characteristic. However at configuration of 3 agents the chaotic search that is executed in case of particle stagnancy, gets the particles more concentrated in short time finding a better personal as well as global best position than the current position without having to reinitialize at random the particle as the PSO does. The penalty of two steps for every generation that the chaotic search executes is negligible towards the benefit of the faster convergence of the CPSO method. Consequently the CPSO method provides a more accurate and faster convergence in case of 3 agents. DE and Chaotic methods show off the same convergence accuracy with the PSO and CPSO method, however the convergence of these methods takes place in more steps than the rest algorithms. Figs. 3.32-3.37 depict the algorithms' steps of convergence at 13:00 configured at central angle of θ=180º.

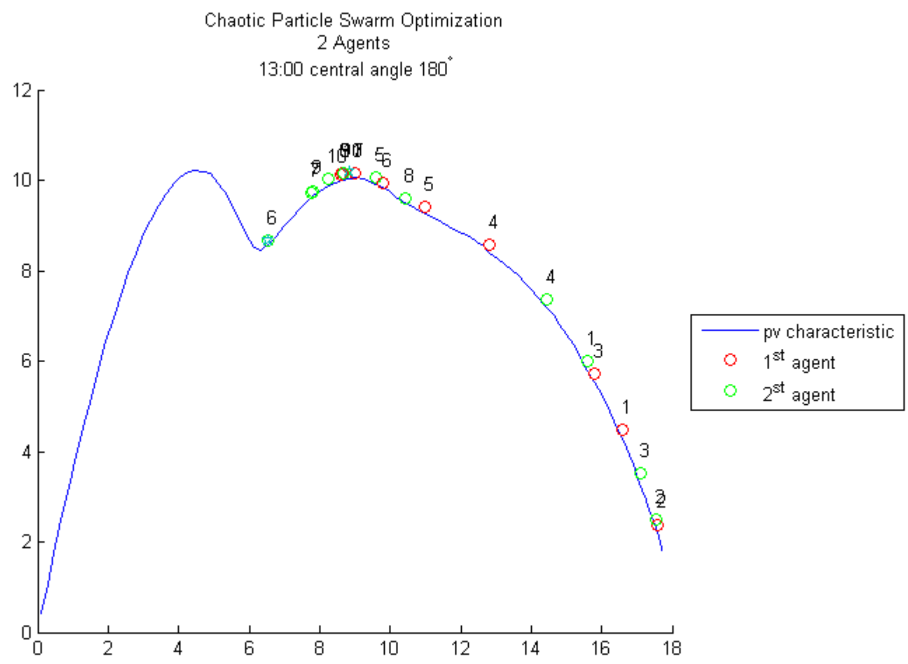

Figure 3.32: Chaotic Particle Swarm Optimization 2 agents central angle θ =180º

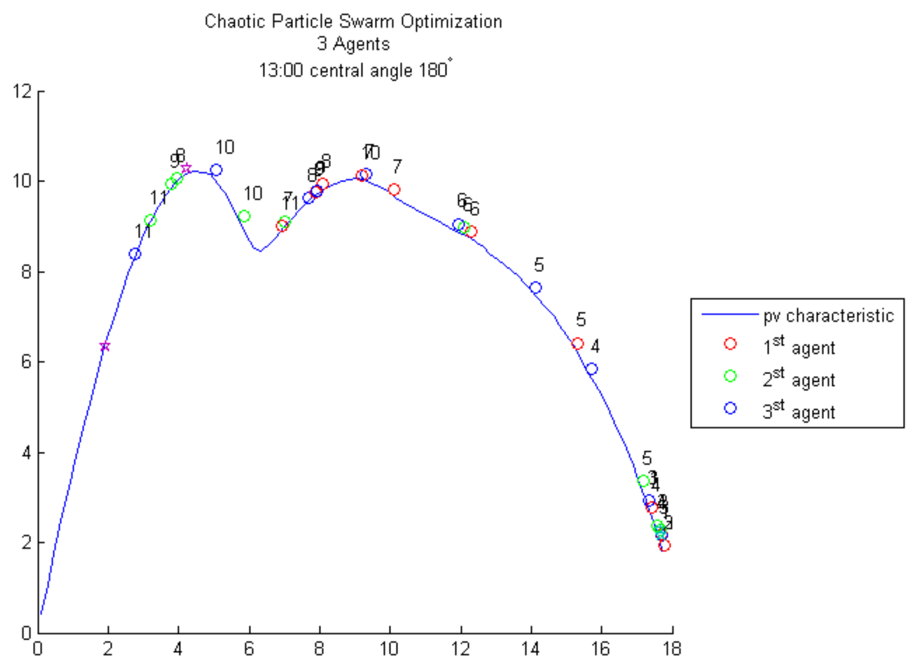

Figure 3.33: Chaotic Particle Swarm Optimization 3 agents central angle θ =180º

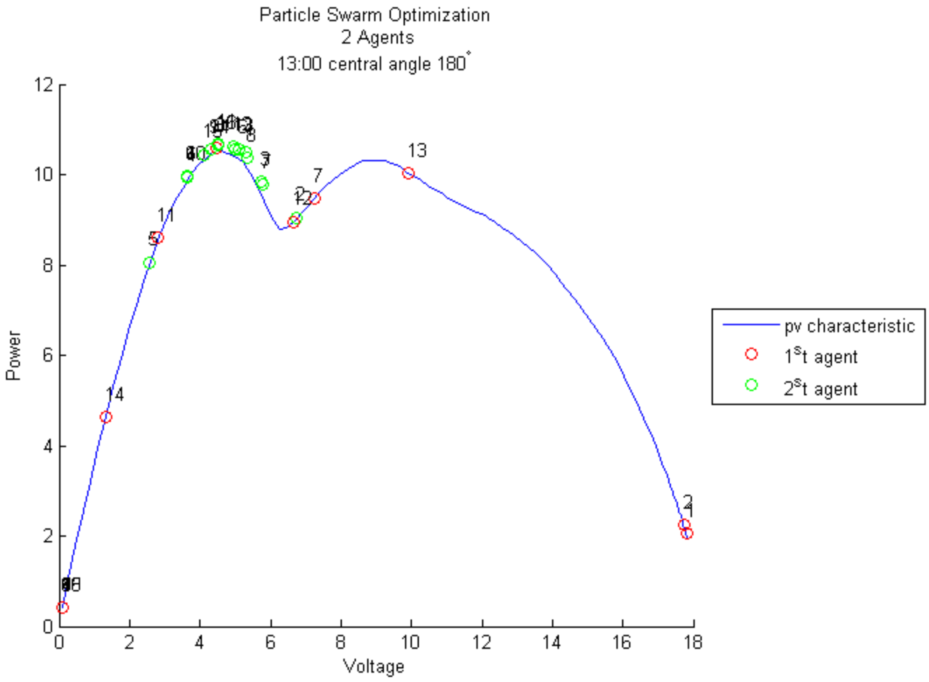

Figure 3.34: Particle Swarm Optimization 2 agents central angle θ =180º

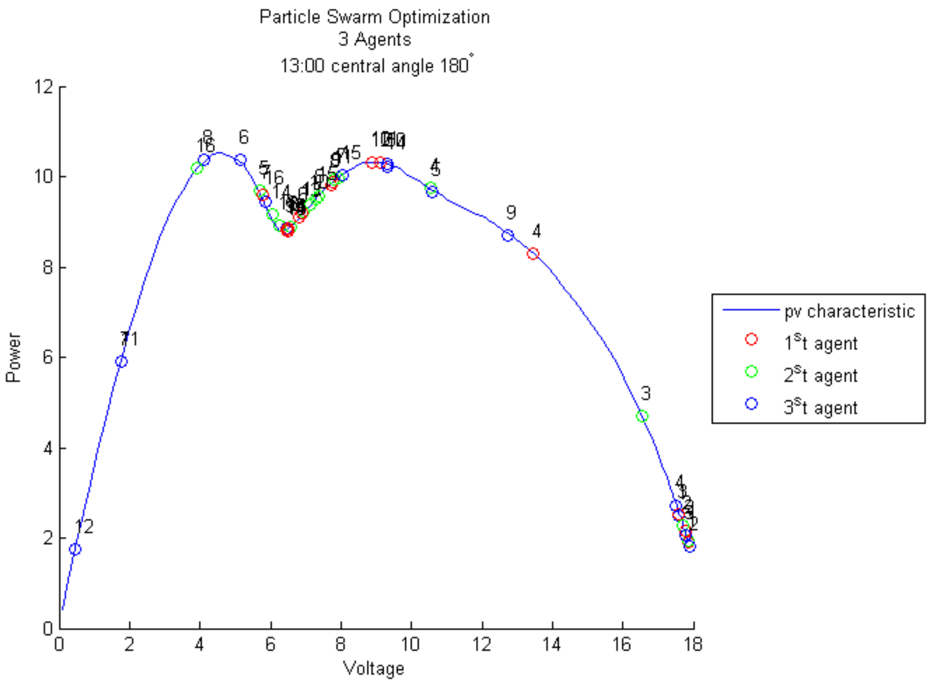

Figure 3.35: Particle Swarm Optimization 3 agents central angle θ =180º

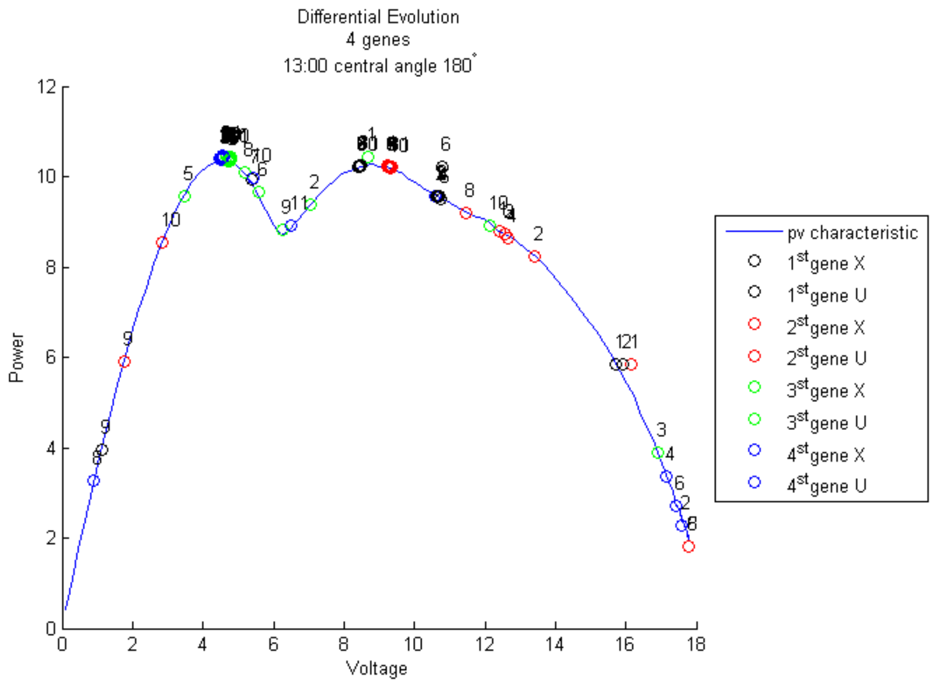

Figure 3.36: Differential Evolution 5 agents central angle θ =180º

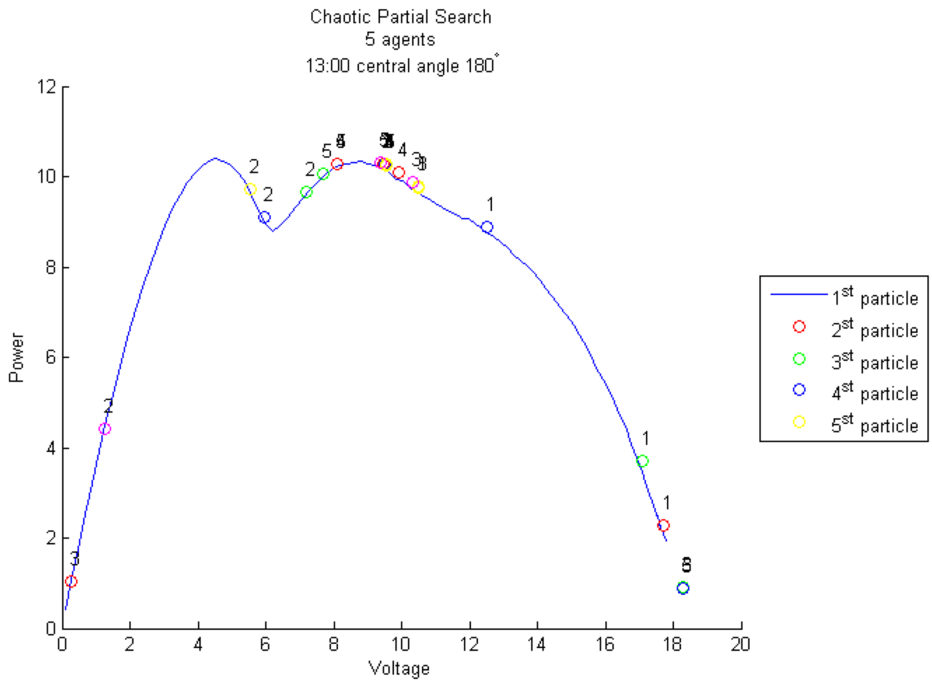

Figure 3.37: Partial Chaotic Search 5 agents central angle θ =180º

Chapter 4

Conclusions

The PV module under non-uniform irradiation exhibits non-convex power-voltage characteristic with several local peaks. The form of the characteristic varies according to solar angle as well as to the degree of bending. Under specific circumstances the position of the maximum power point is unpredictable. Conventional MPPT methods fail to maximize the power-voltage characteristic under these conditions. The results of the algorithm evaluation shown that the Chaotic Particle Swarm Optimization exhibits a rapid and accurate convergence that makes use of the PSO's convergence mechanism without the random initialization and reinitialization of the particles that the PSO does. Better results are expected by the centralized initialization of the agents. The Differential Evolution and Chaotic Partial Search presents the same convergence accuracy overall. However the steps that these methods are needed to converge, outnumbers the steps of PSO and CPSO.

Future Work The examination of BIPV architecture that exploits the flexibility and the lightweight structure of the flexible pv modules reveals new application possibilities.Future work includes the development of a distributed power production system for BIPV applications.

Bibliography

[1] M. Pagliaro, R. Ciriminna, and G. Palmisano, "Flexible solar cells," *ChemSusChem*, vol. 1, no. 11, pp. 880–891, 2008.

[2] K. Jansen, S. Kadam, and J. Groelinger, "The advantages of amorphous silicon photovoltaic modules in grid-tied systems," in *Conference Record of the 2006 IEEE 4th World Conference on Photovoltaic Energy Conversion*, vol. 2. IEEE, 2006, pp. 2363–2366.

[3] P. Jackson, D. Hariskos, E. Lotter, S. Paetel, R. Wuerz, R. Menner, W. Wischmann, and M. Powalla, "New world record efficiency for cu (in, ga) se2 thin-film solar cells beyond 20%," *Progress in Photovoltaics: Research and Applications*, vol. 19, no. 7, pp. 894–897, 2011.

[4] S. Aksu and M. Pinarbasi, "Electrodeposition methods and chemistries for deposition of cigs precursor thin films," in *Photovoltaic Specialists Conference (PVSC), 2011 37th IEEE*, june 2011, pp. 310–314.

[5] G. Dennler and N. Sariciftci, "Flexible conjugated polymer-based plastic solar cells: From basics to applications," *Proceedings of the IEEE*, vol. 93, no. 8, pp. 1429–1439, aug. 2005.

[6] R. Ramabadran and B. Mathur, "Effect of shading on series and parallel connected solar pv modules," *Modern Applied Science*, vol. 3, no. 10, p. P32, 2009.

[7] H. Patel and V. Agarwal, "Matlab-based modeling to study the effects of partial shading on pv array characteristics," *IEEE Transactions on Energy Conversion*, vol. 23, no. 1, pp. 302–310, march 2008.

[8] A. Sayal, "Mppt techniques for photovoltaic system under uniform insolation and partial shading conditions."

[9] K. Ishaque and Z. Salam, "A deterministic particle swarm optimization maximum power point tracker for photovoltaic system under partial shading condition," *IEEE Transactions on Industrial Electronics*, vol. PP, no. 99, p. 1, 2012.

[10] W. Xu, S. Choi, and M. Allen, "Hairlike carbon-fiber-based solar cell," in *Micro Electro Mechanical Systems (MEMS), 2010 IEEE 23rd International Conference on*, jan. 2010, pp. 1187–1190.

[11] M. Schubert and J. Werner, "Flexible solar cells for clothing," *Materials Today*, vol. 9, no. 6, pp. 42–50, 2006.

[12] M. B. Schubert and J. H. Werner, "Flexible solar cells Integration of flexible solar cells into clothing can provide power for," vol. 9, no. 6, pp. 42–50, 2006.

[13] M. Tocher, "Modular cylindrical photovoltaic array for fixed and portable applications," in *Sustainable Energy Technologies, 2008. ICSET 2008. IEEE International Conference on*, nov. 2008, pp. 601–606.

[14] C. Clark, J. Summers *et al.*, "Innovative flexible lightweight thin-film power generation and storage for space applications," in *Energy Conversion Engineering Conference and Exhibit, 2000.(IECEC) 35th Intersociety*, vol. 1. IEEE, 2000, pp. 692–698.

[15] M. Schuber, Y. Ishikawa, J. Kramer, C. Gemmer, and J. Werner, "Clothing integrated photovoltaics," in *Photovoltaic Specialists Conference, 2005. Conference Record of the Thirty-first IEEE.* IEEE, 2005, pp. 1488–1491.

[16] A. Mestre and J. Diehl, "Ecodesign and renewable energy: How to integrate renewable energy technologies into consumer products," in *Environmentally Conscious Design and Inverse Manufacturing, 2005. Eco Design 2005. Fourth International Symposium on.* IEEE, 2005, pp. 282–288.

[17] K. Edmondson, D. Law, G. Glenn, A. Paredes, R. King, and N. Karam, "Flexible iii-v multijunction solar blanket," in *Conference Record of the 2006 IEEE 4th World Conference on Photovoltaic Energy Conversion*, vol. 2. IEEE, 2006, pp. 1935–1938.

[18] W. Zuckermandel, S. Enger, N. Gupta, and J. Summers, "Modular, thin film solar arrays for operationally responsive spacecraft," in *2007 IEEE Aerospace Conference.* IEEE, 2007, pp. 1–6.

[19] M. Tocher, "Modular cylindrical photovoltaic array for fixed and portable applications," in *IEEE International Conference on Sustainable Energy Technologies, 2008. ICSET 2008.* IEEE, 2008, pp. 601–606.

[20] J.-M. Kwon, B.-H. Kwon, and K.-H. Nam, "Grid-connected photovoltaic multistring pcs with pv current variation reduction control," *IEEE Transactions on Industrial Electronics*, vol. 56, no. 11, pp. 4381–4388, nov. 2009.

[21] Q. Li and P. Wolfs, "Recent development in the topologies for photovoltaic module integrated converters," in *Power Electronics Specialists Conference, 2006. PESC'06. 37th IEEE.* IEEE, 2006, pp. 1–8.

[22] S. Araujo, P. Zacharias, B. Sahan, R. Torrico Bascope, and F. Antunes, "Analysis and proposition of a pv module integrated converter with high voltage gain capability in a non-isolated topology," in *7th Internatonal Conference on Power Electronics, 2007. ICPE'07.* IEEE, 2007, pp. 511–517.

[23] W. Bower, R. West, and A. Dickerson, "Innovative pv micro-inverter topology eliminates electrolytic capacitors for longer lifetime," in *Conference Record of the 2006 IEEE 4th World Conference on Photovoltaic Energy Conversion*, vol. 2. IEEE, 2006, pp. 2038–2041.

[24] B. Liu, S. Duan, and T. Cai, "Photovoltaic dc building module based bipv system-concept and design considerations," *IEEE Transactions on Power Electronics*, no. 99, pp. 1–1, 2011.

[25] N. Mohan and T. Undeland, *Power electronics: converters, applications, and design.* Wiley, 2007.

[26] B. Liu, S. Duan, and T. Cai, "Photovoltaic DC-Building-Module-Based BIPV System—Concept and Design Considerations," *IEEE Transactions on Power Electronics*, vol. 26, no. 5, pp. 1418–1429, May 2011. [Online]. Available: http://ieeexplore.ieee.org/lpdocs/epic03/wrapper.htm?arnumber=5597953

[27] Y. Ji, D. Jung, C. Won, B. Lee, and J. Kim, "Maximum power point tracking method for pv array under partially shaded condition," in *Energy Conversion Congress and Exposition, 2009. ECCE 2009. IEEE.* IEEE, 2009, pp. 307–312.

[28] S. Kazmi, H. Goto, O. Ichinokura, and H. Guo, "An improved and very efficient mppt controller for pv systems subjected to rapidly varying atmospheric conditions and partial shading," in *Power Engineering Conference 2009. AUPEC 2009. Australasian Universities.* IEEE, 2009, pp. 1–6.

[29] B. Alajmi, K. Ahmed, S. Finney, and B. Wayne Williams, "A maximum power point tracking technique for partially shaded photovoltaic systems in microgrids," *IEEE Transactions on Industrial Electronics*, no. 99, pp. 1–1, 2011.

[30] M. Veerachary, T. Senjyu, and K. Uezato, "Neural-network-based maximum-power-point tracking of coupled-inductor interleaved-boost-converter-supplied pv system using fuzzy controller," *IEEE Transactions on Industrial Electronics*, vol. 50, no. 4, pp. 749–758, 2003.

[31] T. Esram and P. Chapman, "Comparison of photovoltaic array maximum power point tracking techniques," *IEEE transactions on Energy conversion*, vol. 22, no. 2, pp. 439–449.

[32] D. Hohm and M. Ropp, "Comparative study of maximum power point tracking algorithms using an experimental, programmable, maximum power point tracking test bed," in *2000. Conference Record of the Twenty-Eighth IEEE Photovoltaic Specialists Conference.* IEEE, 2000, pp. 1699–1702.

[33] M. Miyatake, M. Veerachary, F. Toriumi, N. Fujii, and H. Ko, "Maximum power point tracking of multiple photovoltaic arrays: A pso approach," *IEEE Transactions on Aerospace and Electronic Systems*, vol. 47, no. 1, pp. 367–380, 2011.

[34] B. Alajmi, K. Ahmed, S. Finney, and B. Williams, "Fuzzy logic controlled approach of a modified hill climbing method for maximum power point in microgrid standalone photovoltaic system," *IEEE Transactions on Power Electronics*, no. 99, pp. 1–1, 2011.

[35] H. Taheri, Z. Salam, K. Ishaque *et al.*, "A novel maximum power point tracking control of photovoltaic system under partial and rapidly fluctuating shadow conditions using differential evolution," in *2010 IEEE Symposium on Industrial Electronics & Applications (ISIEA).* IEEE, 2010, pp. 82–87.

[36] S. Das, A. Abraham, U. Chakraborty, and A. Konar, "Differential evolution using a neighborhood-based mutation operator," *IEEE Transactions on Evolutionary Computation*, vol. 13, no. 3, pp. 526–553, 2009.

[37] L. Zhou, Y. Chen, K. Guo, and F. Jia, "New approach for mppt control of photovoltaic system with mutative scale dual carrier chaotic search," *IEEE Transactions on Power Electronics*, no. 99, pp. 1–1, 2011.

[38] H. Liu, A. Abraham, and V. Snasel, "Convergence analysis of swarm algorithm," in *2009. NaBIC 2009. World Congress on Nature & Biologically Inspired Computing.* IEEE, 2009, pp. 1714–1719.

[39] H. Meng, P. Zheng, R. Wu, X. Hao, and Z. Xie, "A hybrid particle swarm algorithm with embedded chaotic search," in *2004 IEEE Conference on Cybernetics and Intelligent Systems*, vol. 1. IEEE, 2004, pp. 367–371.

Appendix A

Photos

Arc shape static model of experimentation

Figures A.1-A.7 depict the PV module installed forming the shape of arch for 7 different central angles: 0°, 30°, 60°,90°, 120°,150° and 180°.

Figure A.1: Central angle $\theta = 0^o$

Figure A.2: Central angle θ =30°

Figure A.3: Central angle θ =60°

Figure A.4: Central angle θ =90^{o}

Figure A.5: Central angle θ =120^{o}

Figure A.6: Central angle θ =150º

Figure A.7: Central angle θ =180º

Instrumentation

Figures A.8 and A.9 depict the module integrated converter which was designed and constructed and supported, with measurement instruments.

Figure A.8: Instrumentation: pyranometer, compass, thermometer.

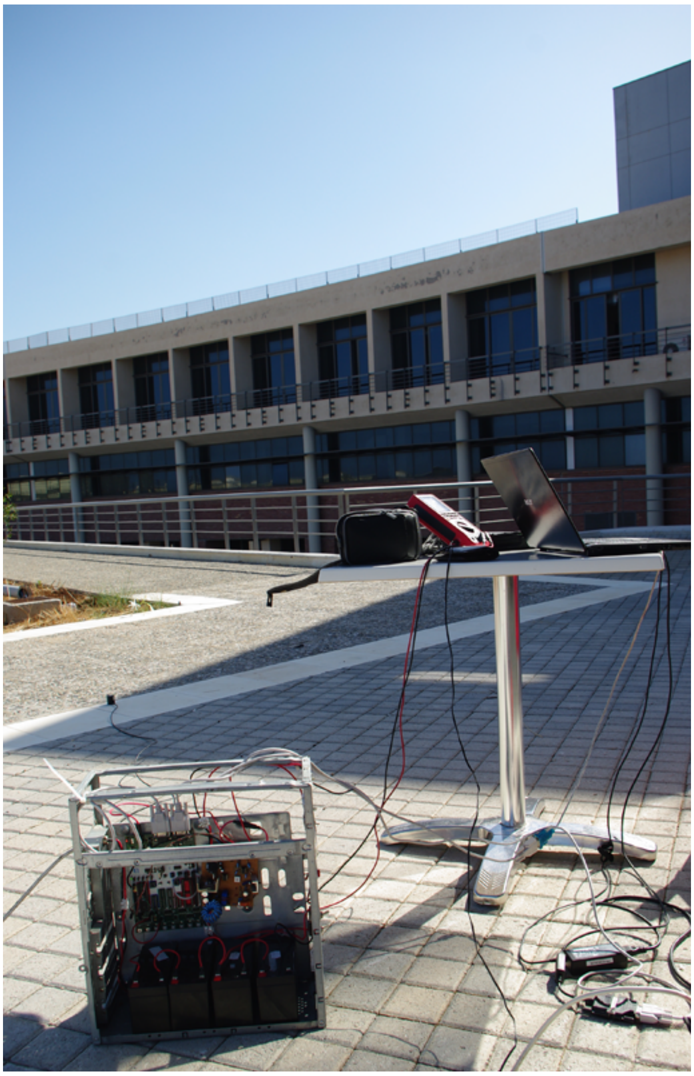

Figure A.9: The Module integrated converter.